AMERICAN MUSEUM NOVITATES

Number 3957, 75 pp. July 17, 2020

Eomakhaira molossus, A New Saber-Toothed Sparassodont (Metatheria: Thylacosmilinae) from the Early Oligocene (?Tinguiririan) Cachapoal Locality, Andean Main Range, Chile

RUSSELL K. ENGELMAN,[1] JOHN J. FLYNN,[2] ANDRÉ R. WYSS,[3] AND DARIN A. CROFT[4]

ABSTRACT

Thylacosmiline sparassodonts (previously recognized as thylacosmilids) are among the most iconic groups of endemic South American Cenozoic mammals due to their distinctive morphology and convergent resemblance to saber-toothed placental carnivores. However, the early evolution of this group and its relationship to other sparassodonts remains poorly understood, primarily because only highly specialized Neogene taxa such as *Thylacosmilus*, *Anachlysictis*, and *Patagosmilus* are well known. Here, we describe a new Paleogene sparassodont, *Eomakhaira molossus*, from the Cachapoal locality of central Chile, the first sparassodont reported from early Oligocene strata of the Abanico Formation. *Eomakhaira* shares features with both Neogene thylacosmilines and Paleogene "proborhyaenids," and phylogenetic analyses recover this taxon as sister to the clade of *Patagosmilus* + *Thylacosmilus*. This broader clade, in turn, is nested within the group conventionally termed Proborhyaenidae. Our analyses support prior hypotheses of a close relationship between thylacosmilines and traditionally recognized proborhyaenids and provide the strongest evidence to date that thylacosmilines are proborhyaenids (i.e, the latter name as conventionally used refers to a paraphyletic group). To reflect the internestedness of these taxa, we

[1] Department of Biology, Case Western Reserve University, Cleveland.
[2] Division of Paleontology and Richard Gilder Graduate School, American Museum of Natural History.
[3] Department of Earth Science, University of California, Santa Barbara.
[4] Department of Anatomy, Case Western Reserve University, Cleveland.

 ISSN 0003-0082

propose use of Riggs' (1933) original name Thylacosmilinae for the less inclusive grouping and Proborhyaenidae for the more inclusive one. Saber teeth arose just once among metatherians (among thylacosmilines), perhaps reflecting a developmental constraint related to nonreplacement of canines in metatherians; hypselodonty may have relaxed this potential constraint in thylacosmilines. The occurrence of *Eomakhaira* in strata of early Oligocene age from the Chilean Andes demonstrates that the stratigraphic range of thylacosmilines spanned almost 30 million years, far surpassing those of saber-toothed placental lineages.

INTRODUCTION

The Sparassodonta, an extinct group of metatherians (marsupials and their extinct relatives), were the dominant group of carnivorous mammals in South America from the early Paleocene (Tiupampan South American Land Mammal "Age," or SALMA; Muizon, 1998; Muizon et al., 2018) to the late early Pliocene (Chapadmalalan SALMA; Goin and Pascual, 1987; Prevosti et al., 2013), sharing the ecological role of large terrestrial predator with phorusrhacid birds (Degrange et al., 2012; Tambussi and Degrange, 2013) and sebecid crocodyliforms (Pol et al., 2012; Molnar and Vasconcellos, 2016) during the continent's long Cenozoic isolation. Sparassodonts occupied many of the niches filled by placental carnivorans and "creodonts" on other continents and often strongly converged with these groups in morphology (Argot, 2004a; Prevosti et al., 2012; Forasiepi et al., 2015). Perhaps the best-known example of this phenomenon is the Thylacosmilinae (Thylacosmilidae of most previous authors), a group of sparassodonts whose striking morphological resemblance to placental sabertooths (Argot, 2004b; Wroe et al., 2013) literally makes them a textbook example of convergent evolution (Futuyma, 1998; Zimmer, 2009).

Thylacosmilines, as traditionally conceived, are characterized by numerous autapomorphies relative to other sparassodonts, including hypselodont (ever-growing) upper canines (Riggs, 1934), a highly reduced incisor series that may have been essentially nonfunctional (Churcher, 1985; Goin and Pascual, 1987), loss of one premolar locus (thought to be the first upper and lower premolar; Forasiepi and Carlini, 2010), retention of the deciduous upper third premolar into adulthood (Goin and Pascual, 1987; Forasiepi and Sánchez-Villagra, 2014), and a highly distinctive basicranium with a compound squamosal/exoccipital bulla, no alisphenoid tympanic process, no external opening for the primary jugular foramen, and large paratympanic spaces (Turnbull and Segall, 1984; Forasiepi et al., 2019). Several of these features appear to be related to a "sabertooth" mode of life, while others occur in various other groups of sparassodonts (i.e., some basicranial features are shared with either hathliacynids or borhyaenoids; Forasiepi et al., 2019), complicating attempts to phylogenetically place thylacosmilines within Sparassodonta. This may reflect the fact that most well-known thylacosmilines come from geologically young deposits (middle Miocene to early Pliocene; Riggs, 1934; Goin and Pascual, 1987; Goin, 1997; Forasiepi and Carlini, 2010) and hence exhibit high numbers of apomorphies not present in non-thylacosmilines.

Both the early evolutionary history of thylacosmilines and the origins of their distinctive saber-toothed morphology remain poorly understood. Phylogenetic analyses indicate that most

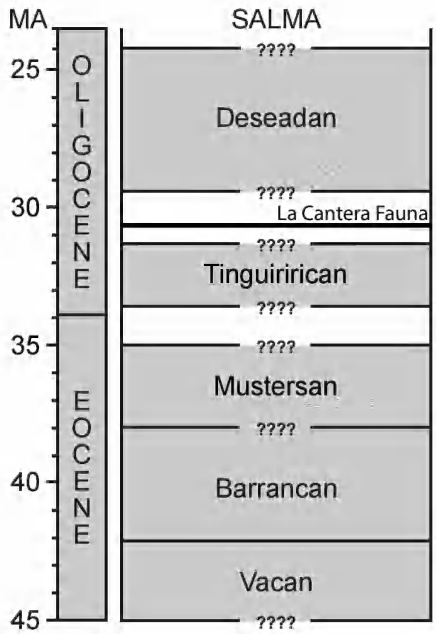

FIG 1. Middle Eocene to Oligocene South American Land Mammal "Ages" (SALMAs). The Tinguiririca or "pre-Deseadan"–aged La Cantera Fauna is represented as a thin bar, as it is thought to represent a very short interval of geologic time (<150 ka; Dunn et al., 2013). Figure modified from Croft et al. (2008b) based on data in Ré et al. (2010), Flynn et al. (2012), Dunn et al. (2013), and Krause et al. (2017).

major Neogene sparassodont lineages, including hathliacynids, borhyaenids, and thylacosmilines, diverged from their nearest relatives prior to the late middle Eocene (e.g., Babot et al., 2002; Babot, 2005; Forasiepi, 2009; Engelman and Croft, 2014; Forasiepi et al., 2015; Suarez et al., 2016; Muizon et al., 2018), but representatives of these groups are unknown prior to the late Oligocene (but see Lorente et al., 2016). The early Oligocene record, in particular, is essential for clarifying whether these long ghost lineages result from poor taxonomic sampling or are an artifact of insufficient sampling of morphological characters in character-taxon matrices.

Unfortunately, the early Oligocene is among the most poorly sampled intervals in the evolutionary history of sparassodonts. Several authors have remarked on the near-absence of sparassodont remains from the earliest Oligocene Tinguiririca SALMA (López-Aguirre et al., 2017; Croft et al., 2018; Prevosti and Forasiepi, 2018) (fig. 1). As of this writing only two specimens have been identified from this interval: a fragmentary upper molar of an extremely small (*Pseudonotictis*-sized) species (Goin et al., 2010; R.K.E., personal obs.), and an isolated premolar of a larger taxon (Goin et al., 2010), both from the La Cancha Fauna of Gran Barranca (Chubut, Argentina). A third specimen, a left dentary tentatively assigned to the borhyaenoid *Pharsophorus lacerans*, has been described from slightly higher early Oligocene levels (La Cantera) at Gran Barranca (Goin et al., 2010). These strata, which postdate the Tinguiririca SALMA and predate the Deseadan SALMA (Ré et al., 2010; Dunn et al., 2013), are informally referred to as the "Canteran" interval (Madden et al., 2010; Dunn et al., 2013) (fig. 1).

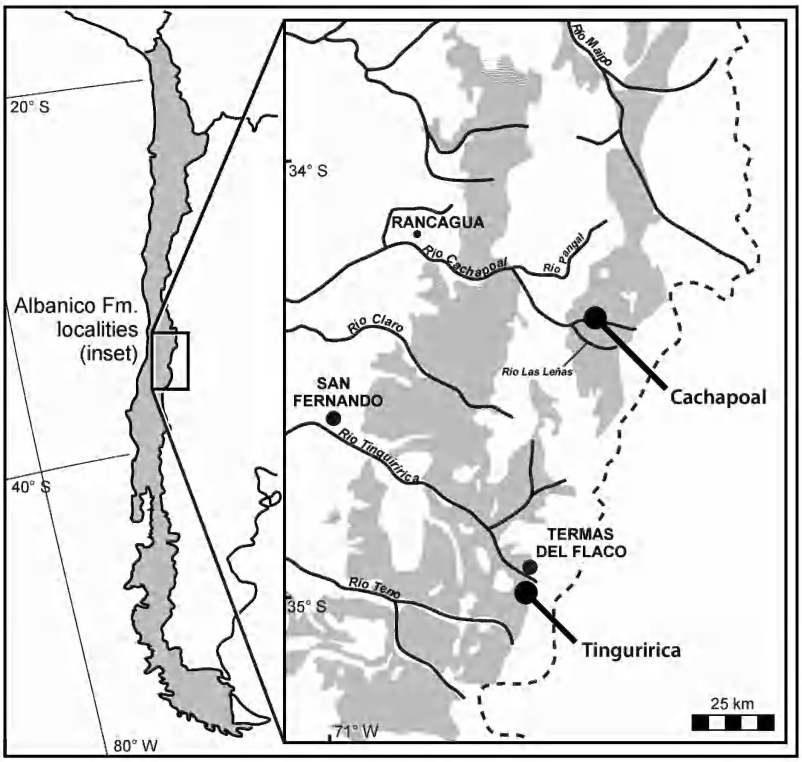

FIG 2. Locations of the Cachapoal locality and the similar-aged (likely coeval) Tinguiririca locality in central Chile. Gray area in inset box represents outcrops of the Abanico Formation.

Here we describe a new sparassodont taxon based on a specimen recovered from the upper Cachapoal River drainage in the Andean Main Range of central Chile, approximately 100 km SSE of Santiago (fig. 2). Taxa recovered from Cachapoal are regarded as Tinguiririca in age based on biochronologic evidence (Hitz et al., 2006; Croft et al., 2008a; Flynn et al., 2012; West et al., 2014), making this the first Oligocene sparassodont to be described from Chile, and only the second to be described from the many diverse faunas of the Abanico Formation (after the late Eocene *Chlorocyon phantasma*; Engelman et al., 2018). This specimen, SGOPV 3490, consists of the anterior portion of the skull of a senescent individual and is the most complete early Oligocene sparassodont known. SGOPV 3490 shows several morphological similarities to thylacosmiline sparassodonts, and phylogenetic analyses indicate that it likely represents an early member of the group.

Materials and Methods

The sparassodont from Cachapoal described here, SGOPV 3490, is preserved in highly indurated volcaniclastic matrix, as is the norm for mammal fossils from the Abanico Formation. Following mechanical preparation, the specimen was scanned at the PaleoCT facility at the University of Chicago using a μCT scanner (GE Phoenix v/tome/x 240kv/180kv scanner)

to elucidate additional details of its morphology. The specimen was scanned at 180 kV and 150 μA with 0.5 mm Cu beam filter, producing a scan of 2021 slices with a voxel size of 0.058 mm. The specimen could not be segmented through automated thresholding due to extreme beam hardening and poor differentiation between rock and bone. As a result, segmentation was completed manually in Amira 5.3.3 (Visage Imaging Inc.). The specimen was visualized in Avizo 7.0.0 (Visualization Science Group) and Dragonfly 2.0 (Object Research Systems Inc.), and the latter was also used for measurements. Rotational movies of the segmented 3D model of this specimen are available as part of the online supplementary information (doi. org/10.5531/sd.sp.41).

Data and measurements of other taxa are based on direct observation by R.K.E. or were taken from the primary literature. A complete list of specimens and references used for comparison is provided in appendix 1.

Saber teeth have evolved repeatedly among carnivorous mammals other than thylacosmiline sparassodonts, most famously in machairodontine felids but also in barbourofelid and nimravid carnivoramorphans as well as machaeroidine "creodonts" (which are probably members of Oxyaenidae; see Zack, 2019a). To avoid confusion, the term "sabertooth" is used here to refer to any carnivorous mammal with large, "saberlike" upper canines (saber teeth), whereas saber-toothed members of the Felidae are specifically referred to as "machairodontines." The term "machairodonty" is used to refer to the saber-toothed condition and the associated morphological complex (Emerson and Radinsky, 1980; Antón, 2013), paralleling terminology used for other specialized craniodental morphologies (e.g., plagiaulacoidy, diprotodonty, hypselodonty).

Proborhyaenid (including thylacosmiline) sparassodonts are unusual among metatherians in having open-rooted, ever-growing (hypselodont) canines (Riggs, 1934; Simpson, 1948; Babot et al., 2002). However, some specimens suggest that canine roots closed and growth ceased in extreme senescence (i.e., MLP 79-XIII-18-1; see Bond and Pascual, 1983; Babot et al., 2002). Here, a tooth is regarded as hypselodont if it continued to grow and its roots remained open into the animal's adult lifespan. This definition mirrors the one used for notoungulates, in which taxa are considered hypselodont if their teeth are open rooted and ever-growing in adults but closed in extreme senescence (e.g., *Adinotherium*, *Nesodon*, and *Trachytherus*; Billet et al., 2008; Cassini et al., 2012, 2017).

The body mass of the new taxon described here was estimated using two methods: (1) lower molar row length (Lm1–4) using the dasyuromorphian regression equation of Myers (2001); and (2) length of m3, using the dasyurid regression equation of Gordon (2003). The first of these equations is the one most closely correlated with body size (i.e., it has the lowest percent prediction error) among the equations of Myers (2001) that can be applied to SGOPV 3490; the second was considered by Zimicz (2012) and Forasiepi et al. (2015) to be the best predictor of body mass in sparassodonts. Although the accuracy of these regression equations for estimating body mass in sparassodonts has been questioned due to extrapolation issues (most sparassodonts are far larger than any living carnivorous marsupial; Forasiepi et al., 2015), the taxon described here is small enough to cluster among the extant species used to construct the regression equation.

Phylogenetic Analysis

To establish the affinities of *Eomakhaira*, we carried out a phylogenetic analysis based primarily on the comprehensive matrix of Suarez et al. (2016), which is the most taxon-rich analysis of relationships within Sparassodonta to date. We augmented this base matrix with character and character-state data from Muizon et al. (2018). Features difficult to score in SGOPV 3490 because of poor preservation or substantial wear were coded as uncertain (i.e., "0/1"). The proborhyaenid *Proborhyaena gigantea* was added to the matrix to elucidate relationships within Proborhyaenidae; MLP 79-XII-18-1 (a specimen referred to *P. gigantea* by Bond and Pascual, 1983) was not included in this coding due to its uncertain taxonomic status (see Babot et al., 2002, and comments on this specimen below). *Vincelestes neuquenianus* was included in the analysis because TNT requires an a priori outgroup (Goloboff, 2009) and the branching sequence of plausible outgroups to Marsupialiformes (e.g., *Holoclemensia*, Deltatheroida, and Eutheria) is debated (see discussion in Beck, in press). A complete list of changes from Suarez et al. (2016) and Muizon et al. (2018), as well as the phylogenetic matrix used in this study in NEXUS format, is provided in the online supplementary information (doi.org/10.5531/sd.sp.41).

Dasyuromorphian taxa (*Dasyurus*, *Sminthopsis*, and *Thylacinus*) were constrained to form a monophyletic group in this study to avoid potential recovery of Sparassodonta within Dasyuromorphia, a problem encountered in previous studies (Forasiepi, 2009; Engelman and Croft, 2014; Forasiepi et al., 2015; Suarez et al., 2016). This problem is likely due to long branch attraction, limited outgroup sampling, and convergent evolution between *Thylacinus* and Sparassodonta. Most of the features shared between *Thylacinus* and Sparassodonta are apomorphies for *Thylacinus* within Dasyuromorphia (and thus do not characterize dasyuromorphians or thylacinids more broadly; Yates, 2014; Kealy and Beck, 2017; Rovinsky et al., 2019) and/or are associated with dietary habits (carnivory) and therefore potentially more homoplastic (Muizon and Lange-Badré, 1997).

The character-taxon matrix was compiled in Mesquite (Maddison and Maddison, 2008) and analyzed in TNT 1.1 (Goloboff et al., 2008) under equal weights, implied weights with a default concavity constant of k = 3, and implied weights with a higher concavity constant of k = 12, following suggestions that higher concavity constants produce more accurate results with larger datasets (Goloboff et al., 2018). Because the use of implied weighting in phylogenetics has been criticized (e.g., Congreve et al., 2016; Madzia and Cau, 2017; but see Goloboff et al., 2018), we used it primarily to evaluate support for hypotheses recovered using equal weights (i.e., topologies recovered using both methods were considered to be more robustly supported than topologies recovered via only one method). Tree analyses were performed in TNT using the "New Technology search" option, applying sectorial search, ratchet, tree drift, and tree fuse options under default parameters, finding the minimum length 1000 times and then searching within the set of recovered trees using tree bisection reconnection branch swapping.

Anatomical Abbreviations: Upper and lower incisors, canines, premolars, and molars are designated as I/i, C/c, P/p, and M/m.

INSTITUTIONAL ABBREVIATIONS: **AC**, Beneski Museum of Natural History, Amherst; **AMNH**, American Museum of Natural History, New York; **CMNH**, Cleveland Museum of Natural History, Cleveland; **CORD-PZ**, Museo de Paleontología, Facultad de Ciencias Exactas, Físicas y Naturales de la Universidad Nacional de Córdoba, Córdoba, Argentina; **FMNH**, the Field Museum, Chicago; **IGM**, Instituto Nacional de Investigaciones Geológico-Mineras, Bogotá, Colombia; **MACN-A**, Ameghino collection, Museo Argentino de Ciencias Naturales "Bernardino Rivadavia," Buenos Aires, Argentina; **MACN-PV**, vertebrate paleontology collection, Museo Argentino de Ciencias Naturales "Bernardino Rivadavia," Buenos Aires, Argentina; **MHNT**, Museu de História Natural de Taubaté, Taubaté, Brazil; **MLP**, Museo de La Plata, La Plata, Argentina; **MMP**, Museo Municipal de Ciencias Naturales de Mar del Plata, Mar del Plata, Argentina; **MNHN**, Muséum national d'Histoire naturelle, Paris, France; **MNHN-Bol**, Museo Nacional de Historia Natural, La Paz, Bolivia; **MNRJ**, Museu Nacional e Universidade Federal do Rio de Janeiro, Rio de Janeiro, Brazil; **MPEF-PV**, Museo Paleontológico Egidio Feruglio, Trelew, Argentina; **MUSM**, Museo de Historia Natural de la Universidad Nacional Mayor San Marcos, Lima, Peru; **PVL**, Paleontología Vertebrados Lillo, Tucumán, Argentina; **SGOPV**, vertebrate paleontology collections, Museo Nacional de Historia Natural, Santiago, Chile; **TMM**, Texas Memorial Museum, Austin; **UATF-V**, Universidad Autónoma Tomás Frías, Potosí, Bolivia; **UCMP**, University of California Museum of Paleontology, Berkeley, California; **UF**, Florida Museum of Natural History, University of Florida, Gainesville; **UNPSJB PV**, vertebrate paleontology collection, Universidad Nacional de La Patagonia San Juan Bosco, Comodoro Rivadavia, Argentina; **YPFB Pal**, paleontology collection, Yacimientos Petrolíferos Fiscales de Bolivia in the Centro de Tecnología Petrolera, Santa Cruz, Bolivia; **YPM-VPPU**, Princeton University Collection, Yale Peabody Museum, New Haven.

SYSTEMATIC PALEONTOLOGY

MAMMALIA Linnaeus, 1754

METATHERIA Huxley, 1880

SPARASSODONTA Ameghino, 1894

BORHYAENOIDEA Simpson, 1930

PROBORHYAENIDAE Ameghino, 1897

PHYLOGENETIC DEFINITION: Proborhyaenidae refers to all sparassodonts more closely related to *Proborhyaena gigantea* than to *Borhyaena tuberata*, *Prothylacynus patagonicus*, *Lycopsis torresi*, *Cladosictis patagonica*, or *Sipalocyon gracilis*. This is a stem-based definition (de Queiroz and Gauthier, 1990).

THYLACOSMILINAE Riggs, 1933

PHYLOGENETIC DEFINITION: Thylacosmilinae refers to all sparassodonts more closely related to *Thylacosmilus atrox* than to *Proborhyaena gigantea*, *Borhyaena tuberata*, *Prothyla-*

cynus patagonicus, *Lycopsis torresi*, *Cladosictis patagonica*, or *Sipalocyon gracilis*. This is a stem-based definition (de Queiroz and Gauthier, 1990).

COMMENTS: Riggs (1933) originally coined the term Thylacosmilinae as a subfamily of Borhyaenidae. Marshall (1976a) raised Thylacosmilinae to family rank (Thylacosmilidae) based on the morphological disparity between this group and other sparassodonts (borhyaenoids of this author), an opinion generally followed by subsequent authors (e.g., Churcher, 1985; Goin and Pascual, 1987; Marshall et al., 1990; Muizon, 1999; Babot et al., 2002; Argot, 2004b; Forasiepi and Carlini, 2010; Wroe et al., 2013; Croft et al., 2018; Muizon et al., 2018; Prevosti and Forasiepi, 2018; and references therein). The distinctiveness of thylacosmilines relative to other sparassodonts has been recognized even by the most extreme taxonomic lumpers, such as Simpson (1945, 1948), who accepted thylacosmilines as distinct but grouped all other sparassodonts within another subfamily, Borhyaeninae. More recently, several phylogenetic analyses, including the present study, have recovered thylacosmilids as deeply nested within Proborhyaenidae (Babot, 2005; Forasiepi et al., 2015; Suarez et al., 2016; Muizon et al., 2018). To avoid having a group bearing a "family level" name (in traditional taxonomy) nested within another family (i.e., Thylacosmilidae nested within Proborhyaenidae) it is necessary to either elevate Proborhyaenidae to Proborhyaenoidea (phylogenetically defined names are rankless) or demote Thylacosmilidae to Thylacosmilinae. We choose the latter option, to follow the initial conceptualization and taxonomy of Riggs (1933; 1934), to avoid the problematic inclusion of a newly elevated Proborhyaenoidea within Borhyaenoidea, and to minimize taxonomic disruption to long-standing naming of many other taxa, such as proborhyaenids. We note that groups of placental saber-toothed carnivores apply similar usage of traditional taxonomic name suffixes, with saber-toothed forms (e.g., Machaeroidinae and Machairodontinae) each within a clade including both them and their non-saber-toothed close relatives (Oxyaenidae and Felidae, respectively).

Eomakhaira molossus, gen. et sp. nov.

Figures 3–4, 6–16; tables 1–2

HOLOTYPE: SGOPV 3490, a partial rostrum of a senescent individual preserving the right maxilla with C-P3, alveoli and partial roots of M1–2, and part of M3; left maxilla with C-P3, anterior root of M1, and M3–4; left and right horizontal rami of the mandible, including both lower canines and most of the postcanine dentition, as well as parts of the coronoid processes; the entire left and parts of the right nasal; parts of the palatine; and the orbital process of the left lacrimal.

DIAGNOSIS: A member of Borhyaenoidea based on its short, robust rostrum, presence of lingual median canine sulci, extremely small protocone, small and unicuspid talonid on m4. Differs from all other borhyaenoid sparassodonts in the following combination of features: small size (smaller than most other borhyaenoids; length of m1–4 = 37.3 mm, comparable to *Fredszalaya hunteri* or the extant dasyuromorphian *Sarcophilus harrisii*); maxilla very deep and maxillary "cheeks" absent; mandibular symphysis unfused and anteroposteriorly narrow; two mental foramina present; length/width ratio of palate >1.5; palate extending to level of M4;

presence of postpalatine tori (shared only with *Arminiheringia* and possibly *Callistoe* among borhyaenoids); absence of postpalatine torus foramen; sphenorbital foramen opening dorsal to M4; large canines; absence of longitudinal striations on the canine roots (shared only with other thylacosmilines and possibly *Lycopsis viverensis*); median keel on the labial face of upper canines; medial sulcus on lingual face of upper and lower canines; short lower canine roots; presence of three premolars with no diastemata between them; premolars large and robust but not globular; asymmetric protoconid of P1 (shared only with *Arminiheringia* and *Callistoe*); P3 significantly longer than p3 (possibly autapomorphic for this taxon); bulbous roots only on p3; preparacingulum absent; M3 with narrow stylar shelf and prominent ectoflexus; M4 extremely narrow anteroposteriorly (only comparable to *Patagosmilus* among borhyaenoids), subequal or greater in width to M3, and with three roots; protocone vestigial (at least on M4); absence of an anteriorly projecting ventral keel of paraconid (which only occurs in proborhyaenids among sparassodonts); protoconid of m4 posteriorly salient; metaconid absent on m4 and probably m2–3; posterolabial cingulid present; talonid of m4 almost absent; and p1–3 short relative to m1–4 (shared with *Paraborhyaena* among borhyaenoids with three premolars). Canines more mediolaterally compressed than in borhyaenoids other than *Patagosmilus*, *Thylacosmilus*, and possibly *Proborhyaena*. P/p3 labiolingually narrower than in *Fredszalaya*, *Plesiofelis*, *Acrocyon*, *Arctodictis*, *Australohyaena*, *Borhyaena*, and *Callistoe*, but wider than in *Prothylacynus* and some individuals of *Pharsophorus*, comparable in relative proportions to *Arminiheringia*, *Paraborhyaena*, and *Proborhyaena*.

Type Locality: Cachapoal locality, west side of Estero Los Llanos of the upper Río Cachapoal drainage, Libertador General Bernardo O'Higgins Region, central Chile (fig. 2).

Stratigraphic Occurrence: Abanico Formation. Most specimens from Estero Los Llanos were recovered from talus cones at the SE nose of a roughly N-S running ridge of ~1,500 m relief. This ridge roughly parallels the strike of the steeply west-dipping beds. The thickness of the Abanico Formation in the Cachapoal region has not been measured in detail but is on the order of 2000–4000 m. Within this thick succession, the exact horizon that produced SGOPV 3490 is not known, as the specimen was collected from talus. For additional geological context of the Cachpaoal locality see Flynn and Wyss (2004), Hitz et al. (2006), and West et al. (2014).

Age: Probably early Oligocene, ?Tinguiririan SALMA. Fossils from the Cachapoal locality are likely at least 29.3 ± 0.1 million years old (at least in part), based on an unpublished date for a volcanic tuff that is thought to either correlate with or overlie the fossil-producing horizons at Los Llanos (Charrier et al., 1997; Flynn and Wyss, 2004). It must be cautioned, however, that this date is from ~5 km to the south, in the neighboring Las Leñas drainage, and that the units involved have not been traced directly between the two locations due to precipitous intervening topography. The only radioisotopic date for the Cachapoal Valley itself is an $^{40}Ar/^{39}Ar$ date of 11.1 ± 1.8 Ma reported by West (2017) from levels far above the fossil-producing strata, which does little to precisely constrain the age of the fossils. The presence of the polydolopid *Kramadolops* (*Polydolops* in Flynn and Wyss, 2004) and the archaeohyracid *Archaeotypotherium* (Croft et al., 2008a) suggest a pre-Deseadan age, and the presence of the interathere *Johnbell hatcheri*, otherwise known only from the Tinguiririan type locality (Hitz

et al., 2006), suggests that fossils from the Cachapoal locality are probably similar in age to those of the Tinguiririca Fauna (~33–32 Ma; Flynn et al., 2003).

ETYMOLOGY: The name of the genus derives from the Greek root *Eos*, meaning "dawn," and *makhaira*, a type of short sword or large knife (often translated as "carving knife"), in reference to the bladelike canines of thylacosmilines. The specific epithet comes from the Greek *molossus*, a term used to refer to short-snouted, robust-skulled dog breeds such as mastiffs and bulldogs and refers to the short, robust snout of this species. Gender is masculine.

DESCRIPTION

SGOPV 3490 is uncharacteristically poorly preserved compared to most fossils described from the Abanico Formation (fig. 3). The specimen was altered syn- or postdepositionally through the actions of heat, fluids, or both, resulting in the thinning or elimination of much of the bone. The density contrast between the volcaniclastic matrix and specimen is low, making it difficult to distinguish rock from bone with the naked eye as well as via CT imagery. Many portions of the specimen were damaged or destroyed during deposition or diagenesis, leaving many surviving elements isolated but "floating" in matrix in near-life position, as has been described for some other specimens from the Abanico Formation (McKenna et al., 2006). For example, the left lower molar row of SGOPV 3490 is preserved in life position, but much of the mandibular ramus is absent labially. Intact toothrows preserved in the absence of bone are occasionally recovered from the Abanico Formation. These specimens may reflect high temperatures or corrosive fluids in the lahar or pyroclastic flow in which the specimens were deposited or subsequent diagenetic processes (the Abanico Formation is locally hydrothermally altered). The specimen also shows clear signs of postmortem crushing and distortion, particularly on the left side, where elements of the skull show signs of breakage and have been displaced anteriorly. By contrast, the right side of the specimen is nearly undistorted; the upper and lower teeth are nearly in occlusion, and the maxilla and mandible show no signs of crushing.

Anatomical positions and directions can be difficult to consistently establish and apply to SGOPV 3490. Many landmarks typically used for orientation (e.g., the alveolar border of the postcanine toothrow or the ventral edge of the dentary) sometimes provide conflicting orientations; orienting the skull based on one landmark results in physically impossible orientations for others (see below). Assuming that the fragments of the palate indicate the horizontal plane and that the roots of several postcanine teeth (P2–3, m1–3) approximate the vertical plane, the canines were procumbent and the lower molar rows were inclined to a degree similar to that observed in other sparassodonts (e.g., *Arctodictis*, *Arminiheringia*, *Australohyaena*, *Callistoe*, some individuals of *Thylacosmilus*). Determining the orientation of the rostrum in *Eomakhaira* more securely would require a more complete or less distorted specimen.

SGOPV 3490 represents a highly senescent individual, as extreme tooth wear obscures much of its dental morphology. The canines are extremely blunt, even compared to many other sparassodonts, with the apices of both the upper and lower canines nearly rounded.

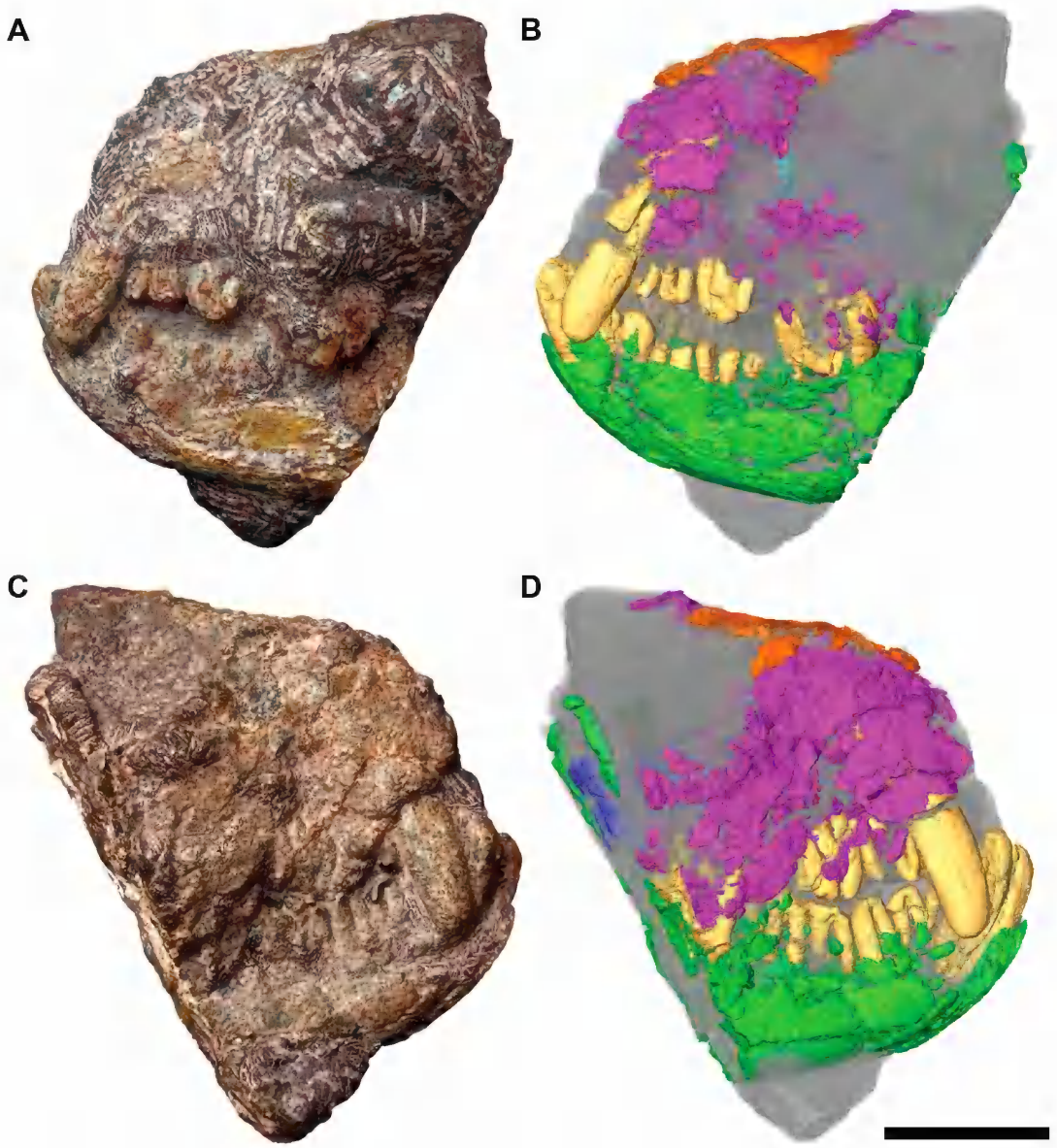

FIG 3. **A**, **C,** Photographs and **B**, **D,** CT segmentation of the holotype of *Eomakhaira molossus*, a partial skull of a senescent individual preserving the rostrum and the anterior portion of the mandible (SGOPV 3490) in left (A, B) and right (C, D) lateral views. In renderings of the CT segmentation, nasal in orange, facial process of the lacrimal in teal, palatine in blue, all other bones of the cranium (maxilla, jugal, frontal, etc.) in purple, teeth in yellow, and dentary in green. Anterior to left in A–B and to right in C–D. Scale = 30 mm.

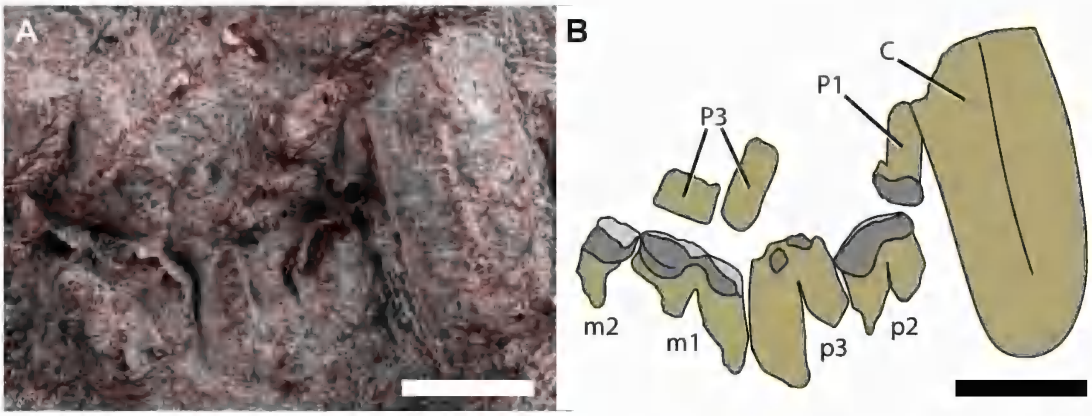

FIG 4. **A,** Photograph and **B,** line drawing of the exposed right upper canine and postcanine dentition of SGOPV 3490, showing their extreme wear. In B, enamel is denoted in dark grey, dentine in brown, and wear surfaces by light grey. The morphology of these teeth is not entirely visible, as much of the occluded upper and lower jaws of the specimen remain encased in matrix (compare with figs. 3 and 9). Scale = 10 mm.

Most of the postcanine dentition is also heavily worn. The main cusp of the left p2 is worn nearly flat, and the occlusal morphology of the right M3 is largely obliterated by wear. The entire crown of the right P3 is worn away, and its roots are in direct occlusion with the lower dentition (fig. 4). The occlusal surfaces of the right m1 and the trigonid of right m2 are virtually flat due to wear. Obliteration of the occlusal morphology of m2 indicates that this specimen pertains to a senile individual (sensu dental age stages of Anders et al., 2011). Even M4, typically the least worn and last tooth to erupt in sparassodonts (Forasiepi and Sánchez-Villagra, 2014; Engelman et al., 2015), exhibits well-developed wear facets in SGOPV 3490. The dentition of SGOPV 3490 is obviously heavily worn through use rather than postmortem abrasion, as the posterior face of P3 and the trigonid of m1 almost occlude and have perfectly matching wear facets. Heavy wear obscures some important morphological details and makes it difficult to determine whether certain features typify the species or are only wear related.

Cranium

The maxilla of SGOPV 3490 is proportionally deeper than in most other sparassodonts, including the robust-skulled proborhyaenids *Arminiheringia* and *Callistoe* and borhyaenid *Arctodictis sinclairi* (fig. 5, table 1). Only *Australohyaena antiquua*, *Arctodictis munizi*, and *Thylacosmilus atrox* have relatively deeper maxillae among the taxa analyzed. A small portion of the dorsal border of the infraorbital foramen is preserved in SGOPV 3490 (fig. 3), indicating that this structure opened dorsal to the P3/M1 embrasure, as in *Patagosmilus*, *Thylacosmilus*, and *Australohyaena* but unlike in: (1) the Eocene taxa *Callistoe* and *Arminiheringia*, in which the infraorbital foramen opens above or anterior to the anterior root of P3; (2) *Borhyaena* and cf. *Proborhyaena* (MLP 79-XIII-18-1), in which the foramen opens slightly more anteriorly

TABLE 1. Measurements of the holotype of *Eomakhaira molossus* (SGOPV 3490) in mm. Greatest dorsoventral height of maxilla measured from alveolar border of P3 to dorsal border of maxilla. Although the outer portion of the maxilla is damaged at this level (see fig. 3), enough of the medial surface of the maxilla and premolar alveoli is preserved to be able to determine that P1–3 are in life position.

Greatest dorsoventral height of maxilla (right)	42.8
Greatest width of nasals (estimated as twice greatest width of right nasal)	24.8
Width of nasals at the level of the canines	6.24
Maximum width of palate between canines	22.9
Approximate width of palate at the level of the infraorbital foramen	28.0
Approximate maximum width of palate (at level of M3)	44.2
Length of C-M3 (approximate)	~49 (right)
Length of P1–3	20.3 (left), 19.5 (right)
Length of M1–3 (approximate)	~26.7 (right)
Length of c-m4	65.0 (right)
Length of p1–3	16.4 (left)
Length of m1–4	37.3 (right)
Length of symphysis	20.2
Depth of dentary below p3	21.2 (left), 21.6 (right)
Depth of dentary below m3	30.3 (right)
Estimated greatest depth of dentary below m4	31.8 (right)

over the posterior root of P3; and (3) species of *Arctodictis*, in which the foramen is more posterior (above or posterior to the posterior root of M1; Forasiepi, 2009).

Although the alveolar border of the maxilla posterior to the infraorbital foramen is fragmentary, the parts preserved suggest that *Eomakhaira* lacked maxillary "cheeks," i.e., protrusions of the maxilla posterior to the infraorbital foramen that extend lateral to the toothrow (best seen in ventral view). Maxillary "cheeks" are a highly variable feature within Sparassodonta. They are present in borhyaenids, *Prothylacynus*, and many hathliacynids but absent in most species of *Lycopsis* (except *L. torresi*), *Acyon*, *Patagosmilus*, and cf. *Proborhyaena* (MLP 79-XII-18-1). Contrary to some reports, maxillary "cheeks" appear to be absent in *Paraborhyaena* and *Thylacosmilus* (FMNH P14531, MLP 35-X-4-1, MMP 1443; see also Petter and Hoffstetter, 1983; Goin and Pascual, 1987). The state in *Arminiheringia* could not be determined based on available information.

Based on the posterior border of the left nasal (fig. S1), the two naso-frontal sutures of *Eomakhaira* form an angle of ~100° in dorsal view, greater than the acute-angled naso-frontal sutures of *Callistoe,* but narrower than those of *Paraborhyaena*, *Patagosmilus*, *Pharsophorus*, and borhyaenids. An internasal projection of the frontals is absent (i.e., the naso-frontal suture is V-shaped rather than W-shaped). The preserved lateral edge of the left nasal is straight, suggesting it represents the border of the naso-lacrimal suture, based on a

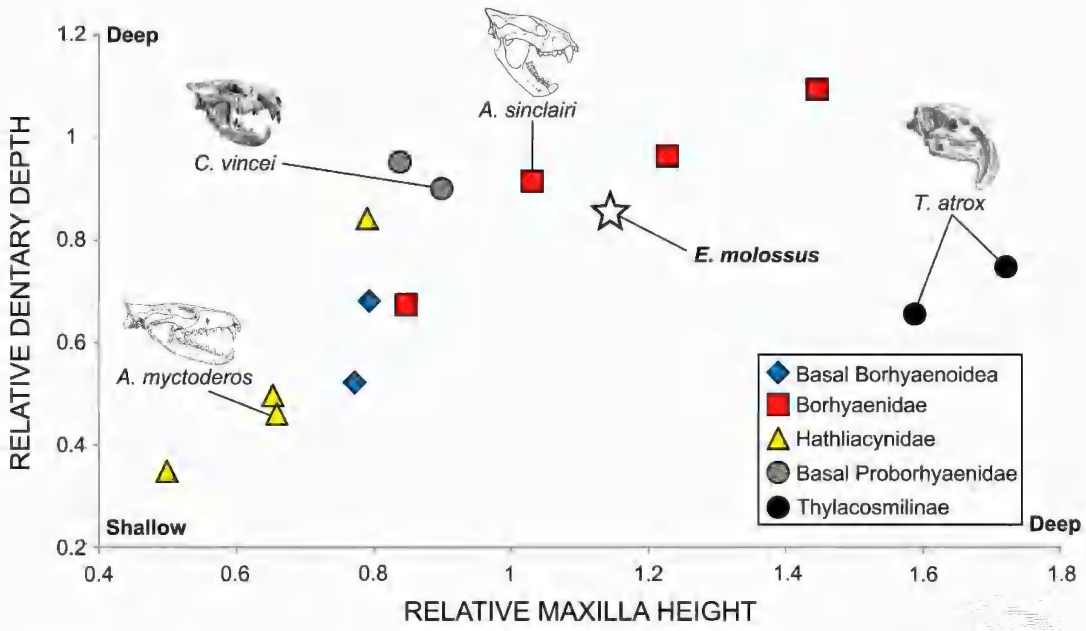

FIG 5. Relative maxilla height and dentary depth (measured at m3–4 embrasure) in sparassodont specimens for which both maxilla and dentary are known, scaled to lower molar row length. *Eomakhaira molossus* is denoted by a star. Skulls of several taxa are illustrated to highlight variation. Skulls of *Arctodictis sinclairi*, *Acyon myctoderos*, *Callistoe vincei*, and *Thylacosmilus atrox* modified from Forasiepi (2009), Forasiepi et al. (2006), Babot et al. (2002), and Riggs (1934), respectively. Data for this figure can be found in table S1.

similar morphology of this suture in other sparassodonts. As in *Callistoe*, a portion of the nasals may have extended onto the lateral surface of the snout, but this cannot be determined with certainty. The nasals are proportionally slender compared to the rest of the skull. Scaling the greatest width of the nasals to the length of M3, the nasals of *Eomakhaira* are narrower than in most borhyaenoids except *Callistoe*, *Patagosmilus*, and a juvenile specimen of *Prothylacynus patagonicus* (MACN-A 5931), and they are much narrower than the nasals of *Paraborhyaena*, *Arminiheringia*, *Patagosmilus*, and borhyaenids (table S2). The nasals of SGOPV 3490 are only about 25% as wide anteriorly as they are at their widest point. In borhyaenoids, this figure is typically ~30% (table S2), with the exception of *Callistoe*, in which the nasals vary less in width along their length (though this may be affected by mediolateral compression of the holotype). Nasal bones of the hathliacynids *Sipalocyon* and *Acyon* show less anterior tapering than in borhyaenoids apart from *Callistoe*, while the proportions of the nasals in *Cladosictis* more closely resemble those of borhyaenoids. Interestingly, the sparassodont UF 27881 from the middle Miocene of Quebrada Honda, Bolivia, originally described as a basal sparassodont (Engelman and Croft, 2014) but recovered as a borhyaenoid in later analyses (Forasiepi et al., 2015; Suarez et al., 2016) does not resemble borhyaenoids in its nasal proportions; rather, it is more similar to a specimen tentatively assigned to the basal sparassodont *Hondadelphys* (IGM 250364; Goin, 1997).

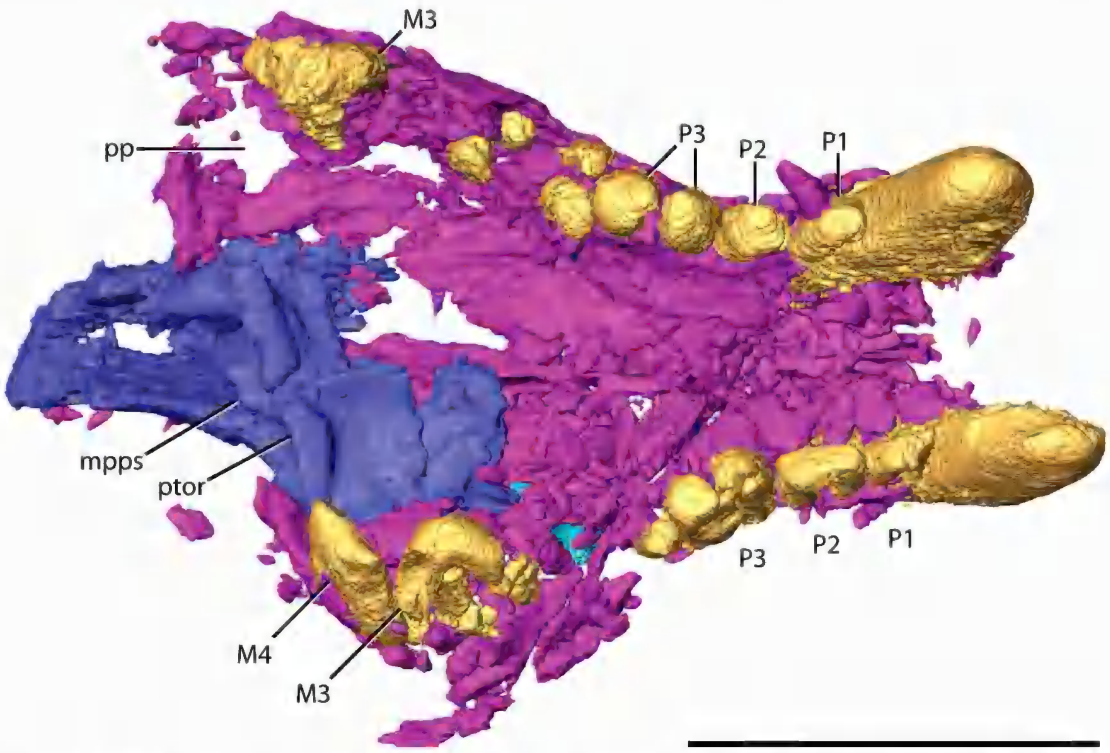

FIG 6. Cranium of the holotype of *Eomakhaira molossus* (SGOPV 3490) in palatal view. Anterior to right. Colors of elements in this CT segmentation are the same as in figure 3. Abbreviations: **mpps**, medial postpalatine spine; **pp**, palatal pit; **ptor**, palatine torus; dental abbreviations as in Materials and Methods. Scale = 30 mm.

The palate of SGOPV 3490 is fragmented and patchily preserved, but enough is present to establish that *Eomakhaira* lacked maxillopalatine fenestrae, as in other sparassodonts (fig. 6). The length/width ratio of the palatal process of the maxilla exceeds 1.5, even taking distortion into account, a value similar to most sparassodonts (with the exception of thylacosmilines and the borhyaenids *Australohyaena* and *Arctodictis*, in which the process is anteroposteriorly shorter and mediolaterally wider and the ratio is less than 1.5). A pair of palatal pits occurs on the palatal process of the maxilla between M3–4; whether an additional pair was present between M2–3 cannot be determined. Accounting for deformation, anterior displacement of the palatine, and the separation of the maxillary and palatine borders of the minor palatine foramen (see below), the horizontal process of the palatine does not appear to have extended posterior to M4, reminiscent of the condition in *Borhyaena*, *Patagosmilus*, and some specimens of *Prothylacynus*.

A pair of low palatine tori are present at the posterior end of the palate. These structures are mediolaterally broad, extending across each palatine bone, but do not contact one another medially (fig. 7). Among metatherians, sparassodonts are unusual in the general absence of a palatine torus, a feature also observed in deltatheroidans (Forasiepi, 2009; Bi et al., 2015), basal didelphids (caluromyines and *Glironia*; Voss and Jansa, 2009), and some dasyuromor-

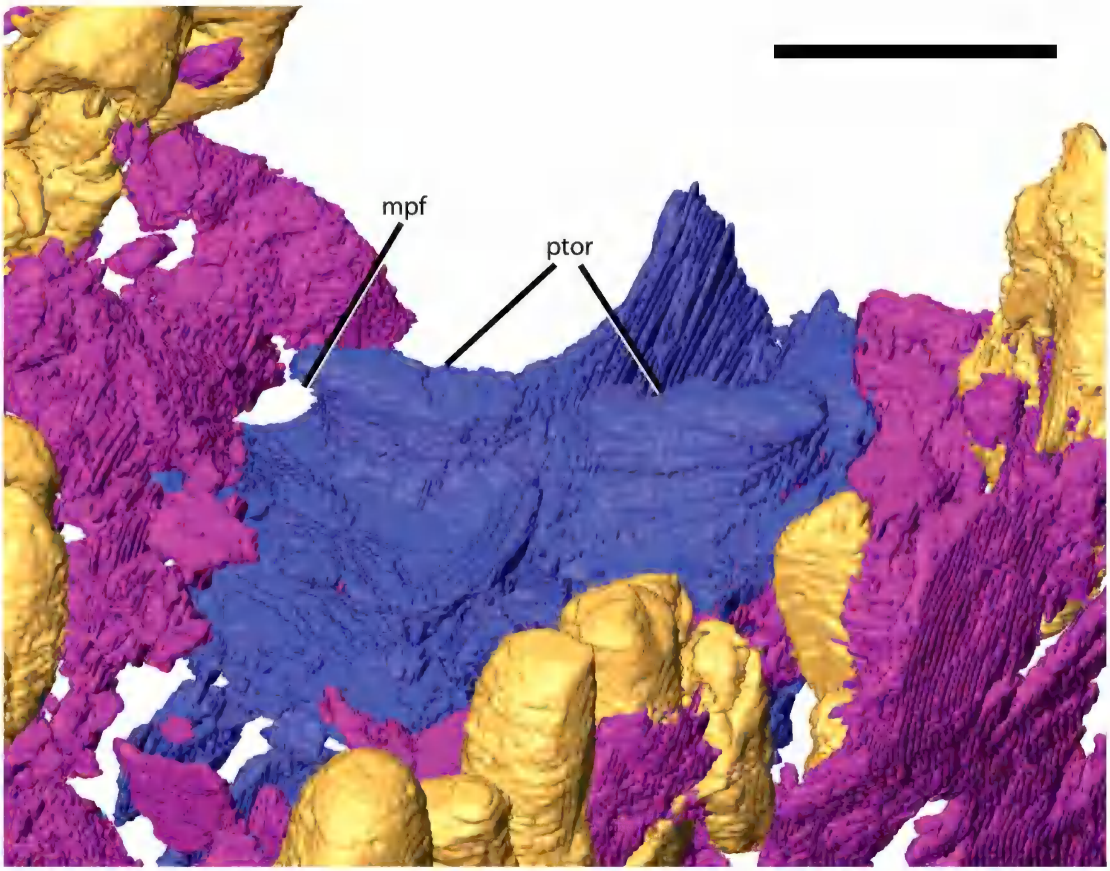

FIG 7. Posterior palate of the holotype of *Eomakhaira molossus* (SGOPV 3490), in oblique anterior view. Anterior to lower left. Shows the paired palatine tori and broken border of the minor palatine foramen. Colors of elements in this CT segmentation are the same as in figure 3. Abbreviations: **mpf**, minor palatine foramen; **ptor,** palatine tori. Scale = 10 mm.

phians (i.e., *Thylacinus*; Wroe, 1999; Warburton et al., 2019; R.K.E., personal obs.). In all of these taxa, the posterior border of the palate is typically single or double arched in ventral view (depending on the presence or absence of a medial postpalatine spine). Although most sparassodonts lack a palatine torus, in many (e.g., UF 27881, *Cladosictis*, *Sipalocyon*, *Borhyaena*, *Australohyaena*, *Arctodictis*, *Thylacosmilus*) the posterior border of the palate is slightly thickened. This thickening can be extremely pronounced (e.g., as in species of *Arctodictis*; Forasiepi et al., 2004; Forasiepi, 2009), but it follows the borders of the choanae rather than forming a straight torus. Other than *Eomakhaira,* the only sparassodonts with true palatine tori are the basal taxon *Allqokirus* and the proborhyaenids *Callistoe* and *Arminiheringia*. However, even in these taxa, the palatine tori do not resemble those of most other metatherians, wherein a straight palatine torus defines the posterior border of the palate. In *Allqokirus*, the palatine torus is well developed but is posteriorly concave rather than straight. *Callistoe* and *Arminiheringia* resemble *Eomakhaira* in having palatine tori that are mediolat-

erally oriented ridges at the back of the palate. Compared to the thickened choanal border of other sparassodonts, these structures are much more prominent in *Eomakhaira*, forming distinct processes that do not follow the borders of the choanae. However, unlike in other metatherians, the palatine tori in *Callistoe* and *Arminiheringia* do not form a single, complete torus; rather, they are paired structures that do not meet at the midline (except possibly in *Callistoe*) and do not constrict the choanae (i.e., in ventral view, the choanae still exhibit the classic "double arch" pattern typical of sparassodonts).

A small foramen occurs just lateral and slightly dorsal to the lateral edge of each palatine torus. It likely represents the minor palatine foramen (fig. 7) based on its position, though it is slightly damaged on both sides of the skull due to anterior displacement of the palatines. In *Eomakhaira*, the minor palatine foramen is located between the maxilla and the palatine, as in most metatherians, including many sparassodonts (including UF 27881, *Cladosictis*, *Arctodictis*, *Callistoe*, *Arminiheringia*, *Patagosmilus*, and some but not all specimens of *Thylacosmilus*). In *Callistoe* and *Arminiheringia*, as in *Eomakhaira*, the minor palatine foramen is dorsal to and slightly tucked under the lateral edge of the palatine torus. The minor palatine foramen is positioned more laterally in *Eomakhaira* than in other sparassodonts; in most sparassodonts, it is closer to the choanae than to the upper teeth, whereas in *Eomakhaira*, it is closer to the upper dentition. In this respect, *Eomakhaira* resembles *Patagosmilus* (but not *Thylacosmilus*). The minor palatine foramen of *Eomakhaira* is fairly large, more comparable in size to that of *Patagosmilus* than *Arminiheringia* or *Callistoe* (in which it is smaller). This foramen is clearly not the postpalatine torus foramen present in most groups of New World metatherians (Wible, 2003), as the homologous structure is either an open notch or absent in sparassodonts (Muizon et al., 2018). The postpalatine torus foramen opens directly posteriorly into the basipharyngeal canal in other metatherians, whereas the inferred minor palatine foramen of *Eomakhaira* opens posterolaterally into the orbitotemporal region (fig. 8), similar to the path of the minor palatine foramen of other sparassodonts. The postpalatine torus foramen appears to be absent in *Eomakhaira*, as it is in proborhyaenids (including thylacosmilines) and borhyaenids (Muizon et al., 2018).

SGOPV 3490 preserves a small portion of the orbital region, primarily on the left side. This consists of part of the ascending process of the palatine posteriorly and several isolated plates of bone separated by distinct gaps and holes that form part of the orbital wall anteriorly (fig. 8). Based on their position and morphology, these bone fragments likely represent parts of the orbital process of the lacrimal and the anterior part of the ascending process of the palatine. No clear suture is visible between the palatine and maxilla in lateral view. Based on size and location, these gaps may represent sutures and foramina that were enlarged postmortem by fragmentation of the fragile surrounding bone. The largest of these openings compares well to the sphenopalatine foramen in location. This foramen opens approximately dorsal to M4, as it does in some other borhyaenoids (borhyaenids, *Callistoe*, *Thylacosmilus*).

The anteriormost fragment of the orbital wall appears to represent a small portion of the orbital process of the lacrimal. Parts of the facial and zygomatic processes of the lacrimal

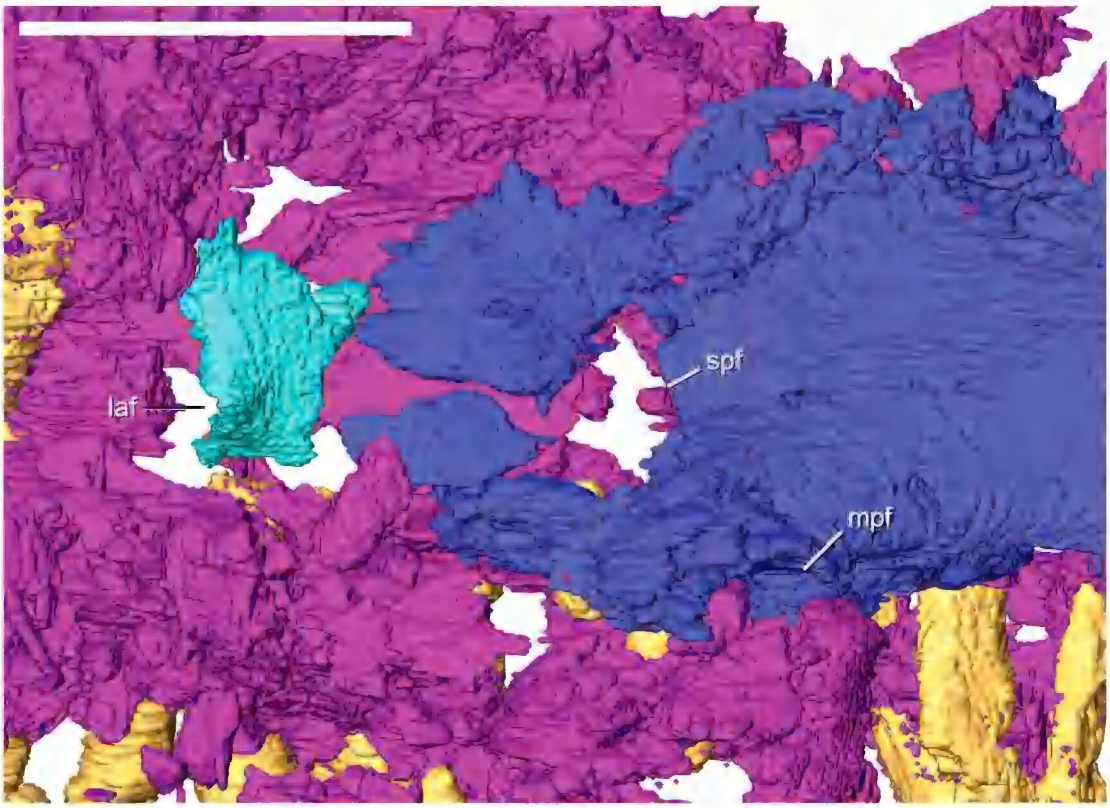

FIG 8. Left orbital region of the holotype of *Eomakhaira molossus* (SGOPV 3490) in oblique posterolateral view. Anterior to left. Colors of elements in this CT segmentation are the same as in figure 3. Abbreviations: **laf**, lacrimal foramen, **mpf**, minor palatine foramen; **spf**, sphenopalatine foramen. Scale = 30 mm.

may be present but cannot be distinguished from surrounding elements (i.e., maxilla). At the anterior end of the fragment of the orbital process is a small, partially preserved canal, likely the lacrimal foramen. Based on its position and surrounding elements, the lacrimal foramen appears to have opened within the orbit. Most sparassodonts have a single lacrimal foramen opening inside the orbit. However, in *Mayulestes*, *Allqokirus*, *Lycopsis padillai*, and *Arminiheringia* there are two lacrimal foramina, and in *Callistoe*, the lacrimal foramen number is polymorphic (Suarez et al., 2016; Muizon et al., 2018). Additionally, in *Allqokirus* and *Mayulestes*, one of the two lacrimal foramina is laterally exposed rather than enclosed within the orbit (Muizon et al., 2018). It is clear that at least one lacrimal foramen that opened within the orbit was present in SGOPV 3490, though the lacrimal foramen count is uncertain due to the limited preservation of this element.

SGOPV 3490 preserves parts of both jugals. On the left side, this element is represented by a fragmentary bone "floating" near the orbital region. Part of the right jugal also seems to be present, represented by small patches of bone (including parts of the rostrum formed by the jugal in other metatherians) and remnants of a marrow cavity dorsal to the upper molars. The shape and location of the maxillo-jugal suture cannot be determined.

Mandible

The mandible of *Eomakhaira* is robust and deep (fig. 9). It is comparatively shallower than the mandible of the proborhyaenids *Callistoe* and *Arminiheringia* (fig. 5, tables S1, S16) and deeper than in *Proborhyaena* and *Paraborhyaena*. The dentary is fractured parallel to the long axis of the horizontal ramus of the dentary, and these complementary fractures are displaced and infilled by matrix (fig. 9C, D). The thickness of these matrix-infilled gaps between complementary bone fragments suggests that the dentary of SGOPV 3490 was originally ~2+ mm shallower than what is reported here. As in *Callistoe*, *Arminiheringia*, and *Pharsophorus tenax*, the horizontal ramus of *Eomakhaira* deepens posteriorly, has a ventral border that is curved in lateral view, and terminates anteriorly in a simple curve. Indeed, the horizontal ramus in *Eomakhaira* strongly resembles that of *Arminiheringia* (MACN-A 10970). This contrasts with the condition in the borhyaenids *Australohyaena* and *Arctodictis*, the proborhyaenids *Proborhyaena* and *Paraborhyaena*, and MPEF-PV 4170, a specimen assigned to *Pharsophorus* cf. *P. lacerans* (but not in the holotype of *P. lacerans*, MACN-A 52-391), in which the horizontal ramus is nearly uniform in depth, its ventral margin is flat, and its anterior end forms a distinct "chin" (fig. S2), with a sharp angle between the anterior border of the symphysis and the ventral border of the horizontal ramus. A distinct "chin" is also present in the basal sparassodonts *Allqokirus* and *Mayulestes* but is absent in most other members of this group in which the anterior border of the dentary is curved. The dentary shows no sign of a genial flange, in contrast to *Thylacosmilus*, *Anachlysictis*, or the unnamed thylacosmilid from La Venta (in which it is present). The deepest point of the horizontal ramus appears to have been below m4 in SGOPV 3490, as in most sparassodonts (table 1).

The left dentary is displaced slightly anteriorly relative to the right. The anteroventromedial edge of the left dentary is straight in ventral view (fig. S3), and the medial face of this element preserves a small portion of the symphyseal surface (fig. 9D). The symphyseal surface does not bear well-developed interdigitating ridges (in contrast to sparassodonts like *Borhyaena*, in which such ridges are present). In dorsal and ventral views, the medial face of the right dentary inflects medially near the p2/3 embrasure, a feature denoting the posteriormost extent of the mandibular symphysis in most mammals, suggesting the symphysis of *Eomakhaira* extended posteriorly to the level of the p2/p3 embrasure, or at most, just slightly below the anterior root of p3 (fig. 9). The symphysis of *Eomakhaira* is thus rather short compared to closely related sparassodonts; in these taxa, the mandibular symphysis reaches its midpoint below the: (1) p3 roots (*Borhyaena macrodonta*, *Borhyaena tuberata*, and *Pharsophorus lacerans* [including MPEF-PV 4190, the specimen of *Pharsophorus* cf. *P. lacerans* from La Cantera]), (2) posterior root of p3 (*Plesiofelis*, *Australohyaena* and *Prothylacynus*), (3) p3/m1 embrasure (*Callistoe*, *Paraborhyaena*, *Proborhyaena*, and *Arctodictis* spp.), or (4) m1 (*Arminiheringia*; Babot et al., 2002; Zimicz, 2012). In *Acrocyon riggsi* (Goin et al., 2007) and *Pharsophorus tenax*, the symphysis extends below the anterior root of p3 but further posteriorly than in SGOPV 3490. In *Thylacosmilus atrox* and *Anachlysictis gracilis*, the symphysis is much shorter than in all aforementioned taxa, ending below the canines.

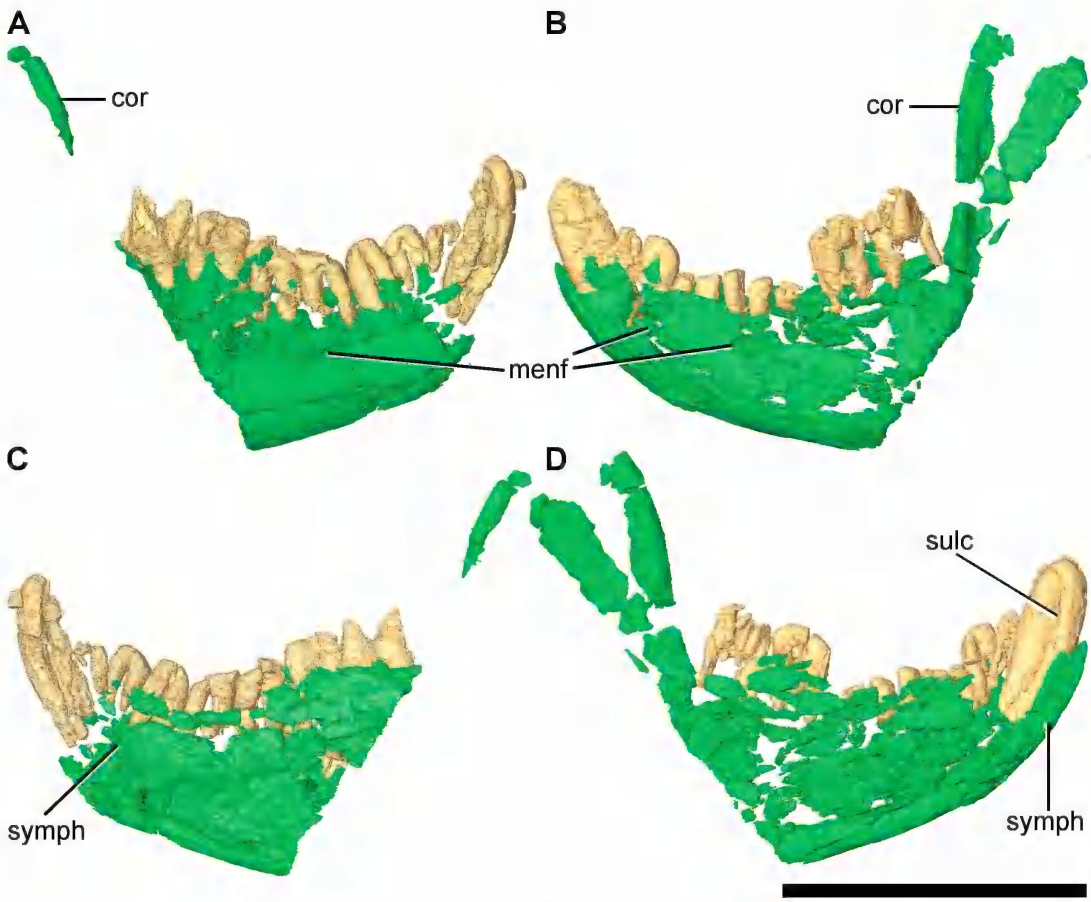

FIG 9. Mandible of the holotype of *Eomakhaira molossus* (SGOPV 3490). Right dentary in **A,** labial and **C,** lingual views. Left dentary in **B,** labial and **D,** lingual views. Colors of elements are the same as in figure 3. Abbreviations: **cor**, coronoid process of dentary; **sulc**, lingual sulcus of the lower canine; **menf**, mental foramina; **symph**, mandibular symphysis. Scale = 50 mm.

Several lines of evidence suggest that the mandibular symphysis of SGOPV 3490 was unfused. The two dentaries are offset anteroposteriorly with respect to one another. The preserved portion of the left symphyseal surface bears a straight ventromedial edge, suggesting a clean break between the two rami, as would be expected if they had been held together by ligaments. This configuration would be unlikely if a fused symphysis were broken postmortem. Had the mandibular symphysis been fused in vivo, one would expect an uneven, jagged break between the two dentaries, or for one or both to be broken immediately posterior to the mandibular symphysis, where the dentary is comparatively the weakest. This is the case in several other sparassodonts with fused symphyses and broken mandibles (e.g., MACN-A 706, *Prothylacynus patagonicus*; MLP 85-VII-3-1, *Arctodictis sinclairi*; UATF-V-000129, *Paraborhyaena boliviana*).

Each dentary of SGOPV 3490 bears only two mental foramina, one located beneath p2–3 and another below the m1–2 embrasure. The posterior foramen is well defined on both den-

taries and opens posteriorly; the anterior foramen is not well preserved on either dentary, but its existence and position can be inferred from a gap in the bone fragments labially beneath the premolar row. The presence of only two mental foramina on each dentary in *Eomakhaira* is unusual for a borhyaenoid. Most hathliacynids, borhyaenoids, and the basal sparassodont *Stylocynus* bear three or more mental foramina on each dentary, and individuals of some species possess as many as five or six (*Acrocyon riggsi*, *Arctodictis sinclairi*, *Australohyaena antiquua*, *Borhyaena tuberata*, and *Lycopsis longirostrus*). Additional mental foramina may have been present in SGOPV 3490, but the location of the preserved bone fragments relative to the positions of mental foramina in other sparassodonts (typically between p2 and m1 or m2) make this unlikely.

Enough of the left coronoid process is preserved to indicate that it is tall and well developed. However, due to crushing and distortion, it is not possible to determine the shape of the masseteric fossa, nor can the angle between the anterior border of the coronoid process and the toothrow be securely determined. A small portion of the right ascending ramus (which is not obviously deformed) indicates that the anterior border of the coronoid process is oriented approximately 110°–113° relative to the toothrow, a value typical for sparassodonts (Forasiepi, 2009).

Dentition

Precanine Dentition: Little of the precanine dentition is preserved in SGOPV 3490. A cylindrical fragment of a small tooth appressed to the lingual side of the lower right canine may represent i3, based on the position of this tooth in other sparassodonts (fig. 15). If this fragment represents part of a lower incisor, then the lower incisors of *Eomakhaira molossus* were proportionally smaller than those of *Arminiheringia auceta*, *Arctodictis sinclairi*, and potentially even *Australohyaena antiquua* and *Paraborhyaena boliviana* (scaling by both p3 and m4) but still larger than in MLP 77-VI-13-1, a specimen assigned to *Arctodictis sinclairi* that has been noted to have relatively small teeth compared with other specimens of this taxon (Goin et al., 2007).

Canines: The most conspicuous feature of the holotype of *Eomakhaira* is its large, robust canines (fig. 3, table 2). These teeth are disproportionately large compared to most sparassodonts, comparable (in relative size) only to proborhyaenids (including thylacosmilines), and the borhyaenids *Australohyaena*, *Acrocyon*, and *Arctodictis* (table 3). The surfaces of the canine roots in SGOPV 3490 are smooth (fig. 4A, 10A). In most borhyaenoids, the canine roots bear a series of small longitudinal grooves that sometimes nearly reach the apex (e.g., in *Arminiheringia* and *Proborhyaena*; figure S4B). The only borhyaenoids that do not have these grooves are thylacosmilines (figure S4C) and possibly *Lycopsis viverensis* (Suarez et al., 2016).

The upper and lower canines of *Eomakhaira* bear a well-developed median sulcus lingually, making them somewhat reniform in cross section (fig. 10B, C). By contrast, no sulcus occurs on the labial side of lower canine or the exposed labial surface of the upper canine. A shallow labial sulcus is present on intralveolar portions of the upper canine but is visible only on CT scans. Although median canine sulci have been considered a synapomorphy of proborhyaenids

TABLE 2. Dental measurements of the holotype of *Eomakhaira molossus* (SGOPV 3490) in mm. Measurements from CT scans, to nearest 0.1 mm. * = estimated measurement due to damaged protocone and missing metastylar corner of M3.

		Upper Dentition				Lower Dentition	
		Left	Right			Left	Right
C	Length	11.4	11.7	C	Length	11.0	—
	Width	6.6	6.9		Width	5.8	—
P1	Length	—	5.2	p1	Length	4.1	—
	Width	—	2.6		Width	2.5	—
P2	Length	6.2	—	p2	Length	6.6	6.5
	Width	3.2	—		Width	4.3	4.3
P3	Length	8.6	9.1	p3	Length	7.5	7.6
	Width	4.9	5.0		Width	4.2	4.1
M1	Length	—	—	m1	Length	—	7.9
	Width	—	—		Width	—	4.2
M2	Length	—	—	m2	Length	—	9.0
	Width	—	—		Width	—	5.3
M3	Length	8.6*	—	m3	Length	—	10.2
	Width	6.9*	—		Width	—	5.5
M4	Length	3.4	—	m4	Length	—	12.0
	Width	8.5	—		Width	—	6.3

(either sensu stricto or including thylacosmilines; Babot et al., 2002), this feature is widely distributed among sparassodonts, with lingual sulci also occurring in the borhyaenids *Australohyaena antiquua*, *Arctodictis sinclairi*, *Arctodictis munizi*, and *Borhyaena macrodonta*, the basal borhyaenoid *Pharsophorus lacerans* (as seen in the holotype MACN-A 32-391, YPM-VPPU 20551, and MPEF-PV 4190, a specimen from La Cantera assigned to *Pharsophorus* cf. *P. lacerans*; Patterson and Marshall, 1978; Goin et al., 2010), and an indeterminate sparassodont from the Fitzcarrald Arch (Tejada-Lara et al., 2015). Sinclair (1930) and Marshall (1978) reported lingual sulci in *Acrocyon riggsi*, but we could not verify this observation in photographs of this taxon. In all sparassodonts in which median sulci occur, the labial ones are less prominent than the lingual ones (e.g., proborhyaenids, *Arctodictis munizi*) or are absent (all other taxa). Although the extraalveolar portion of the upper canine of *Thylacosmilus* lacks a median sulcus, a shallow median sulcus is present on the intralveolar portion of this tooth (FMNH P14344, FMNH P14531). The lower canines of *Thylacosmilus* bear median sulci labially and lingually (Goin and Pascual, 1987).

In cross section, the lingual side of the upper canines of SGOPV 3490 is slightly flatter than the labial side but not as flat as in *Thylacosmilus atrox* (Riggs, 1934). The labial surface of the right upper canine of *Eomakhaira* is slightly keeled (fig. 4A, 10B, C), similar to but less pro-

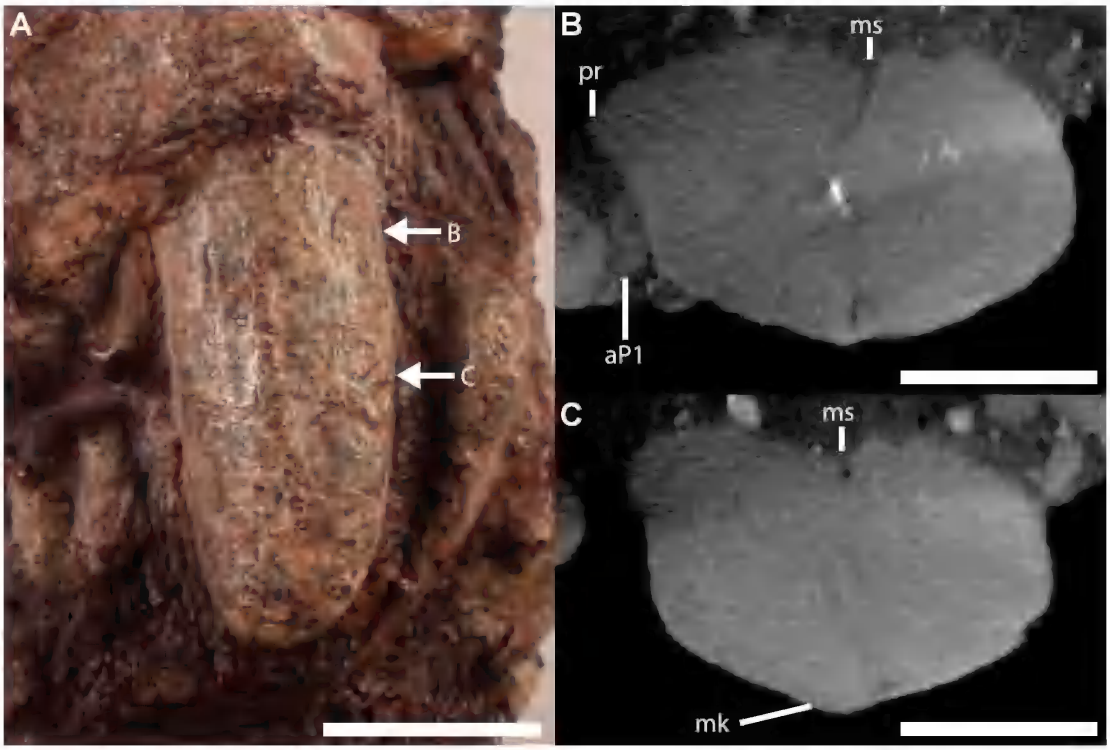

FIG 10. **A,** Photograph and **B, C,** CT images of the right upper canine of the holotype of *Eomakhaira molossus* (SGOPV 3490). **A**, Lateral view, showing bluntness of canine apex and the absence of enamel, longitudinal ridges, and labial median canine sulcus. **B**, Transverse section of canine, slightly below alveolar border (actual point at alveolar border obscured by a crack), showing posterior keel. Anterior root of P1 (**aP1**) marked to show that the longitudinal ridge is not an artifact of postmortem damage. **C**, Transverse section of canine, at level of tooth row, showing presence of median labial keel and lingual median sulcus. Approximate location of sections in B, C denoted by arrows on A. Anterior to right in all images, and lingual to top in B, C. Abbreviations: **aP1**, anterior root of P1; **mk**, labial median keel; **ms**, lingual median sulcus; **pr**, posterior ridge. Scale = 10 mm (A); 5 mm (B, C).

nounced than in *Thylacosmilus* (Riggs, 1934; Turnbull, 1978). This feature is not evident on the more poorly preserved left upper canine. A small carina occurs on the posterior edge of the upper canine, slightly more marked on the right tooth than the left (fig. 10B). Carinae appear to be absent in the upper canines of *Arminiheringia auceta*, cf. *Proborhyaena* (MLP 79-XII-18-1), and other borhyaenids we have observed. By contrast, the upper canines of thylacosmilines, like those of most saber-toothed mammals, bear well-defined carinae that lend the tooth a knifelike appearance. In *Patagosmilus,* the upper canine is blunt anteriorly but bears a sharp posterior carina (Forasiepi and Carlini, 2010), similar to the condition in *Eomakhaira.* The anterior and posterior faces of the upper canines form well-defined carinae in *Thylacosmilus,* the posterior of which is much sharper (Riggs, 1934; Turnbull, 1978; Goin and Pascual, 1987).

The upper canines of *Eomakhaira* are mediolaterally compressed compared to non-thylacosmiline borhyaenoids (table 3). The L/W ratio of the upper canines ranges from 1.50–1.77, depending on orientation of the skull during measurement. The lower end of this range likely

TABLE 3. Upper canine cross-sectional shape (ratio of anteroposterior length [L] to mediolateral width [W]) and relative canine size of SGOPV 3490 compared with other sparassodonts. * = juvenile individuals. For raw measurements and relative canine size calculation method, see table S3.

Taxon	Specimen	Higher Taxon	L/W Ratio	Relative Size
Eomakhaira molossus	SGOPV 3490	Thylacosmilinae	1.71	1.12
Arminiheringia auceta	MACN-A 10792	Proborhyaenidae	1.48	1.04
Callistoe vincei	PVL 4187	Proborhyaenidae	1.38	1.28
Paraborhyaena boliviana	MNHN SAL 51	Proborhyaenidae	1.45	0.85
cf. *Proborhyaena*	MLP 79-XII-18-1	Proborhyaenidae	1.75	—
Proborhyaenidae sp. nov?	MHNT-VT-1400/1401	Proborhyaenidae	1.45	0.64
Thylacosmilus atrox	MLP 35-X-4-1	Thylacosmilinae	2.45	1.13
Thylacosmilus atrox	FMNH P14531	Thylacosmilinae	2.50	1.11
Thylacosmilus atrox	MMP 1470	Thylacosmilinae	2.63	0.84
?Thylacosmilinae sp. nov.	IGM 251108	?Thylacosmilinae	1.56	—
cf. *Dukecynus* sp.*	UCMP 32950	Basal Borhyaenoidea	1.41	—
*Lycopsis longirostrus**	UCMP 38061	Basal Borhyaenoidea	1.27	0.51
Pharsophorus lacerans	MNHN SAL 96	Basal Borhyaenoidea	1.35	—
cf. *Pharsophorus**	AMNH 29591	Basal Borhyaenoidea	1.55	—
Prothylacynus patagonicus	MACN 11453	Basal Borhyaenoidea	1.45	0.75
*Prothylacynus patagonicus**	MACN-A 5931	Basal Borhyaenoidea	1.26	0.67
Hondadelphys fieldsi	UCMP 37960	Basal Sparassodonta	1.81	0.80
Acrocyon riggsi	FMNH P13433	Borhyaenidae	1.36	1.00
Arctodictis munizi	MLP 11-65	Borhyaenidae	1.60	1.29
Arctodictis munizi	CORD-PZ 1210-1/5	Borhyaenidae	1.46	1.27
Arctodictis sinclairi	MLP 85-VII-3-1	Borhyaenidae	1.30	1.16
Australohyaena antiquua	UNPSJB-PV 113	Borhyaenidae	1.34	1.12
Australohyaena antiquua	FMNH P13633	Borhyaenidae	1.42	—
Borhyaena macrodonta	MACN 52-390	Borhyaenidae	1.51	0.92
Borhyaena tuberata	MACN 6203-6265	Borhyaenidae	1.47	0.85
Borhyaena tuberata	MACN 5780	Borhyaenidae	1.52	—
Borhyaena tuberata	YPM-VPPU 15701	Borhyaenidae	1.22	0.99
Borhyaena tuberata	YPM-VPPU 15120	Borhyaenidae	1.45	0.86
Acyon myctoderos	MNHN-Bol-V-003668	Hathliacynidae	1.42	0.60
Borhyaenidium riggsi	FMNH P14409	Hathliacynidae	1.43	0.46
Cladosictis centralis	MACN 11639	Hathliacynidae	1.64	0.84
Cladosictis patagonica	MACN 5927	Hathliacynidae	1.49	0.91

TABLE 3 *continued*

Taxon	Specimen	Higher Taxon	L/W Ratio	Relative Size
Cladosictis patagonica	MACN 6280-6285	Hathliacynidae	1.42	0.62
Cladosictis patagonica	AMNH 9134	Hathliacynidae	1.52	0.72
Cladosictis patagonica	YPM-VPPU 15046	Hathliacynidae	1.50	0.71
Cladosictis patagonica	YPM-VPPU 15170	Hathliacynidae	1.64	0.83
Cladosictis patagonica	YPM-VPPU 15702	Hathliacynidae	1.43	0.95
Notogale mitis	YPM-VPPU 21871	Hathliacynidae	1.47	—
Sipalocyon externa	MACN-A 52-383	Hathliacynidae	1.44	0.72
Sipalocyon gracilis	MACN-A 692	Hathliacynidae	1.51	0.79
Sipalocyon gracilis	YPM-VPPU 15373	Hathliacynidae	1.48	0.61
Sipalocyon gracilis	AMNH 9254	Hathliacynidae	1.55	0.80
Sipalocyon gracilis	YPM-VPPU 15029	Hathliacynidae	1.45	0.71
Sipalocyon gracilis	YPM-VPPU 15154	Hathliacynidae	1.43	0.91
Sparassodonta gen. et sp. nov.	UF 27881	incertae sedis	1.22	0.90
Sparassodonta indet.	MUSM 1649	incertae sedis	1.26	—

underestimates the degree of mediolateral compression of the tooth, however, as it requires an anatomically unlikely orientation of the specimen (one where the palate is highly inclined and the tooth roots are far from vertical). More reasonable orientations of the specimen yield higher estimates. The most reasonable orientations of SGOPV 3490 produce canine L/W ratios of 1.65–1.70. Orientation aside, the upper canines of *Eomakhaira* are clearly more mediolaterally compressed than in most other borhyaenoids, including *Pharsophorus*, *Prothylacynus*, all borhyaenids (*Acrocyon*, *Arctodictis*, *Australohyaena*, and *Borhyaena*), IGM 251108 (the putative thylacosmiline from La Venta), most non-thylacosmiline proborhyaenids (*Arminiheringia*, *Paraborhyaena*, *Callistoe*), and the indeterminate proborhyaenid from the Tremembé Formation (Couto-Ribeiro, 2010). However, they are less compressed than in *Patagosmilus*, *Thylacosmilus*, and cf. *Proborhyaena* (MLP 79-XII-18-1). In terms of nonsparassodont carnivores, the canine proportions of *Eomakhaira* are comparable to the machaeroidine oxyaenid "creodont" *Machaeroides eothen* (see Gazin, 1946), the nimravid carnivoramorphans *Dinictis felina* and *Nimravus brachyops* (see Barrett, 2016), and the machairodontine felid carnivoran *Pseudaelurus quadridentatus* (see Antón et al., 2012). The resemblance to the latter three placental taxa is noteworthy, as each is among the least-specialized members of their respective clades in terms of machairodonty (Meachen-Samuels, 2012; Antón, 2013).

CT imaging indicates that the canine roots of SGOPV 3490 were closed at the time of death. The canine roots are closed in adulthood in sparassodonts except in non-thylacosmiline proborhyaenids, in which the upper and lower canines are hypselodont and their roots remain open throughout life (Simpson, 1948; Marshall, 1978; Babot et al., 2002; but see Bond and Pascual, 1983). In thylacosmilines, only the upper canines are hypselodont (Riggs, 1934;

Forasiepi and Carlini, 2010). However, the closed roots of the lower canines may be a secondary reversal from a hypselodont ancestral condition (Babot et al., 2002). Canine pulp cavities in SGOPV 3490 are relatively narrow and lack a well-developed opening. Additionally, the canine roots taper slightly apically rather than being uniformly wide with outwardly flaring edges as is typically observed in open-rooted taxa. Nevertheless, several features suggest that the canines of *Eomakhaira* were open rooted earlier in ontogeny, closing only in extreme senescence, as in the proborhyaenid *Proborhyaena* (Bond and Pascual, 1983; but see Babot et al., 2002). First, the canines of SGOPV 3490 lack any trace of enamel, being composed solely of dentine. This contrasts with the typical condition in sparassodonts with non-hypselodont canines (e.g., borhyaenids), where some enamel occurs on nonoccluding surfaces near the apex of the tooth (such as the lateral side of the upper canines), even in old individuals. The hypselodont canines of *Patagosmilus* and *Thylacosmilus* have enamel (Turnbull, 1978; Forasiepi and Carlini, 2010), but only in a band covering the labial surface of these teeth rather than a simple cap. Postmortem damage and/or unusual wear are unlikely to account for the complete absence of enamel on all four canines of SGOPV 3940, particularly considering that enamel occurs on the right P1 and p2, located only a few millimeters posterior to the canines (fig. 4). A similar condition (enamel absent on the canines but present on the postcanines) is also observed in the proborhyaenids *Proborhyaena* and *Callistoe*. The absence of enamel in *Eomakhaira* is consistent with this taxon having had open-rooted canines until near the end of its lifespan.

The upper canines of SGOPV 3490 are tall given their high degree of wear (table S4). The upper canine roots extend almost to the dorsal border of the maxilla within their alveoli (measuring over 46 mm in total length), indicating that the height of the exposed portion (23 mm) is natural and not the result of the canine slipping ventrally from the alveolus. Scaled to the anteroposterior length of the tooth, the exposed height of the upper canine in SGOPV 3490 exceeds that of most other borhyaenoids and far exceeds that of other sparassodonts with a comparable degree of canine wear. Scaled to M3 length, the upper canine is longer than in almost any other taxon, except those with hypselodont upper canines.

The pulp cavities of the upper and lower canines appear to extend to their apices. The cavity is difficult to discern in the right upper canine, but an area of seemingly less dense, nodule-containing material runs the entire length of the tooth. The pulp cavities of the upper canines are much smaller than those of the lower canines. A pulp cavity extending to the apex of the tooth would be expected if these teeth were worn but hypselodont (O'Connor et al., 2019), as is seen in other mammals with hypselodont caniniforms (i.e., *Choloepus*; DigiMorph Staff, 2003), though this condition can also result from extreme wear in some sparassodonts without hypselodont canines (e.g., the holotype of *Pharsophorus lacerans*, MACN-A 52-391).

The left lower canine, which has the best-preserved root among the four canines, may not have a fully closed root. Although its pulp cavity is very narrow along most of its length, a deep depression occurs near its base, where the edges of the root flare outward in cross section (fig. 11). This depression connects with the pulp cavity of the tooth. This is reminiscent of the condition in non-thylacosmiline proborhyaenids, all of which have hypselodont lower canines

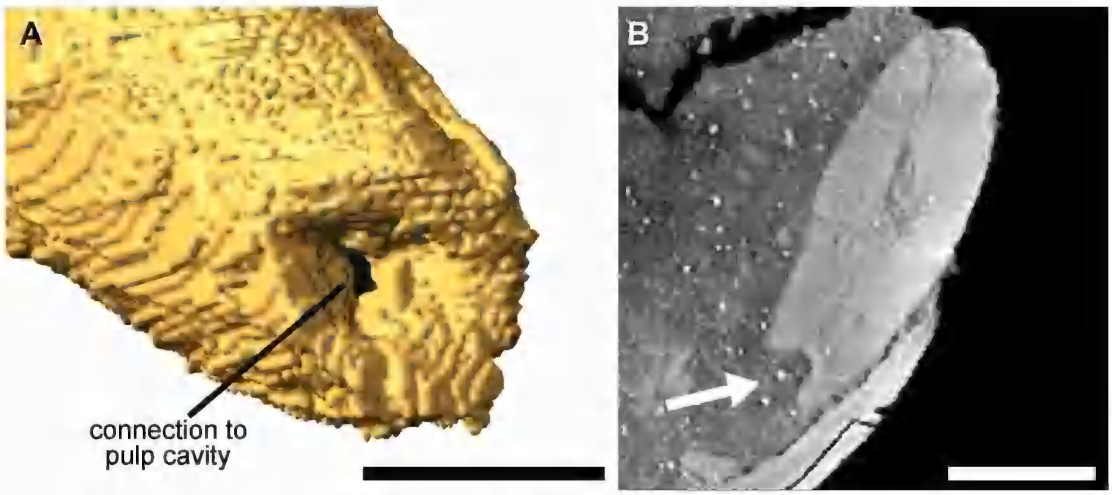

FIG 11. Morphology of the left lower canine root in the holotype of *Eomakhaira molossus* (SGOPV 3490). **A**, CT reconstruction in oblique lateral view, showing prominent depression on proximal end of canine and its connection to the pulp cavity. Connection to pulp cavity has been artificially darkened for contrast. **B**, Oblique lateral CT image slice of SGOPV 3490, showing flared, smooth distal end of left lower canine (denoted by arrow). Scale = 10 mm.

(Babot et al., 2002: fig. 4B, E). The lack of a basal tip on the left lower canine of SGOPV 3490 cannot be ascribed to damage, as the base of the alveolus is intact and the edges of the apical depression are smooth and rounded rather than jagged, as they would be if broken. Given the advanced ontogenetic age of SGOPV 3490, details of the root of the lower left canine suggest that it had been open for much of the animal's life and had only very recently closed. The conditions of the roots of the upper canines are uncertain, as their bases cannot be confidently distinguished from the surrounding matrix and bone. Together, the observations above suggest that the canines of *Eomakhaira* were hypselodont throughout most of their ontogeny, with roots closing and tooth growth ceasing only in extremely senescent individuals.

The roots of the canines in *Eomakhaira*, particularly the lower canines, are shorter and less curved than those of other sparassodonts. The upper canine roots end above P3 in *Eomakhaira* but are still relatively large above P3 in *Callistoe* and *Arminiheringia* (based on coronal cross sections; Babot et al., 2002), suggesting that the roots extended further posteriorly in those taxa. A condition similar to that of *Callistoe* and *Arminiheringia* occurs in *Australohyaena* (UNPSJB PV 113; Forasiepi et al., 2015). The lower canines of SGOPV 3490 are emplaced nearly subvertically within the alveoli, similar to what has been described for most borhyaenoids, with the notable exception of *Arminiheringia*, in which the lower canines are procumbent. The lower canine roots are much shorter and more vertical than their upper counterparts and probably end at the level of the p1–2 embrasure. However, they certainly do not extend beyond the anterior root of p2. This differs from *Callistoe*, *Proborhyaena*, and *Arctodictis*, in which the lower canine roots reach the level of p3 (Babot et al., 2002; Forasiepi, 2009), and from *Arminiheringia*, in which they reach the molar row (Zimicz, 2012). The lower canine roots are more curved in *Callistoe* and *Arctodictis* than in *Eomakhaira*.

PREMOLARS: SGOPV 3490 possesses the typical metatherian postcanine dental formula of three premolars and four molars (fig. 15). In the dentary, the alveolar margin of the postcanine dentition is higher lingually than labially, a feature noted in other sparassodonts (Forasiepi et al., 2015). The postcanine toothrow of *Eomakhaira* is straight in occlusal view (fig. 6), as in most sparassodonts. In the thylacosmilines *Patagosmilus* and *Thylacosmilus*, the postcanine toothrow is strongly curved and concave medially (Forasiepi and Carlini, 2010), but this does not appear to be the case for the more basal thylacosmiline *Anachlysictis* (Goin, 1997). In *Arctodictis* and *Australohyaena*, the postcanine toothrow is neither straight nor curved. Instead, the long axes of the molar and premolar rows are offset from one another rather than aligned (fig. S5), a feature often associated with an obliquely oriented P3. This condition is more pronounced in *Arctodictis munizi* and *Australohyaena antiquua* than in *Arctodictis sinclairi*. The condition in the borhyaenid *Acrocyon riggsi* is unclear; in the holotype (FMNH P13433), the toothrow is straight, but P3 is slightly oblique. This unusual configuration may be an artifact of poor restoration of the holotype skull (Sinclair, 1930). FMNH P13433 is also unusual in having postcanine toothrows that do not diverge posteriorly to form a triangular palate. Posteriorly diverging toothrows characterize every sparassodont for which the shape of the palate can be determined except *Hondadelphys* (thought be a basal member of the clade), an observation that supports the interpretation of Sinclair (1930) that the straight postcanine toothrows of FMNH P13433 are an artifact. The long axis of P3 in *Eomakhaira* is parallel to the long axis of the postcanine toothrow (fig. 6), as in *Pharsophorus, Borhyaena*, and proborhyaenids, rather than being obliquely oriented as in *Australohyaena* and *Arctodictis*.

As in other sparassodonts, the upper and lower premolars of *Eomakhaira* increase in size from P1 to P3 and p1 to p3. However, the relative disparity in sizes among the premolars differs between the upper and lower toothrows. P3 is much larger than P1and P2, which are of similar size. By contrast, p1 is distinctly smaller than p2 and p3, which are of similar size. The first upper and lower premolars are both very small. In lateral view, the dorsal alveolar border of the lower premolars slopes anterodorsally-posteroventrally from p1 to p3, a common pattern also seen in *Prothylacynus patagonicus*, *Pharsophorus* cf. *P. lacerans* (MPEF-PV 4170), *Borhyaena macrodonta*, *Arctodictis sinclairi*, *Australohyaena antiquua*, *Callistoe vincei*, and *Proborhyaena gigantea*. The premolar row is relatively short in *Eomakhaira* compared to other sparassodonts (table S5).

The right P1 and both p1s are oriented obliquely relative to the remainder of the toothrow (~35° anterolabially-posterolingually for both loci), but the left P1 is nearly parallel to the toothrow. Given that the left maxilla is poorly preserved, the anterior root of its P1 is damaged, and natural bilateral asymmetry of tooth orientation has never been documented in Sparassodonta, the orientation of this tooth almost certainly reflects postmortem deformation.

The P1 of *Eomakhaira* is asymmetric in lateral view, with its main cusp located over the anterior root (fig. 4) rather than equidistant between the anterior and posterior roots, as in most sparassodonts. Similarly asymmetric premolars occur in *Allqokirus* and *Mayulestes* but not in hathliacynids, borhyaenids, or most basal borhyaenoids (Muizon et al., 2018). They do occur in the proborhyaenids *Callistoe* and *Arminiheringia*, the only other proborhyaenids for

which P1 is known. P/p1 is thought to have been lost in thylacosmilines (Forasiepi and Carlini, 2010), but the putative basal thylacosmiline from La Venta retains P/p1 (as evidenced by the presence of the roots of these teeth in IGM 251108). What remains of p1 in SGOPV 3490 suggests that its apex was more centrally positioned than that of P1, as in other sparassodonts.

The crowns and roots of P/p2 of *Eomakhaira* are aligned with the rest of the postcanine toothrow, as in *Pharsophorus* (though possibly not as in MPEF-PV 4170 from La Cantera, which more closely resembles *Arctodictis sinclairi* in this respect), *Callistoe*, *Arminiheringia auceta*, and *Borhyaena*, rather than oblique to the toothrow, as in *Proborhyaena*, *Paraborhyaena*, *Arminiheringia contigua* (MACN-A 10317), *Arctodictis*, *Acrocyon*, and *Australohyaena*.

The robust P/p3 bear large, stout roots. Nevertheless, these teeth are proportionally narrower labiolingually than the more bulbous teeth of borhyaenids (P3 L/W ratio = 1.75 in *Eomakhaira* vs. an average of 1.43 in borhyaenids; table S6) and those of species of *Pharsophorus* (*P. lacerans*, YPM-VPPU 20551; *P. tenax*, AC 3192). Borhyaenid taxa closely resembling *Eomakhaira* in other respects (e.g., *Arctodictis* and *Australohyaena*) also have the most bulbous P/p3s. The P3 of *Eomakhaira* is more elongate than that of *Callistoe vincei*, less elongate than that of cf. *Proborhyaena* (MLP 79-XII-18-1), but comparable to those of specimens of *Arminiheringia*. Like P3, the p3 of *Eomakhaira* is proportionally narrower labiolingually than in most borhyaenids, the basal borhyaenoid *Plesiofelis*, and the proborhyaenids *Proborhyaena* and *Arminiheringia*. The L/W ratio of this tooth is comparable to that in the proborhyaenids *Paraborhyaena* and *Callistoe*, but is less narrow than its counterparts in the basal borhyaenoids *Prothylacynus* and *Pharsophorus*.

The P3 of *Eomakhaira* is ~13%–19% longer than p3. In most sparassodonts resembling *Eomakhaira* (borhyaenids, proborhyaenids, and *Pharsophorus*), P3 and p3 are of similar length (table S6). The only borhyaenoid potentially resembling *Eomakhaira* in this respect is *Proborhyaena gigantea*. The P3 of MLP 79-XII-18-1, assigned to *Proborhyaena* by Bond and Pascual (1983) but referred to as cf. *Proborhyaena* here, is extremely large (nearly 30 mm long, judging from its preserved roots). This is considerably longer than the p3 of the largest known specimen of *Proborhyaena gigantea* (AMNH 29576, where this tooth is ~24 mm long). If MLP 79-XII-18-1 pertains to *Proborhyaena*, it implies the P3 of this taxon was >50% longer than p3, a more extreme size disparity than in *Eomakhaira*. The tooth at the P3 locus in *Thylacosmilus* is also much longer than its p3, but since the upper tooth represents dP3 rather than P3 (Goin and Pascual, 1987; Forasiepi and Carlini, 2010; Forasiepi and Sánchez-Villagra, 2014), direct comparisons with other sparassodonts are not possible. No other thylacosmilines are known from associated upper and lower dentitions.

The p3 of *Eomakhaira* appears to have been inclined posteriorly. This is common among borhyaenoids, occurring also in the basal forms *Plesiofelis schlosseri* and *Pharsophorus lacerans*; the borhyaenids *Australohyaena antiquua*, *Arctodictis sinclairi*, and *Borhyaena macrodonta* (Marshall, 1978; Forasiepi et al., 2015); and the proborhyaenid *Proborhyaena gigantea* (R.K.E., personal obs.). Most of the enamel is missing from p3 in SGOPV 3490, with only a small patch preserved near the apex of the left p3. It is not clear whether this paucity of enamel represents a normal feature of *Eomakhaira* or is an artifact of preservation, because in most other sparas-

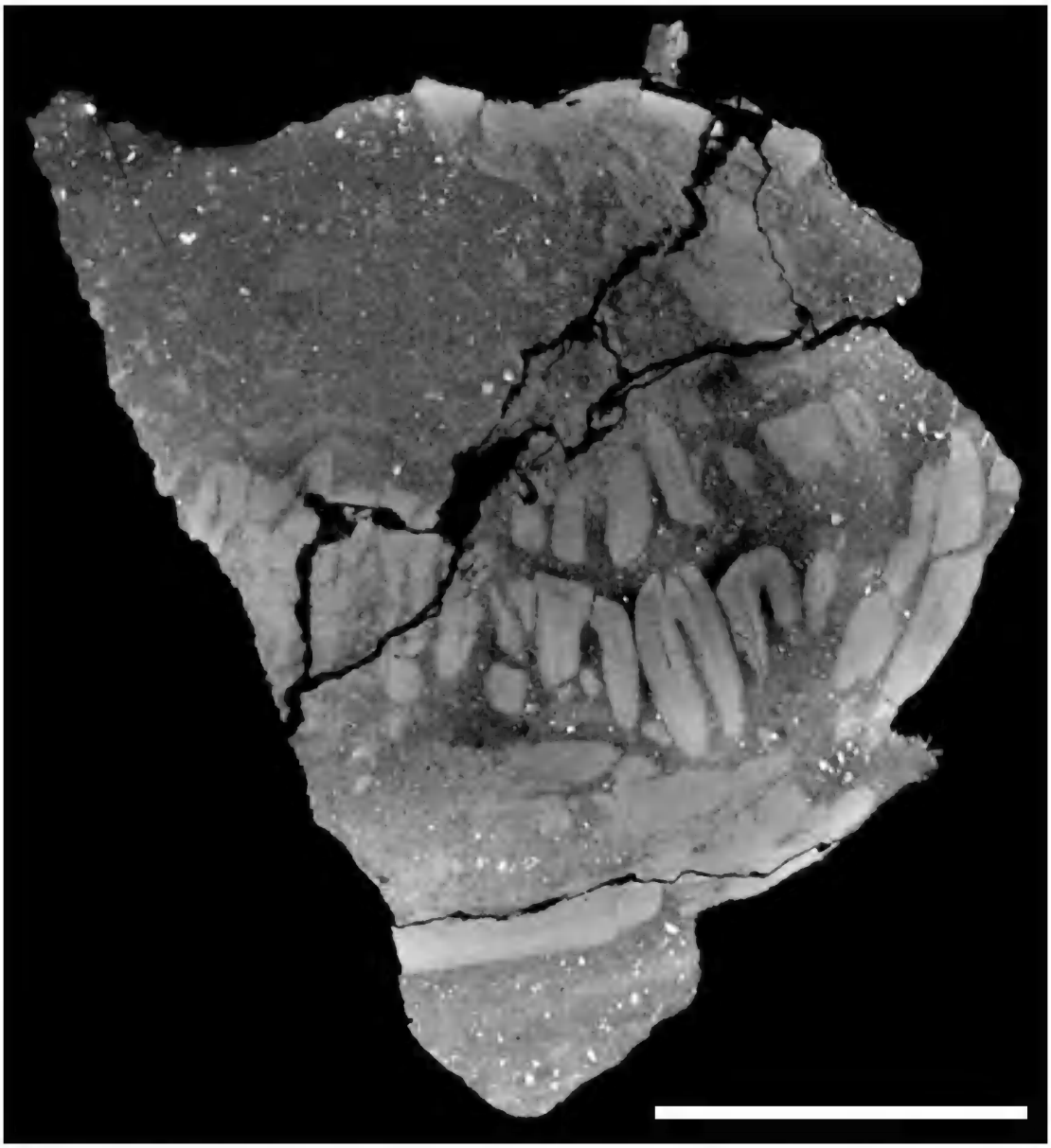

FIG 12. Oblique lateral CT image slice of SGOPV 3490 along the postcanine tooth row, showing position of lower molars and depth of horizontal ramus. Note how worn surfaces of P3 and m1 closely match one another. Scale = 30 mm.

sodonts (e.g., *Pharsophorus*, borhyaenids) the enamel of p3 extends inferiorly to the same level as in the other postcanine teeth, although in *Proborhyaena* (AMNH 29576, MACN-A 52-382) and *Callistoe* (PVL 4187), the enamel of p3 is restricted to the apex of this tooth.

The roots of the lower postcanines of many borhyaenoids (borhyaenids, proborhyaenids, and closely related taxa) are often robust and "bulbous." The degree to which this condition is

expressed is variable, ranging from taxa with bulbous roots only on p3 (e.g., *Borhyaena*) to taxa in which the roots of all premolars are bulbous, but the roots of the molars are not (e.g., *Thylacosmilus*) to those having bulbous roots on all lower premolars and some molars (e.g., *Australohyaena antiquua* and most proborhyaenids). The roots of p3 in *Eomakhaira* are extremely robust (fig. 12) and nearly in contact, resulting in little interradicular space. Whether this condition qualifies as bulbous is uncertain, as previous studies have typically defined roots as bulbous when they are wider than the crown in occlusal view (see Forasiepi, 2009), but the crown of p3 is incompletely preserved in SGOPV 3490. Nevertheless, the morphology of the roots of p3 in SGOPV 3490 closely resembles that of sparassodonts considered to have bulbous roots, such as *Arctodictis sinclairi*, in which the p2–m2 roots are so swollen that the interradicular space is nearly eliminated (Forasiepi, 2009: fig. 19). The crowns of right p2 and m1 are preserved in SGOPV 3490, but their roots are not wider than their crowns, suggesting that these roots are not bulbous if prior definitions are strictly applied. The roots of right p2 are comparatively more robust than the roots of the molars (fig. 4) but still much less bulbous than in *A. sinclairi*. SGOPV 3490 resembles *Thylacosmilus* in that the roots of the lower premolars are more robust than those of the molars, though in contrast to *Eomakhaira* the premolar roots of *Thylacosmilus* are bulbous (Forasiepi, 2009).

Molars: Left M3–4 (fig. 13) and the partial crown of right M3 are the best preserved of the heavily worn upper molars. The left M3 appears to have been displaced posterolingually relative to the left M4. In most sparassodonts, the distal tip of the M3 postmetacrista contacts the anterior end of the M4 preparacrista, whereas in SGOPV 3490, the metastylar corner of M3 is located labial to the end of the M4 preparacrista. Nevertheless, the length of the M3 can be roughly estimated based on preserved parts of this tooth. The M3 is so heavily worn that it is essentially pyramidal in shape, bearing only a single, poorly distinguished cusp. This cusp is located near the labial edge of the tooth, suggesting that the stylar shelf was extremely narrow. Based on comparisons with other sparassodonts, the main cusp represents either the metacone (which is typically the tallest upper molar cusp in sparassodonts) or the remnants of a single, completely connate, merged paracone and metacone. In most sparassodonts that have a very small paracone (e.g., *Borhyaena*, *Arctodictis*, *Australohyaena*, *Prothylacynus*, and the proborhyaenid from the Tremembé Formation), this cusp is typically half (or less) the height of the metacone. However, in *Callistoe*, *Arminiheringia*, and *Patagosmilus*, the paracone is very tall (despite its small base), often nearly as high as the metacone (or only slightly lower). The condition in *Proborhyaena* is ambiguous; the relative heights of the paracone and metacone in the molars of AMNH 29576 are obscured by wear and damage.

Evidence of an anterolabial cingulum, paracone, or stylar cusps on M3 of SGOPV 3490 is lacking. Whether these structures were once present but obliterated by heavy wear cannot be determined. The ectoflexus on M3 is >10% the labiolingual width of the tooth (fig. 13B), qualifying it as "deep" sensu Davis (2007) and Williamson et al. (2012). Among short-snouted borhyaenoids, a deep ectoflexus on M3 occurs in *Prothylacynus patagonicus*, *Proborhyaena gigantea*, and *Callistoe vincei* (table S7). By contrast, upper molar ectoflexi are shallow or absent in *Pharsophorus tenax* and all borhyaenids (*Borhyaena* spp., *Arcto-*

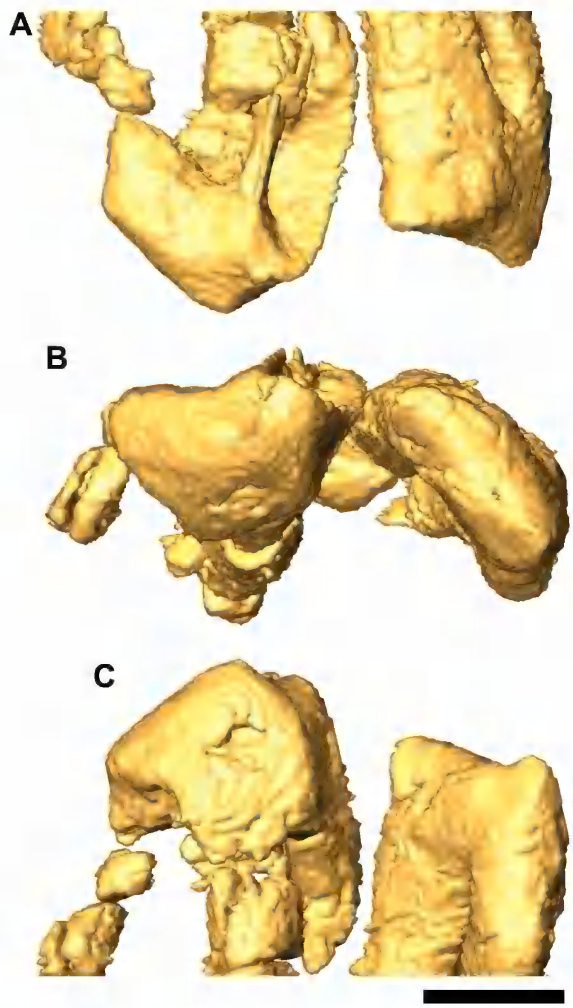

FIG. 13. Left M3–4 of SGOPV 3490 in **A,** labial, **B,** occlusal, and **C,** lingual views (C rotated upside down for easier comparison with A, B). Anterior to left in all CT segmentation images. Scale = 3 mm.

dictis spp., *Acrocyon riggsi*, *Australohyaena antiquua*). Although the M3 ectoflexus of *Patagosmilus goini* is classified here as "shallow," it is deeper than in borhyaenids and *Pharsophorus tenax* (close to the threshold between "deep" and "shallow"; table S7) and contrasts with the condition in *Thylacosmilus atrox* and an indeterminate Colhuehuapian thylacosmiline (Goin et al., 2007), in which the ectoflexus is extremely shallow or absent. CT images show that the M3 roots are extremely splayed in SGOPV 3490. A similar condition occurs in *Proborhyaena*, *Paraborhyaena*, and MLP 79-XII-1-1. Other sparassodonts may also exhibit this condition, but this is difficult to assess without isolated molars or CT imaging data. Goin et al. (2007) considered anterolabially-posterolingually narrow molar roots to characterize Thylacosmilinae. This condition cannot be scored for *Eomakhaira* due to distortion of these roots in SGOPV 3490.

The M3 protocone of SGOPV 3490 appears to have been extremely small. This inference is based on: (1) the position of the lingual root M3, which is mostly superior to the trigon rather than directly above it, leaving little space for a talon (unlike the condition in sparassodonts with a larger protocone); and (2) the presence of a small but poorly preserved protocone on right M3. On the left M3, the protocone is entirely missing and the lingual face is dominated by a nearly vertical surface (fig. 13B, C). It is unclear whether this feature formed in vivo or resulted from postmortem damage. The flat lingual face of the left M3 does not appear to be due to carnassial rotation, as carnassial rotation in other sparassodonts produces wear facets that parallel the preparacrista and postmetacrista (see below), whereas in SGOPV 3490, this feature is oblique to these crests. Significantly, this feature does not occur on the left M3, suggesting that its presence on the right tooth is a preservational artifact.

A small, freshly broken area of enamel on the posterolabial face of the left M3 of SGOPV 3490 shows that the enamel is remarkably thin (~0.06 mm). The enamel seems to be of similar thickness on the lower teeth, but this is uncertain given the lack of other clean breaks and sufficient density contrast and resolution for distinguishing thin enamel from dentine in CT scans. In sparassodonts, extremely thin molar enamel has been reported in a proborhyaenid (0.17 mm in MLP 79-XII-19-1, cf. *Proborhyaena*; Koenigswald and Goin, 2000) and large hathliacynids (0.07–0.10 mm in *Acyon* and *Cladosictis*; Koenigswald and Goin, 2000; Engelman et al., 2015). Enamel is generally thicker in borhyaenids and basal borhyaenoids (~0.23 mm, *Prothylacynus patagonicus*; ~0.34 mm, *Arctodictis sinclari*; Koenigswald and Goin, 2000). Postcanine enamel thickness is unknown in thylacosmilines, but their canine enamel has been reported to be extremely thin (Turnbull, 1978; Koenigswald and Goin, 2000). Although the enamel thickness in *Eomakhaira* is more similar to that in other proborhyaenids than in other borhyaenoids, allometry may play a role, given that *Eomakhaira* is much smaller than both *Prothylacynus* and *Arctodictis*.

The best-preserved upper molar in SGOPV 3490, left M4 (figs. 13, S6), is very short anteroposteriorly. In this respect, *Eomakhaira* more closely resembles *Patagosmilus* (where the M4 is also very narrow) than other short-snouted borhyaenoids (e.g., *Prothylacynus*, *Pharsophorus*, *Arminiheringia*, *Borhyaena*, *Arctodictis*, and *Thylacosmilus*) in which the M4 is more robust and less anteroposteriorly narrow (table S8). The preparacrista is parallel to the axis of the greatest width of the tooth. The M4 crown is oriented obliquely (anterolabially-posterolingually) to the rest of the toothrow. An oblique M4 occurs in many sparassodonts (*Cladosictis patagonica*, *Acyon myctoderos*, *Prothylacynus patagonicus*, *Callistoe vincei*, *Arminiheringia auceta*, *Arctodictis sinclairi*, *Arctodictis munizi*, *Thylacosmilus atrox*) but can be variable (e.g., M4 is oriented obliquely in some but not all individuals of *Arctodictis sinclairi* and *Acyon mycteros*). The M4 of SGOPV 3490 is almost as wide or wider labiolingually than M3, even accounting for damage to the latter tooth, a pattern otherwise seen only in *Pharsophorus tenax*, *Arctodictis sinclairi*, *Patagosmilus goini*, and possibly *Borhyaena macrodonta* among short-snouted borhyaenoids.

The simple M4 crown of SGOPV 3490 consists of two poorly distinguished trigon cusps, a paracone and stylar cusp B, in addition to an extremely small protocone. There is no meta-

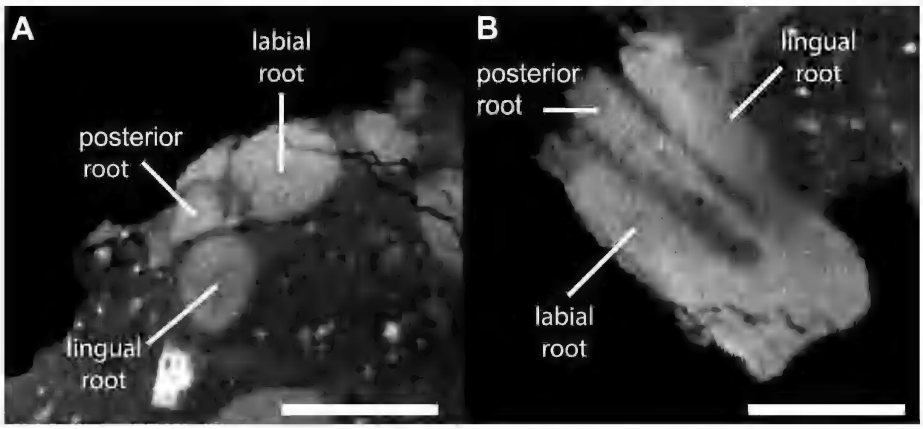

FIG. 14. Cross-sectional CT image of left M4 of SGOPV 3490 in **A,** oblique occlusal and **B,** posterior views. Shows presence of three roots. Scale bars = 5 mm.

cone. Both the paracone and stylar cusp B are nearly subsumed within the extremely well-developed preparacrista, though this may be exaggerated by wear. There is no anterior cingulum (preparacingulum) on M4. A labial cingulum, which occurs in some sparassodonts with simplified M4s (e.g., *Prothylacynus patagonicus*, MACN-A 707), is also absent in *Eomakhaira*. No vestigial postparacrista occurs posterior to the paracone, the presence of which has been described for *Patagosmilus* (Forasiepi and Carlini, 2010) and *Arctodictis* (Forasiepi, 2009).

The M4 protocone of *Eomakhaira* is tiny, barely a swelling of enamel on the lingual side of the paracone. This differs from the condition in *Callistoe* and *Patagosmilus*, in which the vestigial protocone is larger and more distinct from the trigon (Babot et al., 2002; Forasiepi and Carlini, 2010), as well as from *Borhyaena macrodonta* (MACN-A 32–390) and *Pharsophorus tenax* (AC 3192), in which the vestigial protocone retains a small basin. The M4 of *Proborhyaena* is unknown, and the M4 of *Paraborhyaena* could not be examined firsthand.

CT images of the left M4 of SGOPV 3490 show that this tooth has three roots despite its highly simplified morphology (fig. 14). The apices of the roots are located labially, lingually, and posteriorly, with the lingual and posterior roots merging basally, resulting in only two roots at the level of the crown. By contrast, most sparassodonts with a highly simplified ("linear") M4 are considered to have only two roots (but see below), including nearly all short-snouted borhyaenoids for which the M4 is known (i.e., *Acrocyon riggsi*, *Arctodictis* spp., *Borhyaena* spp., *Callistoe vincei*, *Paraborhyaena boliviana*, *Patagosmilus goini*, *Pharsophorus tenax*, *Prothylacynus patagonicus*, and *Thylacosmilus atrox*). *Australohyaena antiquua*, the only short-snouted borhyaenoid with a definitively three-rooted M4, is deeply nested within a clade otherwise characterized by double-rooted M4s (Forasiepi et al., 2015). This observation, combined with the fact that the third root in M4 of SGOPV 3490 could be identified only through CT imagery, raises the question of whether some sparassodonts currently identified as having a two-rooted M4 might instead have a three-rooted M4.

Despite the senescence of SGOPV 3490, there is no evidence of carnassial rotation like that seen in some sparassodonts (see Discussion for more details). Carnassial rotation results in a

unique wear pattern of completely flat wear facets with exposed dentine on the posterolingual faces of M1–3 (extending from the metastyle to the protocone) and the anterolingual face of M4 (fig. S7). Such wear facets are not seen in SGOPV 3490. Although the posterolingual corners of the left and right M3s are poorly preserved, these wear facets are clearly absent on the anterolingual face of M4. At the same time, the crowns of right M3 and left M3 and M4 appear to have been medially canted, a feature usually considered indicative of carnassial rotation (Mellett, 1969; Bond and Pascual, 1983). This canting is clearly not an artifact of postmortem distortion, as the crowns are slanted in opposite, complimentary directions on the left and right sides. Medially canted molars occur in all other borhyaenoids and hathliacynids, including many species that show no signs of carnassial rotation, even in the oldest individuals (see discussion). This demonstrates that molar canting occurs independently of, and is thus not necessarily indicative of, carnassial rotation. Whereas the posterior upper molars of *Eomakhaira* are medially canted, the posterior lower molars are laterally canted. Laterally canted posterior lower molars occur in other sparassodonts, such as *Australohyaena* (Forasiepi et al., 2015), *Arminiheringia*, and *Arctodictis*. Labial canting of the lower molars is possibly correlated with the lingual canting of the upper molars in many sparassodonts.

The lower molars of SGOPV 3490 are not strongly imbricated (fig. 15), at least not to the degree seen in the borhyaenids *Australohyaena*, *Acrocyon*, and *Arctodictis*, or the thylacosmiline *Thylacosmilus*. The m3–4 are slightly angled relative to the long axis of the toothrow, comparable in degree of imbrication to that seen in *Arminiheringia* and *Proborhyaena* but more imbricated than in *Paraborhyaena*, *Pharsophorus* (specifically the holotype, MACN-A 52-391), and possibly *Borhyaena* (based on MACN-A 52-366, assigned to *Borhyaena macrodonta*). In lateral view, the alveolar border of the lower molars, as approximated by the bases of the crowns (in the absence of most of the alveolar bone in this region), rises posteriorly at an angle of ~5°–6° relative to horizontal. Several factors suggest this is real rather than taphonomic. First, when the specimen is positioned such that the alveolar border is horizontal, the nasals point anterodorsally, a biologically unreasonable orientation. Second, the right P3/m1 are preserved in occlusion, and the alveolus of the right P3 is partially preserved, indicating that the right dentary has not moved relative to the cranium. Finally, a lower toothrow that rises posteriorly occurs in a few other sparassodonts, including *Arminiheringia auceta*, *Paraborhyaena boliviana*, *Arctodictis sinclairi*, *Australohyaena antiquua*, and possibly *Acrocyon riggsi* (Goin et al., 2007; fig. 8A). In those taxa, the alveolar border of the lower molars is angled at about 8° relative to horizontal, similar to the inferred angle in SGOPV 3490.

Little can be said about m1–2 of SGOPV 3490. As mentioned above, the occlusal morphology of right m1–2 has been obliterated by wear, whereas on the left side, m1 is missing its crown, and no trace of m2 is preserved, possibly due to greater distortion of the left side of the skull. The posterior lobes of the crowns of m1–2 are not lower than the anterior lobes, a condition that occurs to a variable degree in all borhyaenids, including *Prothylacynus*, *Plesiofelis*, *Pharsophorus* (including *P. lacerans* and *P. tenax* but not MPEF-PV 4170, the specimen from La Cantera assigned to *Pharsophorus*), *Proborhyaena*, and *Thylacosmilus*. In this respect, SGOPV 3490 resembles *Arminiheringia*. A small posterolabial cingulid occurs on the labial side of m1 in SGOPV

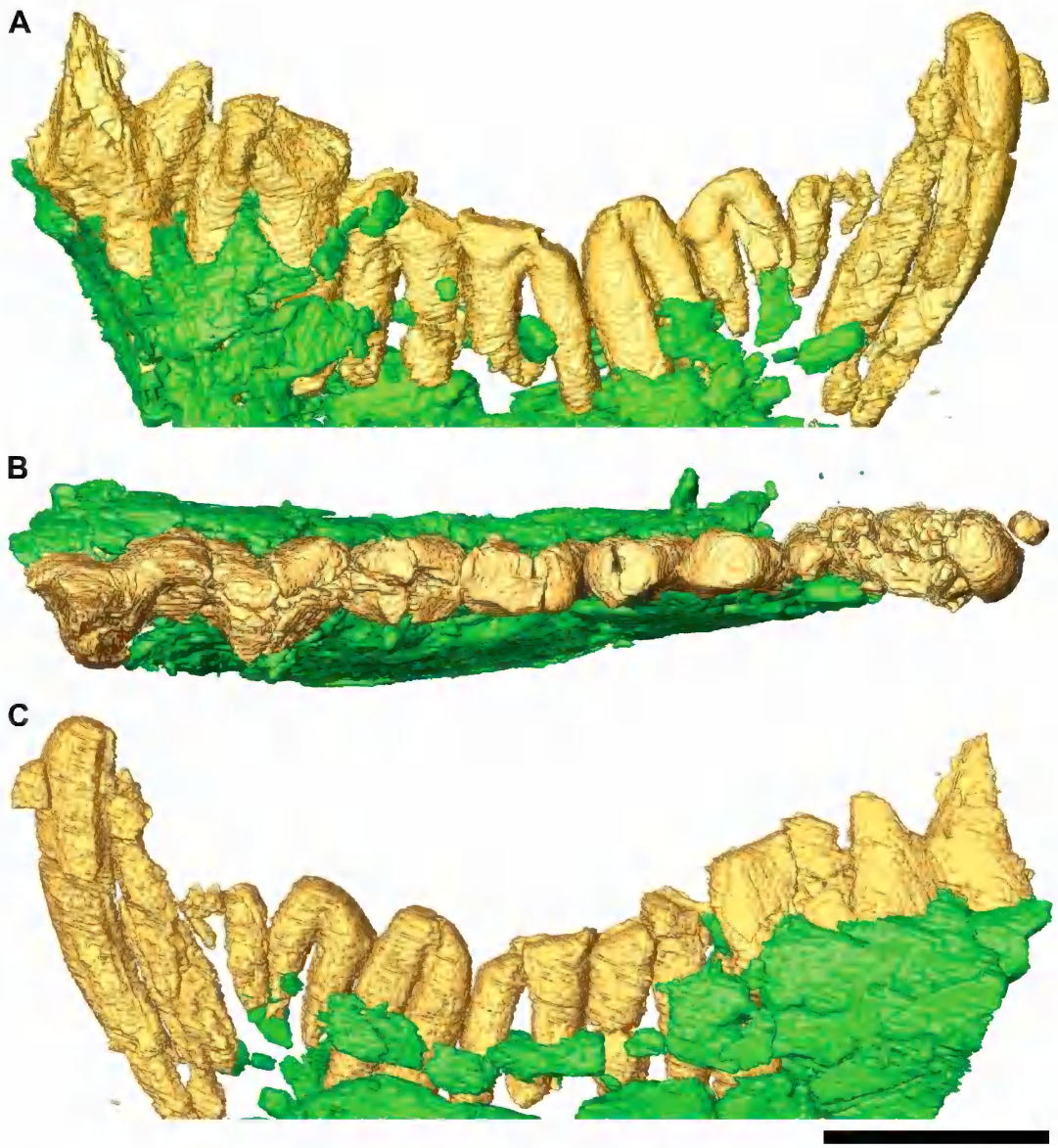

FIG. 15. Lower right dentition of SGOPV 3490 in **A,** labial, **B,** occlusal, and **C,** lingual views. Colors of elements in this CT segmentation are the same as in figure 3. Anterior to right in A, B and to left in C. Scale = 30 mm.

3490 (fig. 4). The presence or absence of a posterolabial cingulid cannot be evaluated in m2 or m3, but it is absent on m4. The presence of a labial postcingulid on m1 is not unexpected given its distribution among sparassodonts. Posterolabial cingulids are absent in the basal borhyaenoids *Lycopsis*, *Pseudothylacynus*, and *Prothylacynus* but are present in cf. *Nemolestes* (AMNH 29433; Forasiepi et al., 2015), *Plesiofelis*, *Pharsophorus* (both *P. lacerans* and *P. tenax*), all borhyaenids (*Acrocyon* spp., *Australohyaena antiquua*, *Arctodictis* spp., and *Borhyaena* spp.), and the proborhyaenid *Callistoe* (Forasiepi et al., 2015). This feature could not be scored for *Arminiheringia*,

Proborhyaena, or *Paraborhyaena*. The condition in thylacosmilines is not entirely clear. Photographs of the holotype of *Anachlysictis gracilis* in Goin (1997) appear to show a posterolabial cingulid, whereas figures of *Thylacosmilus* (Riggs, 1934; Marshall, 1976a) show a structure that could be a posterolabial cingulid. Most phylogenies of sparassodonts (Forasiepi, 2009; Engelman and Croft, 2014; Forasiepi et al., 2015; Suarez et al., 2016) imply at least six independent losses of the posterolabial cingulid (in *Hondadelphys*, *Stylocynus*, *Lycopsis*, *Prothylacynus*, and at least twice among hathliacynids, but see Phylogenetic Analysis below), or repeated loss and reacquisition of the posterolabial cingulid within Sparassodonta.

The right m4 is the best-preserved lower molar in SGOPV 3940 and the only tooth in which crown morphology has not been largely obliterated by wear. Nevertheless, its paracristid still is highly worn, comparable to the degree of wear in the holotype of *Angelocabrerus daptes* (MMP 967M; Simpson, 1970) and a specimen assigned to *Pharsophorus* cf. *P. lacerans* (MPEF-PV 4190; Goin et al., 2010). As in all borhyaenoids, the m4 of SGOPV 3490 is characterized by two main cusps, a tall protoconid and a slightly shorter paraconid. The m4 paraconid of SGOPV 3940 lacks an anteriorly projecting ventral keel, unlike most sparassodonts but as in proborhyaenids and possibly *Thylacosmilus*. The protoconid is tall relative to the anteroposterior length of the tooth (i.e., the height is greater than 90% the length of the tooth; see Muizon et al., 2018) and is wider at its midpoint that at its base, as in other sparassodonts. The m4 of SGOPV 3490 closely resembles that of *Proborhyaena* and *Paraborhyaena* in having a posteriorly salient protoconid at the posterior end of the tooth and a barely discernable talonid. The latter feature contrasts with m1–3, each of which shows evidence of a talonid that is very small and worn but nevertheless slightly larger.

The metaconid is clearly absent on the m4 of SGOPV 3490 (fig. 15). Assessing whether a metaconid was present or absent on m2–3 is more difficult due to the worn and highly fragmented preservation of these teeth, but this cusp appears to be absent on at least m3. In borhyaenoids with a metaconid (e.g., borhyaenids, *Pharsophorus*), this cusp often occurs as a small, low protuberance at the posterolingual corner of the tooth (see Forasiepi et al., 2015: figs. 10, 11). In SGOPV 3490, on the other hand, the posterolingual surface of m3–4 is smooth, and the base of the protoconid extends to the lingual margin of the tooth; there is no evidence that a distinct metaconid was present. In fact, the posterior margin of m3 is very similar to the holotype of *Arminiheringia auceta* (MACN-A 10970), consisting of a cuspless ridge that is oriented dorsolingually-ventrolabially.

The anterior root of the posterior lower molars (primarily m3–4) in SGOPV 3490 is much larger and more robust than the posterior one. This condition is also seen in several other proborhyaenids and borhyaenids, including *Borhyaena macrodonta*, *Borhyaena tuberata*, *Arctodictis sinclairi*, *Arctodictis munizi*, *Acrocyon riggsi*, *Acrocyon sectorius*, MLP 88-V-10-4 (the proborhyaenid from Antofagasta de la Sierra), *Arminiheringia auceta*, *Paraborhyaena boliviana*, *Proborhyaena gigantea*, and *Thylacosmilus atrox* (table S9). However, this condition is not present in the borhyaenid *Australohyaena antiquua*, the proborhyaenid *Callistoe vincei*, and all species of non-proborhyaenid, non-borhyaenid sparassodonts in which the state of the roots of the lower molars could be determined (e.g., *Hondadelphys*, hathliacynids, *Pharsophorus* spp.,

Prothylacynus patagonicus; see table S9). Disparity in size between the anterior and posterior roots varies among taxa. In *Arctodictis sinclairi* and *Arminiheringia auceta*, only the roots of m3–4 are unequal in size, whereas in *Arctodictis munizi*, *Proborhyaena gigantea*, *Paraborhyaena boliviana*, and *Thylacosmilus atrox*, it is the roots of m2–4 that are unequal. In SGOPV 3490, the anterior roots of m2–4 are larger than the posterior ones, but the disparity is much less in m2 than in m3–4. Molar roots differ in size among other groups of carnivorous mammals. The roots of m2–3 are similar in length and robustness in the extant bone-cracking *Sarcophilus harrisii*, while the anterior root of m4 is slightly more robust than, but the same length as, the posterior one (Fiani, 2015). This size disparity is also present in the lower carnassial (m1) of some carnivorans that are not specialized bone-crackers, including some species of barbourofelids (Tseng et al., 2010), felids, and *Cryptoprocta* (R.K.E., personal obs.).

PHYLOGENETIC ANALYSES

The equal-weights analysis produced 12 most-parsimonious trees (MPTs), each 1624 steps in length, with a consistency index of 0.302 and a retention index of 0.663. A strict consensus of these trees is shown in figure 16. The implied-weights analysis with k = 3 produced a single MPT with a best score of 179.21909 (fig. 17). The implied-weights analysis with k = 12 produced a single MPT with a best score of 72.67280 (fig. 18). Since the topologies of the MPTs in the three analyses are nearly identical, they are discussed together below.

In all three analyses, *Eomakhaira* is recovered as the basalmost member of Thylacosmilinae (basal to a clade of *Patagosmilus* + *Thylacosmilus*) within Proborhyaenidae (as defined above). *Eomakhaira* is recovered as a thylacosmiline in every equal-weights MPT, despite several characters coded as uncertainties (which results in TNT considering all possible coded character states when determining the MPT). Recovery of Thylacosmilinae within Proborhyaenidae is not due solely to the inclusion of *Eomakhaira*, as Thylacosmilinae is nested within Proborhyaenidae even when *Eomakhaira* is excluded from the analysis. Among proborhyaenids, the clade of *Paraborhyaena* + *Proborhyaena* and *Callistoe vincei* (as a distinct branch) represent successive outgroups to Thylacosmilinae. Proborhyaenidae (including Thylacosmilinae) has a high bootstrap support value (71) and a high Bremer support value (4) in the equal-weights analysis; in both implied-weights analyses (76 in the analysis where k = 3, 71 where k = 12), it has a high bootstrap support value. Proborhyaenidae is recovered as the sister group of Borhyaenidae, and the clade of Proborhyaenidae + Borhyaenidae has high bootstrap support values in all three analyses (84 under equal weights, 92 in the implied-weights analysis where k = 3, and 89 in the implied-weights analysis where k = 12).

Eomakhaira could only be coded for ~19.5% of the characters in this analysis (78 of 400 characters), and accurately coding some characters was hindered by the extreme dental wear and challenging preservation of the specimen. *Eomakhaira* is almost certainly a member of the clade composed of Borhyaenidae, Proborhyaenidae (including Thylacosmilinae), and their closest relatives (i.e., *Pharsophorus*) based on the unambiguous synapomorphies preserved (e.g., lingual median sulci on the canines, absence of the postpalatine torus foramen). It is

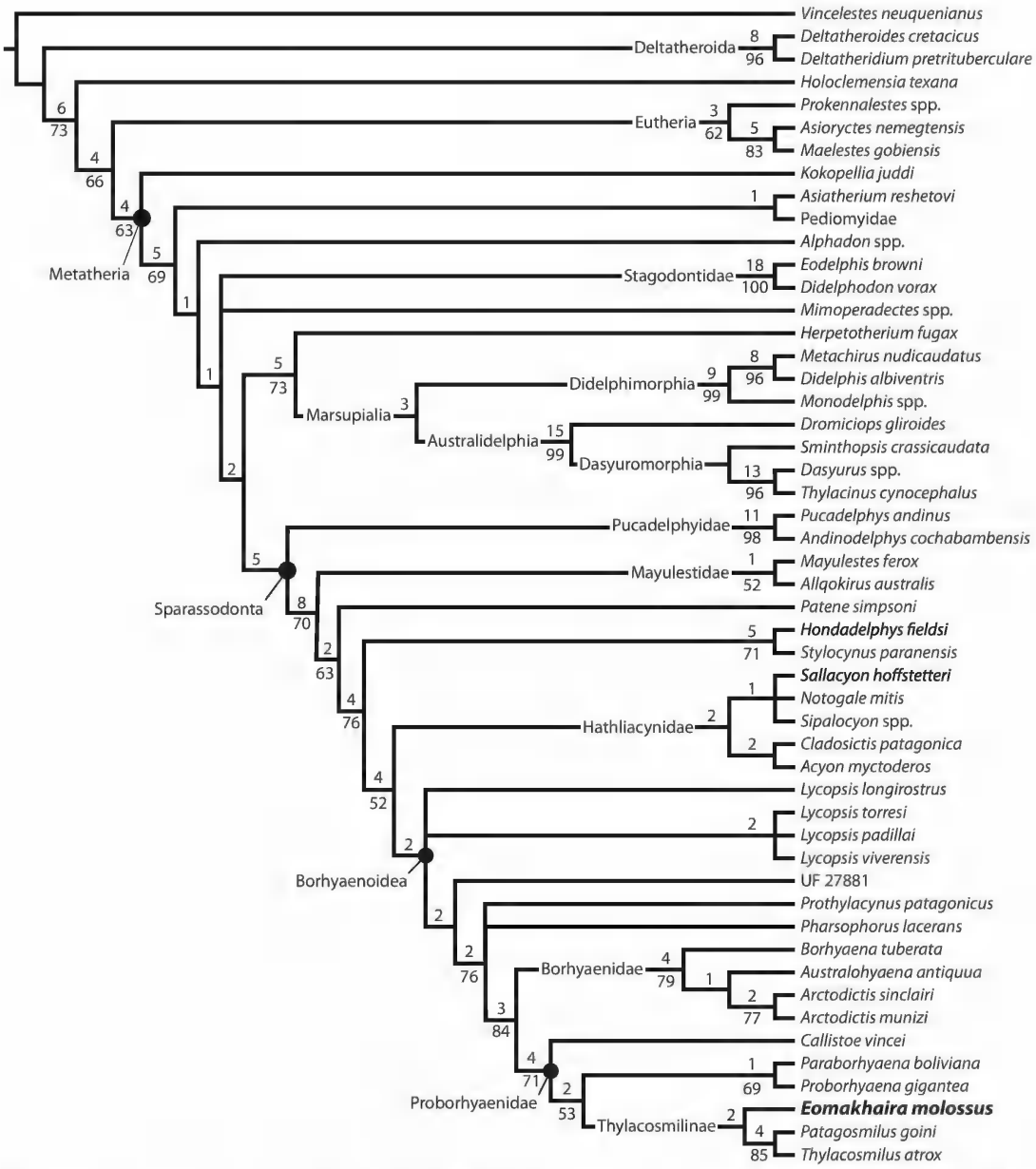

FIG. 16. Results of parsimony phylogenetic analysis under equal weights, showing the strict consensus of 12 most parsimonious trees (MPTs). *Eomakhaira molossus* in bold. Numbers to upper left of each node represent Bremer supports/decay indices, numbers to lower left of each node represent bootstrap values. Support values not given for Dasyuromorphia, as this node was constrained a priori (see text).

highly likely that it represents a proborhyaenid, though there is a small chance it could instead represent a borhyaenid or a *Pharsophorus*-like borhyaenoid. All most-parsimonious trees place it with Thylacosmilinae rather than among other proborhyaenids. Excluding *Eomakhaira* from Thylacosmilinae requires two additional steps to the MPTs and results in the new taxon occupying various more basal positions within Proborhyaenidae (as the most basal proborhyaenid, as sister to *Proborhyaena* + *Paraborhyaena*, etc.). Constraining *Eomakhaira* to be outside of Proborhyaenidae also requires two steps more than the MPTs, placing *Eomakhaira* as the nearest outgroup to Proborhyaenidae. Constraining *Eomakhaira* as a borhyaenid requires five steps more than the MPTs, and recovers *Eomakhaira* as the basalmost member of this group. Constraining *Eomakhaira* to be outside the clade of Borhyaenidae + Proborhyaenidae also requires five steps more than the MPTs, and results in *Eomakhaira* being recovered as the sister taxon of that clade. In all these analyses, *Patagosmilus* + *Thylacosmilus* remain nested within Proborhyaenidae. Constraining Proborhyaenidae (excluding Thylacosmilinae) and Thylacosmilinae to each be monophyletic (leaving *Eomakhaira* as a floating taxon) requires three steps more than the MPTs and recovers *Eomakhaira* as either the basalmost "proborhyaenid" or the basalmost thylacosmiline in different MPTs.

Deltatheroida and *Holoclemensia* are recovered as the most basal taxa in this analysis, outside of Theria. The placement of Deltatheroida may reflect the selection of *Vincelestes* as the outgroup, as deltatheroidans and other carnivorous mammals frequently exhibit secondarily simplified dentitions (Muizon and Lange-Badré, 1997; Solé and Ladevèze, 2017) that superficially resemble the nontribosphenic dentition of *Vincelestes*. Within Marsupialiformes, sparassodonts are recovered crownward of *Kokopellia*, *Asiatherium*, Pediomyidae, *Alphadon*, Stagodontidae, and *Mimoperadectes* (in the equal-weights analysis), sister to the Pucadelphyidae (*Pucadelphys* + *Andinodelphys*) within Pucadelphyida. Pucadelphyida is recovered either as sister to a clade of *Herpetotherium* + crown group Marsupialia (in the equal-weights analysis and implied-weights analysis with k = 12) or *Herpetotherium* is recovered as sister to Pucadelphyida and this clade is recovered as sister to crown-group Marsupialia (in the implied-weights analysis with k = 3).

Mayulestes, *Allqokirus*, and *Patene* are recovered as the earliest-diverging branches of Sparassodonta, with *Mayulestes* and *Allqokirus* as sister taxa and *Patene* apical to the clade of *Mayulestes* + *Allqokirus* but basal to the remainder of the group. This result resembles that of Rangel et al. (in press), who recovered *Mayulestes*, *Allqokirus*, and *Patene* as successively diverging lineages at the base of Sparassodonta, but it contrasts with that of Muizon et al. (2018), who recovered these three taxa as a monophyletic clade (Mayulestidae sensu Muizon et al., 2018). We agree with the assessment by Rangel et al. (2019) that the recovery of Mayulestidae in Muizon et al. (2018) is due to the latter study optimizing sparassodont or pucadelphyidan symplesiomorphies as apomorphies of *Mayulestes*, *Allqokirus*, and *Patene*.

In all three of our analyses, *Hondadelphys* and *Stylocynus* form a well-supported clade (Bremer support of 5 and bootstrap support of 71 in the equal-weights analysis, bootstrap support of 59 in the implied-weights analysis with k = 3, bootstrap support of 70 in the implied-weights analysis with k = 12) that is apical to *Mayulestes*, *Allqokirus*, and *Patene* but basal to

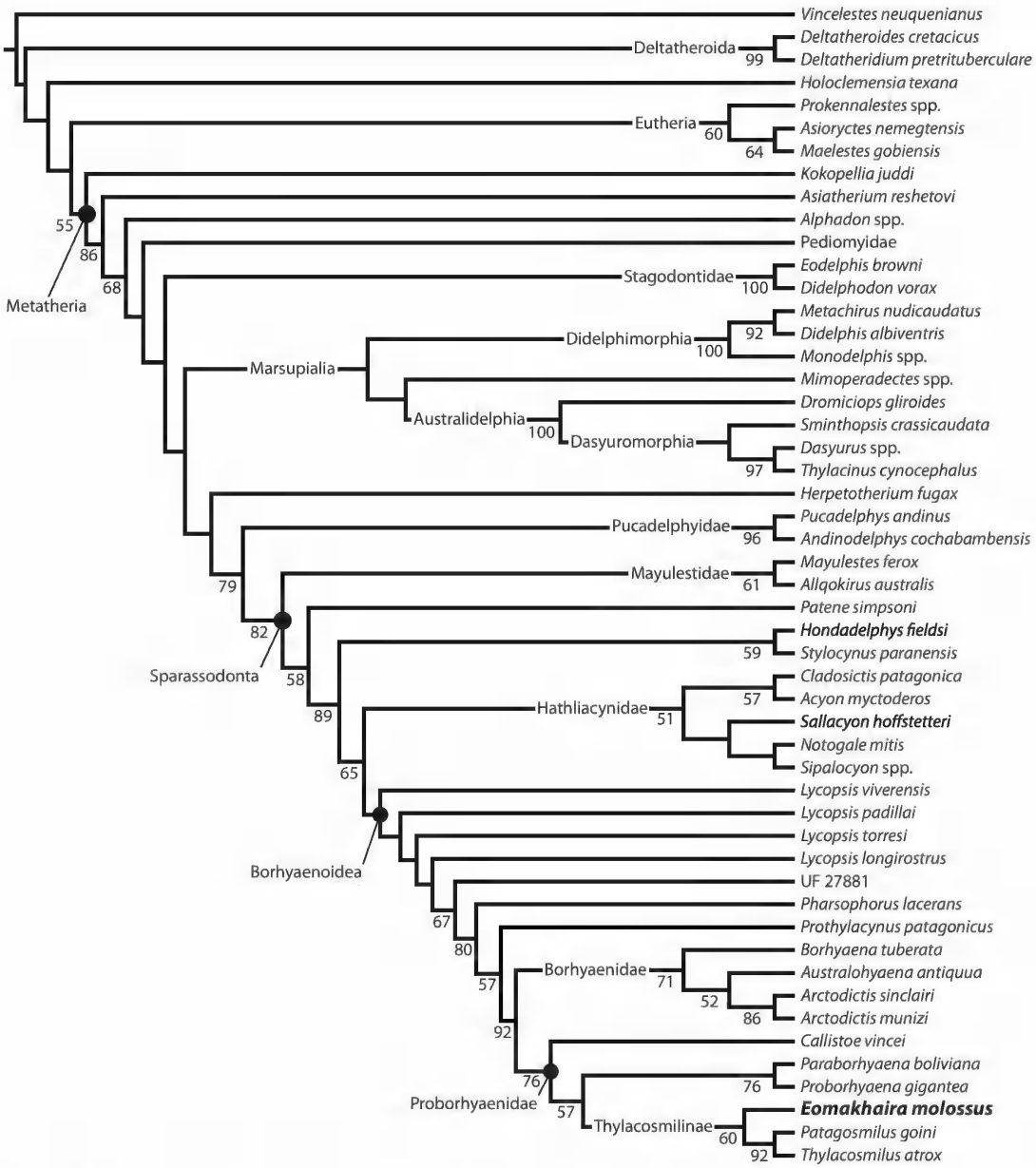

FIG. 17. Results of parsimony phylogenetic analysis under implied weights with concavity constant k = 3, showing the single recovered most parsimonious tree (MPT). *Eomakhaira molossus* in bold. Numbers to lower left represent bootstrap values. Support values not given for Dasyuromorphia, as this node was constrained a priori (see text).

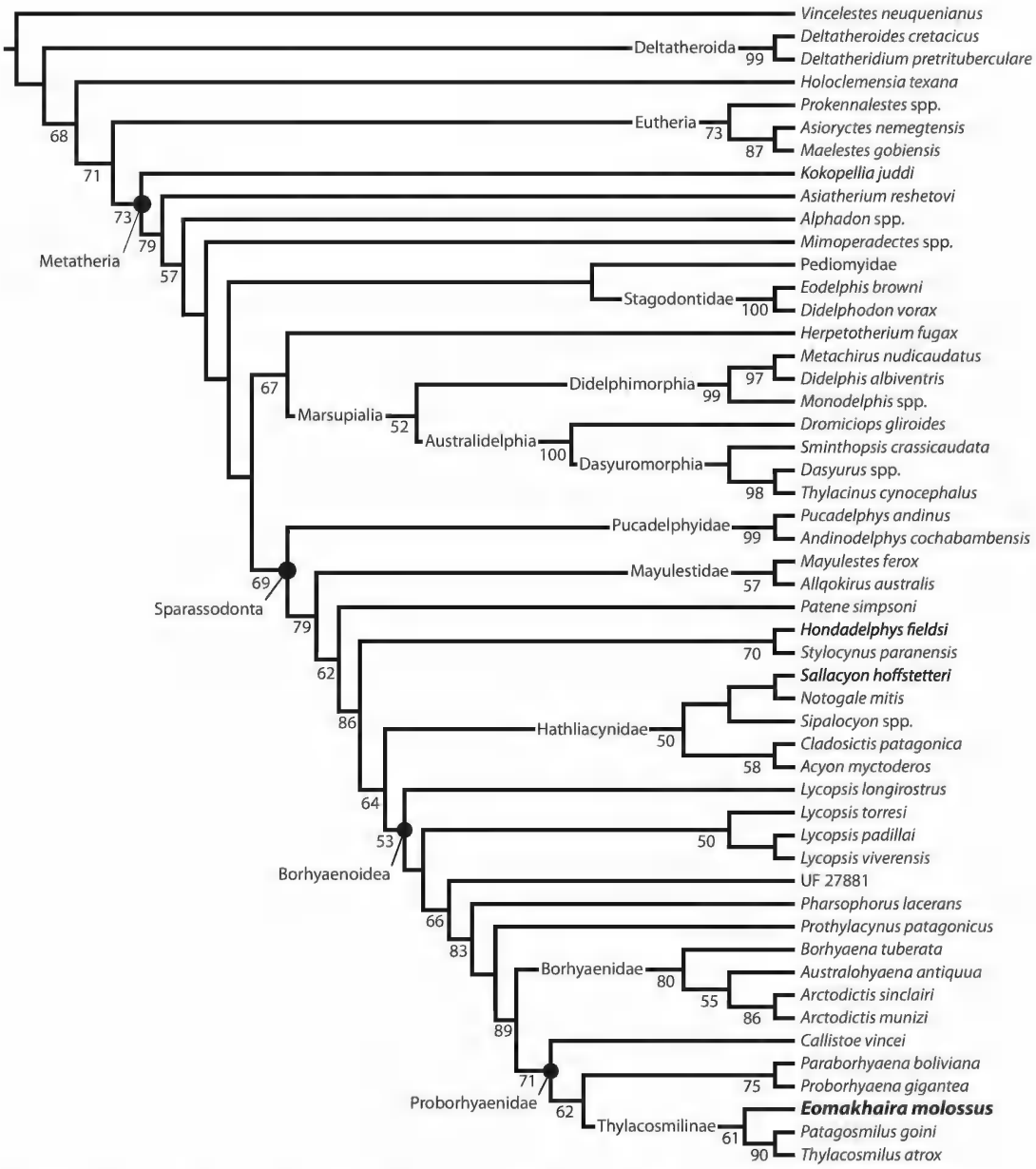

FIG. 18. Results of parsimony phylogenetic analysis under implied weights with concavity constant k = 12, showing the single recovered most parsimonious tree (MPT). *Eomakhaira molossus* in bold. Numbers to lower left represent bootstrap values. Support values not given for Dasyuromorphia, as this node was constrained a priori (see text).

Hathliacynidae + Borhyaenoidea. This contrasts with previous analyses (e.g., Forasiepi, 2009; Engelman and Croft, 2014; Forasiepi et al., 2015; Suarez et al., 2016), in which these two taxa were recovered as successively diverging branches just outside of Hathliacynidae + Borhyaenoidea. If the grouping of *Hondadelphys* + *Stylocynus* is upheld in future analyses, Hondadelphidae (Marshall et al., 1990: previously monotypic) might be the appropriate name for this clade. *Hondadelphys* and *Stylocynus* are united by several apomorphies, including a metacone positioned lingual to the paracone (char. 203: 1), well-separated paracone and metacone (char. 205: 0), large protocone (char. 209: 2), absence of StB (char. 228: 2), talonid wider than the trigonid (char. 244: 2), relatively short protoconid (char. 253: 0), and transverse posthypocristid (char. 270: 1). Several of these traits are often considered metatherian symplesiomorphies (all but chars. 228 and 244 are optimized as marsupialiform symplesiomorphies here), but in the current analysis, the character states of *Hondadelphys* and *Stylocynus* appear to be synapomorphic reversals within Sparassodonta. This is supported by the observation that these features are not observed in any Paleogene sparassodont (including additional taxa not considered in the present phylogenetic analysis, e.g., *Patene coluapiensis*, *Procladosictis anomala*). Some of these features may be functionally linked (i.e., width of the talonid and size of the protocone; chars. 209 and 244) or correlated with omnivory, but others are not (i.e., absence of StB) or are unique to *Hondadelphys* + *Stylocynus* within Sparassodonta. A clade of *Hondadelphys* + *Stylocynus* is also more congruent with the stratigraphic record of these taxa than previous phylogenetic analyses. *Hondadelphys* and *Stylocynus* date to the middle and late Miocene, respectively (Marshall, 1976b, 1979), and previous phylogenies that recovered them as successively diverging branches basal to Hathliacynidae + Borhyaenoidea imply a separate ghost lineage for each that extends back to the middle Eocene. By contrast, the present phylogeny requires only a single ghost lineage extending into the Paleogene (representing the common ancestor of the *Hondadelphys* + *Stylocynus* clade).

Relationships within Hathliacynidae are slightly better resolved in this analysis than in previous studies. The group is recovered as monophyletic with two major subclades in all analyses: one that includes the large-bodied hathliacynids *Cladosictis* and *Acyon*, and the other that consists a polytomy of *Sallacyon*, *Notogale*, and *Sipalocyon*. In the implied-weights analyses, the polytomy is resolved, with *Sallacyon* as the sister to *Notogale* + *Sipalocyon*. There has been little consensus regarding relationships within Hathliacynidae (Muizon, 1999; Forasiepi et al., 2006; Forasiepi, 2009; Suarez et al., 2016), as noted previously (Forasiepi et al., 2015). Some studies have even failed to recover a monophyletic Hathliacynidae (Muizon et al., 2018; Rangel et al., 2019).

The borhyaenoid *Lycopsis* is not unambiguously recovered as monophyletic. In some MTPs of the equal-weights analysis, *Lycopsis longirostrus* is sister to remaining species of *Lycopsis* (resulting in a monophyletic *Lycopsis*). In others, *L. longirostrus* is sister to all other borhyaenoids (including other species of *Lycopsis*, which form their own clade distinct from *L. longirostrus* and all other borhyaenoids), resulting in a paraphyletic *Lycopsis*. Thus, *L. longirostrus* forms part of a basal borhyaenoid polytomy in the consensus tree. In the implied-weights analysis with k = 3, the four species of *Lycopsis* form a series of successively diverging branches

at the base of Borhyaenoidea. *Lycopsis* is also recovered as paraphyletic in the implied-weights analysis with k = 12; *L. longirostrus* is at the base of Borhyaenoidea, and the remaining species of *Lycopsis* form a monophyletic clade. The paraphyly of *Lycopsis* is not surprising, as this taxon is not currently diagnosed by any synapomorphies uniquely shared by its four species (*Lycopsis torresi*, *L. longirostrus*, *L. padillai*, and *L. viverensis*) to the exclusion of other sparassodonts. Instead, *Lycopsis* has been diagnosed by general borhyaenoid apomorphies (Suarez et al., 2016) and a combination of features that are plesiomorphic relative to later-diverging borhyaenoids (e.g., *Prothylacynus*, Borhyaenidae, Proborhyaenidae). Even in cases where *Lycopsis* has been recovered as monophyletic (i.e., Suarez et al., 2016 and some of the equal-weights MPTs in this study), its monophyly is only supported by two characters: an infraorbital foramen located over the anterior root of P3 (char. 22: 0 of this study) and p3 with an anterior edge more convex than the posterior edge (ch. 194 [0] of this study). Neither of these character states are unique to *Lycopsis* spp. among sparassodonts nor definitely present in all four species referred to this genus (the former cannot be coded in *L. padillai* and *L. torresi*, and the latter cannot be coded in *L. padillai* and *L. viverensis*). Therefore, *Lycopsis sensu lato* may represent a grade of basal borhyaenoids rather than a monophyletic group.

DISCUSSION

Paleobiology of SGOPV 3490

Body Mass: Compared to other borhyaenoids, *Eomakhaira molossus* is notable for its small size. Regression equations of the lower dentition from Myers (2001) and Gordon (2003) yield body mass estimates of 9.5–10 kg for *Eomakhaira molossus* (table S10), comparable to a male Tasmanian devil (*Sarcophilus harrisii*; Rose et al., 2016). The holotype specimen, SGOPV 3490, is comparable in size to a skull of *Sarcophilus*, though SGOPV 3490 is deeper and narrower. This unusual shape is unlikely to be attributable to postmortem compression. While the skull has been subjected to shear deformation, there are no signs of significant dorsoventral or mediolateral crushing.

Eomakhaira is by far the smallest known Paleogene proborhyaenid (fig. 19, table S11), its estimated body mass being only ~40% of that of the next smallest, *Callistoe vincei* (~23 kg; Argot and Babot, 2011). Such a small proborhyaenid is quite unexpected during the Oligocene, given that non-thylacosmiline proborhyaenids reached their largest size during this interval. The two previously described Oligocene proborhyaenids, *Proborhyaena* and *Paraborhyaena*, both likely exceeded 50 kg in body mass (Zimicz, 2012; Prevosti et al., 2013; Croft et al., 2018). The small size of *Eomakhaira* indicates that proborhyaenids exhibited significantly more ecomorphological diversity than previously recognized during the Oligocene. This conclusion is corroborated by an unnamed proborhyaenid from the late Oligocene (Deseadan SALMA) locality of Taubaté (Couto-Ribeiro, 2010) that is comparable in size to *Arminiheringia auceta* (table S11), making it much larger than *Eomakhaira* but still smaller than *Paraborhyaena* and *Proborhyaena* (probably about 30–40 kg based on comparison with *A. auceta*; Prevosti et al., 2013; Croft et al., 2018). There are two possible explanations for the high ecomorphological diversity of proborhyaenids during the Oligocene. First, Oligocene proborhyaenids could rep-

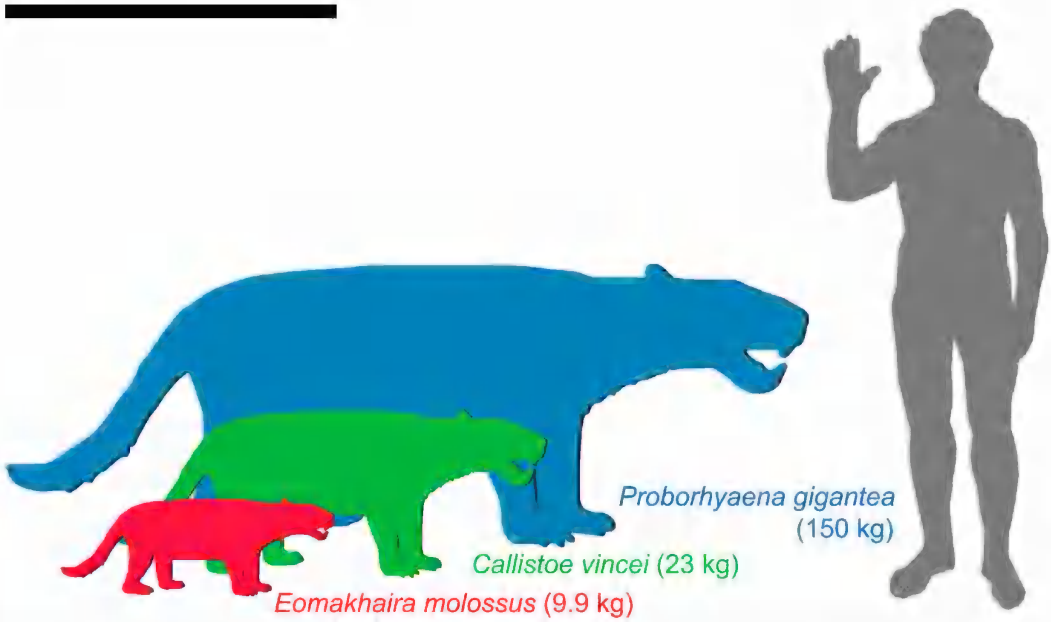

FIG. 19. Size comparison of representative Paleogene proborhyaenids. From largest to smallest, *Proborhyaena gigantea* (in blue), the largest known proborhyaenid (scaled after AMNH 29576, the largest specimen of this taxon); *Callistoe vincei* (in green), the smallest named proborhyaenid prior to this study (scaled after the holotype specimen, PVL 4187); *Eomakhaira molossus* (in red), scaled after SGOPV 3490. *Homo sapiens* (170 cm tall) to right for comparison. Body mass for *Proborhyaena* from Prevosti et al. (2013) and Croft et al. (2018), *Callistoe* from Argot and Babot (2011), and *Eomakhaira* from the present study. Silhouettes for *Proborhyaena* (CC-BY-SA 3.0), duplicated for *Callistoe* and *Eomakhaira*, and *Homo* (CC0 1.0) by Zimices, and NASA, respectively, from PhyloPic. Scale bar = 1 m.

resent holdovers from a much older unsampled Eocene radiation, of which only a few lineages (such as those that gave rise to *Proborhyaena* + *Paraborhyaena* and Thylacosmilinae) survived into the Oligocene. Alternatively, the high Oligocene diversity of Proborhyaenidae might reflect an Oligocene radiation related to faunal turnover at the Eocene-Oligocene transition, of which gigantism and small size/incipient machairodonty were but two evolutionary experiments. South American metatherians underwent a large faunal turnover during the Oligocene, likely in response to climatic change. This turnover (termed the Bisagra Patagónica) has been associated with the Eocene-Oligocene transition (EOT) by previous authors and has been considered analogous to the Grande Coupure in Europe and the Mongollian Remodelling in Asia (Goin et al., 2010; 2016; Abello et al., 2020). However, the peak of the turnover does not correlate with the EOT (and the faunal events associated with it on other continents) but instead occurs nearly 4 million years later, during the "middle" Oligocene (~30.6–30.7 Ma; "Canteran"; see Goin et al., 2010; Dunn et al., 2013). Regardless of its exact correlation with the EOT, this Oligocene turnover resulted in the extinction of many formerly dominant metatherian groups and subsequent radiation of the survivors (Goin et al., 2010; 2016; Abello et al., 2020). Among sparassodonts, these changes included the appearance of hathliacynids and borhyaenids in the

late Oligocene (Petter and Hoffstetter, 1983; Forasiepi et al., 2015). The extinction of non-thylacosmiline proborhyaenids at the end of the Oligocene has been considered an example of the long-term decline of a previously dominant group stemming from climatic changes during the Oligocene (Goin et al., 2016). However, given that gigantism and machairodonty do not occur in middle Eocene proborhyaenids such as *Callistoe* or *Arminiheringia*, proborhyaenids may have radiated in response to the environmental changes and faunal turnover during the Oligocene in a manner similar to hathliacynids and borhyaenids. The fossil record of proborhyaenids is too incomplete at present to favor either hypothesis, though they both represent avenues for future research.

The small size of *Eomakhaira* raises the possibility that an isolated m4 from the late Eocene (Mustersan) of Antofagasta de la Sierra in northwestern Argentina (MLP 88-V-10-4) belongs to the same taxon or a closely related form. Originally assigned to *Arminiheringia* by Goin et al. (1998), later authors (Babot et al., 2002; Babot, 2005; Powell et al., 2011) have referred this specimen to *Callistoe* based on its smaller size and reduced talonid. Although MLP 88-V-10-4 is larger than the corresponding tooth of the holotype of *Eomakhaira* (m4 length is 14.0 mm in MLP 88-V-10-4 versus 12.0 mm in SGOPV 3490), it is smaller than the corresponding tooth in the holotype of *Callistoe* (length = 17 mm; Babot et al., 2002). MLP 88-V-10-4 also more closely resembles SGOPV 3490 in the more posterior position of its protoconid and near absence of a talonid; in *Callistoe*, the protoconid is positioned more anteriorly and is less salient posteriorly, and the talonid is larger. Furthermore, MLP 88-V-10-4 lacks an anterolabial cingulid (Goin et al., 1998: fig. 7A), similar to *Proborhyaena*, *Paraborhyaena*, and *Thylacosmilus* (but apparently not the thylacosmiline *Anachlysictis*, see Goin, 1997: fig. 11.6B). This suggests that MLP 88-V-10-4 cannot be assigned to either of the currently recognized genera of Eocene proborhyaenids, *Callistoe* or *Arminiheringia*, in which an anterolabial cingulid is present on m4 (Babot et al., 2002). While the size and morphological resemblance support a potential close relationship with *Eomakhaira*, this is not definitive, as the state of the anterolabial cingulid cannot be determined in SGOPV 3490.

The small size of *Eomakhaira* relative to other proborhyaenids suggests that thylacosmilines were ancestrally characterized by small body size compared to other members of this group. *Eomakhaira* is small (9.5–10 kg) not only relative to Paleogene proborhyaenids but also to many late Cenozoic thylacosmilines (table S11). The proborhyaenid taxa stemward of the base of Thylacosmilinae are all relatively large (>20 kg), with the smallest of these species, *Callistoe*, being two and a half times larger than *Eomakhaira*. The only members of Proborhyaenidae (including thylacosmilines) comparable to *Eomakhaira* in size (table S11) are other geologically old thylacosmilines such as the Colhuehuapian thylacosmiline from Gran Barranca and the possible plesiomorphic thylacosmiline from La Venta (the latter being substantially smaller than *Eomakhaira*). The slightly larger *Patagosmilus goini* is estimated to have been less than 20 kg (Prevosti et al., 2013). If MLP 88-V-10-4 from the late Eocene of Antofagasta de la Sierra also pertains to *Eomakhaira* or a closely related form, it would further support the idea that thylacosmilines were ancestrally characterized by small body size, as MLP 88-V-10-4 is slightly larger than SGOPV 3490, potentially implying a decrease in size across the Eocene-Oligocene

boundary. The large body size and highly specialized morphology of non-thylacosmiline proborhyaenids has previously been used to argue against a close relationship between thylacosmilines and proborhyaenids sensu stricto (Simpson, 1948; Bond and Pascual, 1983), as large, morphologically specialized carnivorous mammal clades generally exist for short timespans (<10 million years) rather than continue to diversify for millions of years (Van Valkenburgh, 1999; Van Valkenburgh et al., 2004). Ancestrally small body size in thylacosmilines may have circumvented this pattern and allowed for a later, secondary acquisition of large body size in this clade later in the Cenozoic.

Dietary Habits: Several features suggest that borhyaenids and non-thylacosmiline proborhyaenids used p3, the largest and most robust premolar in all sparassodonts, to crack bones. These include an interlocking or fused mandibular symphysis, deep dentary, bulbous premolars (especially P/p3) with long roots, enamel microfractures, and high estimated bite force (Blanco et al., 2011; Ercoli et al., 2014; Forasiepi et al., 2015; Echarri et al., 2017). Contrary to a possible first impression of this robust-skulled new taxon, *Eomakhaira* does not seem to have been specialized for bone cracking (sensu Werdelin, 1989). Previous authors have noted that mandible depth in bone-cracking carnivorous mammals is often that same below the primary carnassial and the bone-cracking premolar, resulting in the ventral border of the horizontal ramus of the dentary to appear straight in lateral view (Palmqvist et al., 2011; Forasiepi et al., 2015). More specifically, Palmqvist et al. (2011) considered a uniformly deep mandible with a straight ventral border between the bone-cracking premolar and primary carnassial to distinguish obligate scavenging hyaenids (*Hyaena hyaena* and *Parahyaena brunnea*) from facultative scavengers that also hunt for prey (i.e., *Crocuta crocuta*, wherein the dentary is deeper beneath the carnassial than the bone-cracking premolar). This observation may not be broadly applicable, however, given that it is only based on extant hyaenids; extinct hyaenid species may have differed in their dietary habits despite similar mandible morphology (DeSantis et al., 2017). Moreover, since *Hyaena* and *Parahyaena* are considered sister taxa among extant hyaenids (e.g., Koepfli et al., 2006), it is not clear whether their similar mandible shape reflects functional morphology or shared ancestry. In extant metatherians, a uniformly deep dentary with a straight ventral border between the primary crushing tooth and carnassial is present not only in bone-cracking *Sarcophilus* but also in non-bone-cracking *Dasyurus*. Thus, this feature cannot be used to securely distinguish obligate bone-cracking scavengers from facultative bone-crackers.

In sparassodonts, a deep mandible with a straight ventral border and roughly uniform depth between p3 and m4 occurs in *Australohyaena*, *Proborhyaena*, *Paraborhyaena*, and *Arctodictis*, and these taxa have all been considered to be bone-crackers (Blanco et al., 2011; Zimicz, 2012; Ercoli et al., 2014; Forasiepi et al., 2015; Echarri et al., 2017). By contrast, the dentary is much shallower under p3 than under m4 in *Eomakhaira*, and the ventral border of the mandible is curved in lateral view. The symphysis of *Eomakhaira* is also much less extensive than in presumed bone-cracking sparassodonts. In most such sparassodonts, the symphysis extends posteriorly to at least the main bone-cracking premolar, often to the p3/m1 embrasure and sometimes to the posterior root of m1 (in *Arminiheringia auceta*; Babot et al., 2002; Zimicz,

2012). In the extant bone-cracking dasyuromorphian *Sarcophilus*, the symphysis extends to the midpoint of m1, which is functionally analogous to the p3 of sparassodonts. In *Eomakhaira*, the symphysis ends approximately at the level of the p2/p3 embrasure. Also, the roof of the skull is not vaulted at the level of the primary bone-cracking teeth in *Eomakhaira*, in contrast to the typical condition in other bone-cracking mammals (Werdelin, 1989), including *Australohyaena*, in which the nasals are vaulted (Forasiepi et al., 2015).

Zimicz (2012; 2014) and Forasiepi et al. (2015) used several metrics modified from Van Valkenburgh (1989) to examine dietary habits in carnivorous metatherians, primarily degree of specializations for bone-cracking (durophagy) and/or a carnivorous diet (i.e., hypercarnivory, mesocarnivory, etc.). Five of these parameters (premolar shape, relative premolar length, relative premolar size, relative trigonid length, and relative grinding area) can be applied to *Eomakhaira* (table 4). Premolar shape of the putative bone-cracking tooth (width/length of p3) reflects the robustness of the last lower premolar; it is 0.54 in *Eomakhaira*, slightly below the threshold separating bone-cracking from non-bone-cracking forms (bone-crackers >0.58). Relative premolar size (width of p3/cube root of body mass in kg) is 1.32, which is substantially lower than the threshold between bone-cracking and non-bone-cracking taxa (bone-crackers >2.6). The relative premolar length (length of p3/length of m4) is 0.63, below the threshold of hypercarnivores (hypercarnivores >0.7). However, extant metatherian hypercarnivores such as *Sarcophilus harrisii* and *Dasyurus maculatus* (see Maga and Beck, 2017), as well as many fossil sparassodonts exhibiting other specializations considered related to hypercarnivory (*Callistoe*, *Arminiheringia*, *Australohyaena*), also fall below this threshold, suggesting that this parameter is not applicable across metatherians.

With regard to the molars, the relative trigonid length (m4 trigonid length/total m4 length) of *Eomakhaira* is 0.91, within the range of specialized ("catlike") hypercarnivores and comparable to some of the most specialized carnivores within Sparassodonta, including the borhyaenoid *Angelocabrerus*; the borhyaenids *Australohyaena*, *Arctodictis*, and *Acrocyon*; the proborhyaenids *Proborhyaena* and *Paraborhyaena*; and the thylacosmiline *Thylacosmilus* (Zimicz, 2012; Forasiepi et al., 2015; Croft et al., 2018). Zimicz (2012) and Forasiepi et al. (2015) considered a relative trigonid length of >0.9 to indicate catlike hypercarnivory and a relative trigonid length of 0.8–0.9 to indicate hypercarnivory with bone-crushing specializations. However, only three extant bone-crushing taxa (*Crocuta crocuta*, *Hyaena hyaena*, and *Parahyaena brunnea*; all placental hyaenids) were included in the comparative dataset of those studies. *Hyaena* and *Parahyaena* are unusual among extant large-bodied hypercarnivores in having small but functional talonids on m1 (Ewer, 1954), whereas *Crocuta* more closely resembles felids in its longer trigonid and a near-vestigial talonid (and has a relative trigonid length >0.9; Van Valkenburgh, 1989). This difference may be related to the substantial amount of fruit consumed by *Parahyaena* and *Hyaena* (~12%–20% of diet by volume) but not by *Crocuta* (Kruuk, 1976; Owens and Owens, 1978; Mills, 2015). Molar trigonid length is unlikely to be correlated with bone-cracking habits in hyaenids, as hyenas primarily employ premolars in this function (Werdelin, 1989). Additionally, the relative trigonid lengths of the extant non-bone-cracking hypercarnivorous canids *Cuon*, *Lycaon*, and *Speothos* are only 0.72–0.74 (Van Valken-

TABLE 4. Morphometric values of the dentition used to infer dietary habits in *Eomakhaira molossus*. Methodology for calculating these parameters and critical values for dietary categories based on Van Valkenburgh (1989), Zimicz (2012), and Forasiepi et al. (2015).

Parameter	Value	Critical Values
Premolar shape (width of p3/length of p3)	0.54	Bone-crackers >0.58, other carnivores <0.58
Relative premolar size (width of p3/cube root of body mass in kg)	1.32	Bone-crackers >2.6, other carnivores <2.6
Relative premolar length (length of p3/length of m4)	0.63	Hypercarnivores >0.7, other carnivores <0.7
Relative trigonid length (length of m4 trigonid/length of m4)	0.91	"Catlike" hypercarnivores >0.9, bone-cracking hypercarnivores 0.8–0.9, other carnivores <0.8
Relative grinding area (square root of grinding area of m4/length of trigonid of m4)	~0	Hypercarnivores <0.48, other carnivores >0.48

burgh, 1989). The narrow range of relative trigonid lengths in living bone-cracking carnivorans (0.8–0.9) most likely reflects their low diversity ($N = 4$, the three hyaenids and *Sarcophilus harrisii*) and phylogenetic signal rather than any unique functional association; three of the four extant bone-crackers (*Crocuta crocuta*, *Hyaena hyaena*, and *Parahyaena brunnea*) belong to the same clade, and this range is within the variation seen in mammalian hypercarnivores more generally.

Relative grinding area (RGA) has been assessed via two methods in sparassodonts, one using only m4 (Prevosti et al., 2013) and the other assessing the entire lower molar row (Croft et al., 2018). Although the latter method is optimal (see Croft et al., 2018), m1–3 in the holotype of *Eomakhaira* are too heavily worn to calculate RGA in this manner. The m4 of *Eomakhaira* most closely resembles that of *Proborhyaena*, *Paraborhyaena*, *Arctodictis*, and *Thylacosmilus*, all of which were characterized by Prevosti et al. (2013) as lacking a functional talonid and therefore considered to have an RGA of 0. Evaluated together, the short mandibular symphysis, shallow dentary below p3, labiolingually narrow premolars that are small in proportion to those of bone-cracking taxa, long trigonid, and very small talonid of *Eomakhaira* suggest it was hypercarnivorous but not clearly specialized for bone crushing.

Carnassial Rotation in Sparassodonts

Mellett (1969) described an unusual phenomenon in the hyaenodont *Hyaenodon* in which the upper molars become progressively more medially oriented throughout ontogeny (carnassial rotation). Mellett (1969) also reported the occurrence of carnassial rotation in the hyaenodont *Hemipsalodon*, the oxyaenid *Patriofelis*, and "an unnamed Pliocene marsupial saber-tooth" (Mellett, 1969; almost certainly referring to *Thylacosmilus atrox*, given that no other well-preserved thylacosmilines were known at the time). Carnassial rotation has been documented in extinct carnivorans, including the barbourofelid *Barbourofelis* (see Baskin, 1981) and the nimravid

Hoplophoneus (see Bryant and Russell, 1995). Marshall (1978) reported carnassial rotation in several sparassodonts, most prominently *Arminiheringia auceta*, but also to a lesser degree in *Acrocyon*, *Arctodictis*, and *Borhyaena* (but see below). Bond and Pascual (1983) described carnassial rotation in a senescent specimen they assigned to *Proborhyaena* (MLP 79-XII-18-1). Carnassial rotation in the placental *Hyaenodon* and the metatherian *Arminiheringia* produces a very distinct form of wear in which the entire posterolingual face of the upper molars is worn flat and the dentine is exposed, even on the talon (fig. S7). This produces a sharp, flat edge with vertical wear facets that roughly parallels the main shearing blade of the tooth (typically the postmetacrista of upper molars) but relatively little apical wear. In the holotype of *Arminiheringia auceta* (MACN-A 10970/10972), in vivo wear had progressed to the point that the pulp cavities of M1–3 were exposed. Additionally, in the holotype of *A. auceta*, a second flat wear facet is present on the anterolingual face of M1–4, roughly parallel to the preparacrista. These facets are not present in *Hyaenodon* (M. Borths, personal commun.).

Aside from *Arminiheringia*, the only other sparassodonts for which true carnassial rotation appears to be present are the proborhyaenid *Callistoe vincei* and thylacosmiline *Thylacosmilus atrox*. The holotype of *Callistoe vincei* (PVL 4187) exhibits the same vertically flat wear facets seen in *Arminiheringia* on the entire posterolingual faces of M2–3 and anterolingual faces of M2–4 (M1 not being preserved in this specimen), including the talons. In *Thylacosmilus*, FMNH P14531 exhibits vertically flat wear facets on the posterolingual face of M3 and anterolingual faces of M4 (as determined from a cast of this specimen). Goin and Pascual (1987) found no evidence of ontogenetic carnassial rotation in *Thylacosmilus*, perhaps because they examined ontogenetically younger specimens (with less-worn teeth) than FMNH P14531, which pertains to an older individual with a highly worn dentition. Contra Marshall (1978), we have not observed carnassial rotation in any borhyaenid. The dentitions of borhyaenids are not characterized by flat wear facets across the entire lingual faces of the teeth; rather, wear facets are predominantly apical and follow the major cusps and crests of the crowns, as in most other faunivorous metatherians (e.g., *Didelphis*; see Crompton and Hiiemae, 1970). Bond and Pascual (1983) reported carnassial rotation in cf. *Proborhyaena* (MLP 79-XII-18-1) based on lingual canting of the upper molars and labial canting of the lower molars. However, as discussed below, neither of these features is necessarily indicative of carnassial rotation. The molars of MLP 79-XII-18-1 are too damaged to determine whether flat wear facets similar to those seen in *Arminiheringia* and *Thylacosmilus* were present. Carnassial rotation does not characterize all proborhyaenids despite its presence in *Callistoe*, *Arminiheringia*, and *Thylacosmilus*. Upper molars of *Proborhyaena gigantea* (AMNH 29576) clearly do not exhibit carnassial rotation. Wear facets on the upper molars of AMNH 29576 are restricted to their occlusal faces, as in most other sparassodonts.

Although only a handful of sparassodonts exhibit true carnassial rotation, many sparassodonts do exhibit upper molars that are medially canted. This condition can be identified by measuring the angle between the bases of the crowns of the posterior upper molars (M3–4) and the horizontal plane in posterior (distal) view; we consider an angle >35° indicative of canted molars. In general, the posteriormost upper molars (M3–4) show the highest degree of

canting, whereas more anterior molars (e.g., M1) are less canted and often comparable in orientation to the canines and premolars. In taxa with canted upper molars, the paracone and metacone are typically canted medially, and the occlusal faces of the upper molars are partially or completely obscured when the palate is in ventral view, sometimes to the point that the protocone is hidden by the trigon (figure S5 illustrates this condition in borhyaenids). In effect, this means that the upper molars are not oriented in occlusal view when the palate is viewed ventrally, something that can readily be seen when sparassodont skulls are figured in ventral view (Sinclair, 1906: pls. 42, 44, 48, 55, 59, 60; Babot et al., 2002: figs. 5C, 6B; Forasiepi, 2009: fig. 20; Forasiepi et al., 2015: figs. 2, 6A). In addition to SGOPV 3490, molars canted at angles >35° are present in the hathliacynids *Acyon myctoderos*, *Cladosictis patagonica*, and *Sipalocyon gracilis*, and in the borhyaenoids *Acrocyon riggsi*, *Arctodictis sinclairi*, *Prothylacynus patagonicus*, *Pharsophorus tenax*, and *Arminiheringia* sp. (table 5; fig. S8). By contrast, the angle between the palate and the crowns of M3–4 is 10°–25° in *Allqokirus australis*, *Patene simpsoni*, *Patene coluapiensis*, *Hondadelphys fieldsi*, and UF 27881 (as indicated by the alveoli of M2–3). Both states contrast with the condition in metatherians such as *Didelphis*, where the crown bases lie nearly level with the palate (angle <10°). The upper molars are also medially canted in *Australohyaena antiquua*, *Borhyaena* spp., *Callistoe vincei*, cf. *Proborhyaena*, *Paraborhyaena boliviana*, and *Thylacosmilus atrox*, but the precise angle cannot be determined from available photographs and published illustrations (which typically do not show the palate in posterior view). All undoubted members of Hathliacynidae + Borhyaenoidea that could be observed directly exhibit strongly medially canted upper molars.

Although the upper molars of many sparassodonts are medially canted, they do not appear to have undergone carnassial rotation as seen in *Hyaenodon* and *Arminiheringia*. Few sparassodonts exhibit the distinctive wear pattern observed in *Arminiheringia*, even in older individuals, suggesting that molar orientation changed little after eruption in those taxa. This interpretation is supported by MACN-A 5931 (*Prothylacynus patagonicus*) and MLP 82-V-1-1 (an undescribed specimen referred to *Arminiheringia* sp.), both subadults with M/m4 still erupting and little to no wear on M3 (Forasiepi and Sánchez-Villagra, 2014). In these individuals, M3 is already medially canted at an angle comparable to that seen in adult specimens, and M4 is erupting in a canted orientation (fig. S8B). Additionally, MLP 82-V-1-1 bears flat wear facets on the posterolingual faces of M1–2 similar those of the (adult) holotype of *Arminiheringia* (Forasiepi and Sánchez-Villagra, 2014: fig. 2B), indicating that carnassial rotation can be identified early in ontogeny in sparassodonts for which this condition is present. Thus, the upper molars of most sparassodonts appear to have erupted in a canted position rather than having rotated into that position later in life.

The morpho-functional significance of medially canted upper molars in sparassodonts is unclear, given that it appears to be uncorrelated to carnassial rotation. Mellett (1969) suggested that carnassial rotation, as occurs in *Hyaenodon*, maintained precise occlusion between the carnassials despite wear and prolonged the functional lifespan of the dentition in this taxon. According to Mellett (1969), a carnivorous mammal like *Hyaenodon*, with multiple shearing teeth, anisognathus lower jaws, and fused mandibular symphysis, cannot compensate for tooth

TABLE 5. Angle of medial canting of posterior upper molars in sparassodonts. Inward canting angle measured as angle between bases of M3–4 and palate in posterior view.

Taxon	Higher Taxon	Specimen	Angle
Eomakhaira molossus	Thylacosmilinae	SGOPV 3490	~42°
Arminiheringia sp.	Proborhyaenidae	MLP 82-V-1-1	43.89°
Acrocyon riggsi	Borhyaenidae	FMNH P13433	48.58°
Arctodictis sinclairi	Borhyaenidae	MLP 85-VII-3-1	49.07°
Pharsophorus tenax	Basal Borhyaenoidea	AC 3192	35.87°
Prothylacynus patagonicus	Basal Borhyaenoidea	MACN-A 5931	45.54°
Prothylacynus patagonicus	Basal Borhyaenoidea	MACN-A 706	38.55°
Acyon myctoderos	Hathliacynidae	UF 26921-26941	40.21°
Cladosictis centralis	Hathliacynidae	MACN-A 11639	34.92°
Cladosictis patagonica	Hathliacynidae	MACN-A 5950	38.45°
Cladosictis patagonica	Hathliacynidae	MACN-A 5927	44.69°
Sipalocyon gracilis	Hathliacynidae	MACN-A 692	46.72°
Sipalocyon gracilis	Hathliacynidae	YPM-VPPU 15373	38.27°
UF 27881	Sparassodonta incertae sedis	UF 27881	24.61°
Allqokirus australis	Basal Sparassodonta	MNHC 8267	22.81°
Hondadelphys fieldsi	Basal Sparassodonta	UCMP 37960	14.57°
Patene coluapiensis	Basal Sparassodonta	AMNH 28448	15.66°
Patene simpsoni	Basal Sparassodonta	MNRJ 1331-V	17.76°
Pucadelphys andinus	Pucadelphyidae	YPFB Pal 6472	5.7°
Didelphis virginiana	Didelphidae	TMM M-2517	8.3°
Dasyurus hallucatus	Dasyuridae	TMM M-6921	24.0°

wear via lateral motion of the lower jaw (as occurs in forms with unfused symphyses, such as most extant carnivorans), and carnassial rotation provided an analogous functional solution. However, medially canted upper molars occur in many sparassodonts with a ligamentous symphysis (e.g., *Acyon*, *Cladosictis*, *Sipalocyon*), which provides some symphyseal flexibility. The same is true for *Barbourofelis* and nimravid carnivorans. Although Baskin (1981) suggested that the long vertical symphysis of *Barbourofelis* would have been functionally equivalent to a fused symphysis, Bryant and Russell (1995) suggested that this taxon was capable of lateral lower jaw mobility. Furthermore, as noted, the upper molars of immature specimens of *Arminiheringia* sp. and *Prothylacynus patagonicus* are medially canted, M4 erupts in a canted orientation, and the angle between the base of the molar and the palate in these specimens is comparable to that of adult sparassodonts (including other specimens of the same taxa). This indicates that medial canting of the upper molars was not attained gradually over an animal's lifespan, as might be expected if canting maintained precise occlusion during wear, since M3–4

are already canted while they erupt. Finally, the lower molars of many sparassodonts are laterally canted (e.g., *Australohyaena antiquua*; see Forasiepi et al., 2015), a condition also present to a lesser degree in *Dasyurus* (see Macrini, 2005a). The lower molars of *Hyaenodon* are not canted, suggesting that the functional explanation for carnassial rotation in *Hyaenodon* by Mellett (1969) may not be applicable to sparassodonts (except possibly to *Arminiheringia*, *Callistoe*, and *Thylacosmilus*). Bryant and Russell (1995) suggested that canting in *Dinictis* and carnassial rotation in *Hoplophoneus* (medial canting and carnassial rotation do not cooccur in these taxa) counter heavy wear stemming from the dental morphology and more posterior location of the carnassials of these taxa compared to other carnivorans. Such reasoning would not apply to most metatherian carnivores (except *Thylacosmilus* and possibly *Patagosmilus*; Goin, 1997; Forasiepi and Carlini, 2010), whose primary carnassials (m4) are located at the anteroposterior midpoint of the mandible (Werdelin, 1987), as in carnivorans.

The mammaliaform *Morganucodon* exhibits medially canted posterior upper molars and uncanted anterior molars (Jäger et al., 2019), similar to what is described here for sparassodonts. *Morganucodon* also resembles many sparassodonts in having prominent pits on the maxilla that receive the main cusp of the lower molars and posterior upper molars positioned lingual to the lateral edge of the maxilla (i.e., "maxillary cheeks"), which suggest analogous jaw mechanics. These features have been argued to minimize "roll" (sensu Grossnickle, 2017) during mastication in *Morganucodon*, allowing precise occlusion despite mainly orthal jaw movements. However, canting of the upper molars in *Morganucodon* is interpreted to have increased tooth wear rates (Jäger et al., 2019), which runs counter to the view that upper molar canting prolongs the functional lifespan of the dentition (Mellett, 1969; Bryant and Russell, 1995).

Alternatively, canting of the posterior molars in sparassodonts may be related to their extremely tall lower molar protoconids compared to those of other carnivorous metatherians (Muizon et al., 2018). Canting may be a way to accommodate these tall teeth when the mouth is closed. The embrasure pits on the palate of many sparassodonts (e.g., Engelman and Croft, 2014) have been suggested to represent a similar adaptation to accommodate the extremely tall protoconids (Forasiepi, 2009; Muizon et al., 2018).

Proborhyaenidae and the Origin of Thylacosmilines

Implications of *Eomakhaira molossus* for Understanding the Evolution of Thylacosmilinae: Ever since the first well-preserved specimens of thylacosmilines were described (Riggs, 1933, 1934), the manner in which these animals acquired their distinctive, highly specialized machairodont morphology has been debated, as has their relationship to other sparassodonts. Based on various similarities, Scott (1937) tentatively linked *Thylacosmilus* and the Eocene proborhyaenid *Arminiheringia*, but this idea was questioned based on substantial morphological and temporal differences between *Thylacosmilus* and non-thylacosmiline proborhyaenids (Simpson, 1948; Marshall, 1976a; Bond and Pascual, 1983). Early workers were hampered in their attempts to link thylacosmilines to other sparassodonts because the only well-known member of the group was *Thylacosmilus atrox*, its geologically

youngest and most autapomorphic member, which shared few features with other taxa known at the time. Only much later did earlier-diverging forms with less extreme machairodont specializations come to light. Goin (1997) described two taxa from the middle Miocene locality of La Venta, Colombia, (Laventan SALMA) exhibiting less machairodont specializations than the Mio-Pliocene *Thylacosmilus*: the thylacosmiline *Anachlysictis gracilis* and a second taxon, questionably assigned to the group (IGM 251108). More recently, even older thylacosmiline remains have been described from the early Miocene (Colhuehuapian SALMA; Goin et al., 2007) and early middle Miocene (Colloncuran SALMA; Forasiepi and Carlini, 2010) of Patagonia. Paradoxically, these older Patagonian taxa appear to be more closely related to *Thylacosmilus* than to the taxa from La Venta, even though *Thylacosmilus* and the La Venta taxa are closer in age; this implies an older (likely pre-Miocene) origin of the clade (Goin et al., 2007; 2016).

Our phylogenetic analysis recovers the early Oligocene *Eomakhaira* as the basalmost member of a clade that includes the thylacosmilines *Patagosmilus* and *Thylacosmilus,* which collectively are nested within Proborhyaenidae. The idea of a close relationship between thylacosmilines and proborhyaenids sensu stricto is not novel. Several studies (Marshall et al., 1990; Muizon, 1999; Babot et al., 2002) have recovered proborhyaenids sensu stricto and thylacosmilines as sister groups, and several others (Babot, 2005; the equal-weights analysis of Forasiepi et al., 2015; Suarez et al., 2016; Muizon et al., 2018) have recovered Thylacosmilinae within a paraphyletic Proborhyaenidae. Carneiro (2018) recovered a paraphyletic Proborhyaenidae, with *Paraborhyaena* as sister group to Thylacosmilinae, but also found Borhyaenidae nested within this group, with *Callistoe* and *Arminiheringia* recovered as basal to a clade composed of Borhyaenidae + (*Paraborhyaena* + Thylacosmilinae). Support for a close relationship between Thylacosmilinae and Proborhyaenidae sensu stricto has not been universal in previous studies, and placements for Thylacosmilinae outside of Proborhyaenidae have also been suggested (Patterson and Marshall, 1978; Bond and Pascual, 1983; Goin, 1997, 2003; Forasiepi, 2009; Engelman and Croft, 2014; the implied-weights analysis of Forasiepi et al., 2015). Recovery of *Eomakhaira* as an Oligocene thylacosmiline not only breaks up the long ghost lineage between thylacosmilines and non-thylacosmiline proborhyaenids but also corroborates the nesting of thylacosmilines within Proborhyaenidae, given that *Eomakhaira* exhibits a combination of derived features occurring in other thylacosmilines and plesiomorphic features retained in non-thylacosmiline proborhyaenids.

Eomakhaira resembles non-thylacosmiline proborhyaenids and differs from other thylacosmilines in retaining lingual sulci on the upper canines, three premolars, replacement of dP3, and absence of a genial flange. Its P1 is asymmetric, which is likely ancestral for proborhyaenids given its presence in *Callistoe* and *Arminiheringia*; the tooth is unknown in *Proborhyaena* and *Paraborhyaena* and is interpreted as absent/lost in other thylacosmilines. SGOPV 3490 lacks enamel on the labial surface of the canines, which suggests that enamel, if present in *Eomakhaira*, was a simple cap lost through wear as in non-thylacosmiline proborhyaenids rather than a persistant band extending to the base of the tooth as in *Patagosmilus* and *Thylacosmilus* (Turnbull, 1978; Forasiepi and Carlini, 2010; Koenigswald, 2011), Finally, *Eomakhaira* may have had open-rooted (hypselodont) lower canines, as in non-thylacosmiline proborhyaenids but unlike

thylacosmilines. Its lower molars lack an anteriorly projecting ventral keel on the paraconid, as in non-thylacosmiline proborhyaenids (present in *Anachlysictis* but evidently absent in *Thylacosmilus* among thylacosmilines).

On the other hand, *Eomakhaira* has canines that lack longitudinal grooves, as other thylacosmilines (and, possibly, *Lycopsis viverensis*). The upper canines are narrow labiolingually compared to other sparassodonts, have a well-developed median keel, and lack a labial median sulcus. The maxilla of *Eomakhaira* is deep, as in other thylacosmilines (a condition acquired independently in borhyaenids), rather than shallow as in proborhyaenids. The dentary of *Eomakhaira* is intermediate in depth between those of other thylacosmilines and non-thylacosmiline proborhyaenids, shallower than in the Eocene proborhyaenids *Callistoe* and *Arminiheringia* (though possibly not the Oligocene *Paraborhyaena* and *Proborhyaena*) but deeper than in the thylacosmilines *Anachlysictis* and *Thylacosmilus*. The infraorbital foramen of *Eomakhaira* is located at the P3/M1 embrasure, a position more similar to thylacosmilines than most non-thylacosmiline proborhyaenids (except possibly *Proborhyaena*), in which it is located more anteriorly. The mandibular symphysis of *Eomakhaira* also more closely resembles that of thylacosmilines than non-thylacosmiline proborhyaenids. In most borhyaenoids (especially non-thylacosmiline proborhyaenids), the symphysis is broad anteroposteriorly and typically fused in adults. In *Eomakhaira*, the symphysis is unfused and much narrower, probably ending at the p2/3 embrasure (but perhaps as far posterior as the anterior root of p3). P3 of *Eomakhaira* is much longer than p3, and the lower premolar row is relatively short. Both conditions are reminiscent of other thylacosmilines, in which dP3 is much longer than p3, and the upper and lower premolar rows are relatively short (though in *Patagosmilus* and *Thylacosmilus*, there is a large diastema between the lower canine and premolars due to a more posterior position of the postcanine teeth; Goin, 1997; Forasiepi and Carlini, 2010). The M4 of *Eomakhaira* resembles that of *Patagosmilus* more than that of any other borhyaenoid examined in being gracile, anteroposteriorly narrow and labiolingually very wide compared with M1–3 and in having a vestigial protocone. Compared with M4 of *Eomakhaira* and *Patagosmilus*, the M4 of *Thylacosmilus* is anteroposteriorly longer than labiolingually wide (resulting in a robust tooth), due partly to the loss of its talon. Some features common to both *Eomakhaira* and later thylacosmilines may also occur in *Proborhyaena gigantea*, especially if MLP 79-XII-18-1 pertains to that species, and potentially represent synapomorphies at a deeper node within Proborhyaenidae; these include a shallow dentary, more posteriorly positioned infraorbital foramen, labiolingually narrow upper canines, and a P3 that is much larger than p3.

Evolution of Saber Teeth in Sparassodonta: Among eutherians, saber teeth have originated independently three or four times: in oxyaenid "creodonts" (Machaeroidinae), in nimravid and barbourofelid carnivoramorphans (if these are not sister taxa that were ancestrally machairodont; Wang et al., 2020), and in felid carnivorans (Machairodontinae) (Antón, 2013). Among metatherians, they are known to have evolved only once, in sparassodonts (suggestions that the extant didelphid *Monodelphis dimidiata* exhibits a saber-toothed morphology have not been supported by later analyses; Blanco et al., 2013; Chemisquy and Prevosti, 2014). This disparity between eutherians and metatherians is curious given the broad range of preda-

tory metatherians, which include deltatheroidans, stagodontids, the marsupialiform *Anatoliadelphys*, other groups of sparassodonts (i.e., hathliacynids), didelphids (i.e., sparassocynins, didelphins, and related forms), dasyurids, thylacinids, and thylacoleonids. One potential reason for the rarity of metatherian sabertooth lineages may be related to how their distinctive upper canines may have functioned. It has been argued that saber teeth would have required a considerable learning period to be used effectively (Emerson and Radinsky, 1980; Akersten, 1985; Antón and Galobart, 1999; Wheeler, 2011). Functional modeling of saber bites has shown that an imprecise bite can cause the canines to snag, can easily be be too shallow to be lethal, or can penetrate too deeply to be extracted from the prey (Wheeler, 2011). Elongate, labiolingually narrow upper canines are also vulnerable to breakage when subjected to sudden, unpredictable loads such as those produced by struggling prey (Van Valkenburgh and Ruff, 1987). Many eutherian sabertooths exhibited prolonged retention of the deciduous canines, which are also large and machairodont in these lineages (Bryant, 1988; Wysocki et al., 2015; Wysocki, 2019). It has been hypothesized that this extended retention time resulted in a longer "training" period, in which breakage would not have had permanent consequences (due to their eventual replacement).

Unlike eutherians, metatherians (including sparassodonts; Marshall, 1976c; Forasiepi and Sánchez-Villagra, 2014) lack deciduous canines and therefore have only one tooth generation at the canine locus, precluding "training" canines. At the same time, thylacosmiline sparassodonts are the only sabertooths with hypselodont canines, and this may be a different means to achieve the same end: a tooth that would eventually be replaced in the event of breakage (albeit by growth at the base rather than by wholesale replacement) (Marshall, 1976a). The results of our phylogenetic analysis suggest that open-rooted canines were not a novel innovation of thylacosmilines but a plesiomorphic feature inherited from non-sabertoothed ancestors (i.e., an apomorphy for proborhyaenids). This suggests that the absence of deciduous canines may have constrained the evolution of saber teeth in metatherians and that hypselodonty is a prerequisite for evolving saber teeth in this clade. This may be one reason why saber-toothed canines only evolved once in metatherians rather than repeatedly, as in eutherians. Deciduous canines are widespread within Eutheria, whereas hypselodont canines in metatherians appear to have a much narrower distribution. Therefore, developing saber teeth in metatherians would require not only selection for machairodonty but also the prerequisite of an uncommon morphology.

Open-rooted, ever-growing (hypselodont) canines in proborhyaenids (including thylacosmilines) are frequently considered a unique feature within Metatheria (Vieira and Astúa de Moraes, 2003; Goswami et al., 2011; Forasiepi and Sánchez-Villagra, 2014). However, they may be more widely distributed than generally realized. Hypselodont canines have been reported in peramelemorphians (Aplin et al., 2010; K. Travouillon, personal commun.), and CT scans of adult peramelemorphians show open-rooted canines with nontapering roots and open pulp cavities (Macrini, 2005b, 2007a). A CT scan of the nonsparassodont pucadelphyidan *Pucadelphys andinus*, interpreted as a sexually mature male (see Ladevèze et al., 2011), appears to show open-rooted upper canines (Macrini, 2007b). The canines of didelphids and dasyuromorphians are reported to be hypselodont by several authors (Jones, 1995, 2003; Voss and Jansa,

2009; Chemisquy and Prevosti, 2014; R. Voss, personal commun.; R. Beck, personal commun.), but we have not been able to confirm these observations. Among the aforementioned studies, Chemisquy and Prevosti (2014) is the only one that provides imagery to support their claim of hypselodonty in *Monodelphis dimidiata*. However, their radiographs are shown only in palatal view, making it difficult to determine whether the canine pulp cavities are actually open (or merely show the apical foramen). In one of the radiographs said to demonstrate an open root (Chemisquy and Prevosti, 2014: fig. 5B), the canine root is closed. Other CT scans (Macrini, 2001; DigiMorph Staff, 2004; Macrini, 2005a, c) and X-rays (Woolley, 2011; Fiani, 2015) of adult didelphids and dasyuromorphians show nonhypselodont canines. None of the canines of didelphids and dasyuromorphians we have observed exhibit the features associated with hypselodonty that have been described previously in proborhyaenids, such as absence of enamel, remodeling of the apex with well-developed compensatory wear facets, and great height of the tooth despite heavy wear (fig. 20).

The development of hypselodont, open-rooted canines in proborhyaenids may be the result of paedomorphosis. The canine roots of extant marsupials remain open much longer during ontogeny than those of most placentals (Jones, 2003; Chemisquy and Prevosti, 2014), and the canine roots of juvenile non-proborhyaenid sparassodonts remain open relatively late in ontogeny (Forasiepi and Sánchez-Villagra, 2014; Engelman et al., 2015). Combined with the observations above, the presence of closed roots in senescent proborhyaenids, such as SGOPV 3490 and MLP 79-XII-18-1 (Bond and Pascual, 1983), suggests that canine hypselodonty was achieved by delaying root closure until extremely late in ontogeny. Similar evolutionary transitions from closed-rooted to fully hypselodont teeth via postponement of root formation have been observed in other mammals, including notoungulates (Madden, 2015). It has also been suggested that paedomorphosis played a role in other aspects of thylacosmiline evolution, such as the retention of dP3 as a functional element in the adult dentition (Forasiepi and Sánchez-Villagra, 2014).

Other features in thylacosmilines typically related to machairodonty, such as those connected with a wide gape (Emerson and Radinsky, 1980; Slater and Van Valkenburgh, 2008; Antón, 2013), appear to have originated prior to the group's origin (i.e., among non-thylacosmiline proborhyaenids). In *Callistoe vincei*, the combined heights of the upper and lower canines are comparable to the height of only the upper canine of *Thylacosmilus* (see Powell et al., 2011). Thus, *Callistoe* and *Thylacosmilus* would have required comparable gapes to achieve clearance between the canines (Powell et al., 2011; Wroe et al., 2013).

The transverse processes of the atlas of *Callistoe* and *Thylacosmilus* are longer (anteroposteriorly) than wide (transversely), and extend far posterior to the caudal facets. This contrasts with the condition in *Prothylacynus*, *Borhyaena*, and *Arctodictis*, in which these processes are subequal in length and width and extend only slightly posterior to the posterior border of the caudal facets (Argot, 2003; Forasiepi, 2009). Similar distinctions in the morphology of the axial transverse processes are seen in comparisons between saber-toothed and non-saber-toothed felids, respectively (Akersten, 1985; Argot, 2004b; Salesa et al., 2005). Elongate transverse processes in saber-toothed felids increased the area of origin for the obliquus capitis cranialis and obliquus capitis

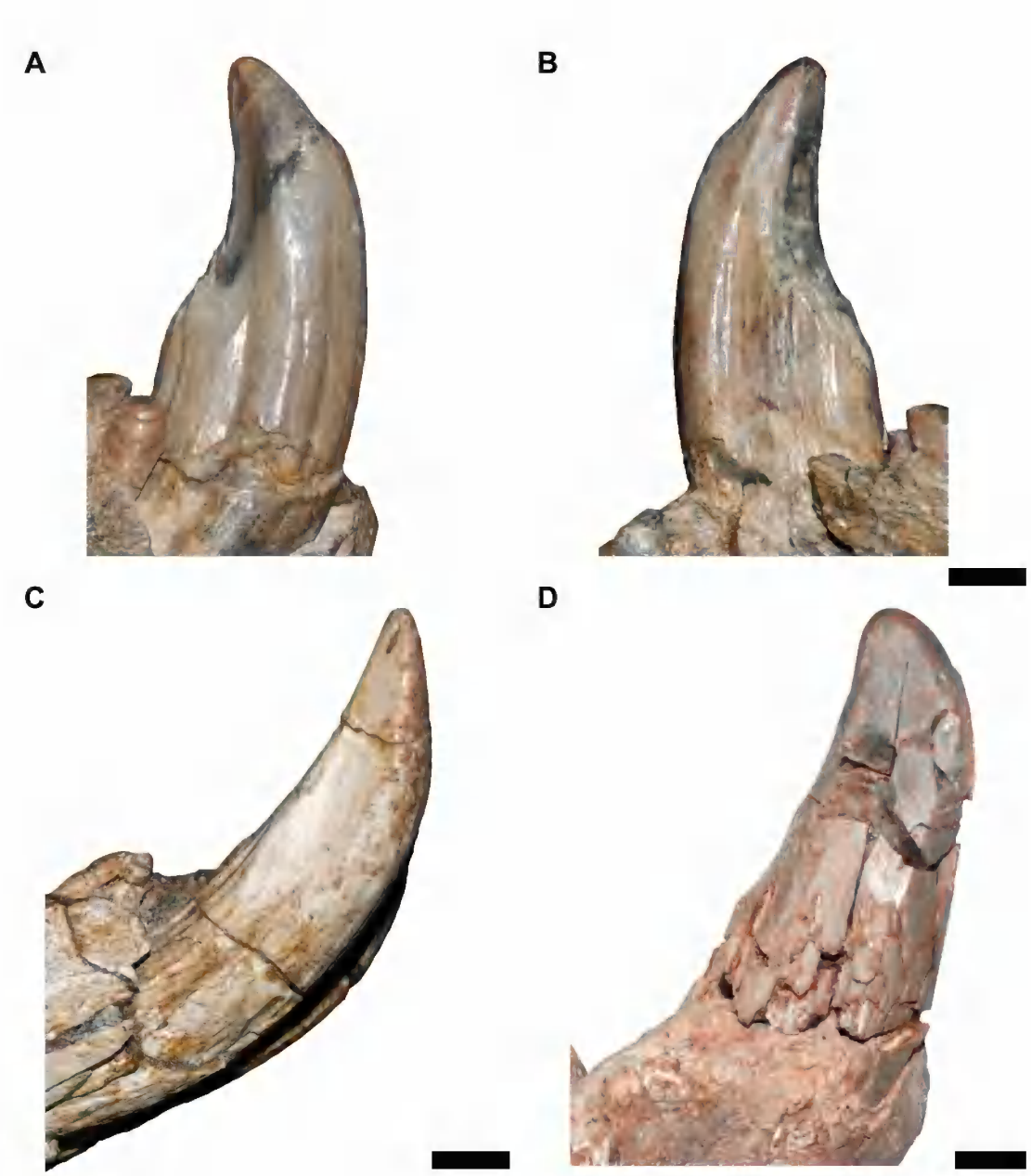

FIG 20. Lower canines of non-thylacosmiline proborhyaenids. **A–B**, *Proborhyaena gigantea* (MACN-A 52-382) in **A,** labial and **B,** lingual views. **C**, *Arminiheringia auceta* (MACN-A 10970) in labial view. **D**, *Paraborhyaena boliviana* (UATF-V-000129; left canine, reversed) in labial view. The upper canines of *Arminiheringia* show a comparable morphology (see fig. S4B; apices of the upper canines are unknown for *Proborhyaena* and *Paraborhyaena*). Scale bars = 10 mm.

caudalis (Antón and Galobart, 1999), which are thought to be the primary muscles involved in the saber bite in saber-toothed mammals (Akersten, 1985; Antón et al., 2004). The transverse processes of the atlas in *Thylacosmilus* resemble those of saber-toothed felids (Argot, 2004b: fig. 1C, D). The transverse processes of *Callistoe* (Argot and Babot, 2011: fig. 2D) extend further posteriorly than those of most sparassodonts but less posteriorly than in *Thylacosmilus*, suggestive of large obliquus capitis cranialis and obliquus capitis caudalis muscles in this non-saber-toothed taxon. This suggests that specialization of the neck musclature occurred in non-thylacosmiline proborhyaenids prior to the evolution of saber teeth in this clade.

The Oligocene *Paraborhyaena*, which is recovered as more closely related to *Thylacosmilus* than to *Callistoe* in our phylogenetic analyses (figs. 16, 17), shows additional similarities to *Thylacosmilus* in the posterior part of the skull not present in the geologically older *Callistoe*. (The posterior cranium is unknown in other proborhyaenids, such as *Proborhyaena* and *Patagosmilus*.) As in *Thylacosmilus*, the braincase of *Paraborhyaena* is short anteroposteriorly (Petter and Hoffstetter, 1983; Muizon et al., 2018), and the nuchal crest is nearly vertical, exposing the occipital condyles in dorsal view (Petter and Hoffstetter, 1983: fig. 2, pl. 4.1B). A shortened temporalis fossa (covarying with an anteroposteriorly short braincase) and vertical occiput, features common among saber-toothed mammals, have been considered to reflect either a wide gape or mechanical compensation of a reduced temporalis muscle lever arm created by a small coronoid process (see Emerson and Radinsky, 1980; Slater and Van Valkenburgh, 2008; Antón, 2013, and references therein). In *Proborhyaena*, *Eomakhaira*, and *Anachlysictis* (in which the temporal and occipital regions of the skull are unknown, but these taxa are phylogenetically bracketed by *Paraborhyaena* and *Thylacosmilus*), the coronoid process is large and dorsoventrally tall (Mones and Ubilla, 1978; Goin, 1997), contradicting the latter hypotheses. This suggests that proborhyaenids differed from placental sabertooths in acquiring a short braincase and vertical occiput early in their history (i.e., prior to appearance of saber teeth), whereas these features generally appeared after the acquisition of saber teeth in placentals (Antón, 2013).

Eomakhaira is considered a saber-toothed sparassodont here because it exhibits a degree of machairodont specialization comparable to that of early-diverging members of other saber-toothed clades, e.g., *Machaeroides*, *Dinictis*, *Nimravus*, and *Pseudaelurus*. Accordingly, saber-toothed sparassodonts (Thylacosmilinae) now have a documented biochron extending from the early Oligocene (32–33 Ma) to the early Pliocene (3 Ma), a duration of almost 30 million years (fig. 21), far longer than that of any placental sabertooth clade. Saber-toothed oxyaenid "creodonts" (Machaeroidinae) span approximately 11 million years (52.8–41.5 Ma; Dawson et al., 1986; Robinson et al., 2004; Kelly et al., 2012; Tomiya, 2013; Zack, 2019a, b), a minimum estimate given the clade's poor fossil record (no more than six species and fewer than 10 specimens). Securely dated and identified nimravids are known from the late Eocene (~37.8 Ma; Averianov et al., 2016; 2019) to the end of the Oligocene (23 Ma; Bryant, 1996; Peigné, 2003), a temporal range of 14.8 million years. Isolated upper canine fragments from Asia (Chow, 1958; Suyin et al., 1977; Averianov et al., 2016) may push the first appearance datum of this clade back into the late middle Eocene (~42 Ma), extending its temporal range to approximately 19 million years. However, given that these specimens consist of isolated fragments of upper canine saber teeth, they may pertain

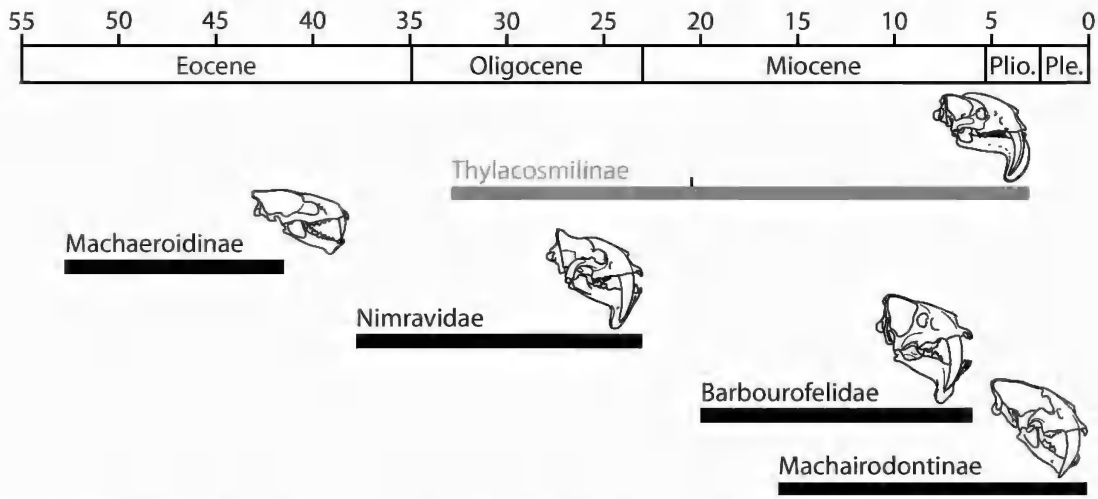

FIG. 21. Temporal durations of major lineages of mammalian saber-toothed carnivores, with metatherian lineage in grey and placental lineages in black. A representative skull of each clade is depicted to the right; from top to bottom: *Thylacosmilus atrox* (Thylacosmilinae), *Machaeroides eothen* (Machaeroidinae), *Hoplophoneus primaevus* (Nimravidae), *Barbourofelis fricki* (Barbourofelidae) and *Smilodon fatalis* (Machairodontinae). Images of *Machaeroides*, *Barbourofelis*, and *Smilodon* modified from Antón (2013), *Thylacosmilus* from Riggs (1934), and *Hoplophoneus* from Scott and Jepsen (1936) and Bryant (1996). Tick mark on Thylacosmilinae record represents the oldest occurrence of this clade (~20.2 Ma) prior to the discovery of *Eomakhaira*. Abbreviations: **Plio.**, Pliocene; **Ple.**, Pleistocene.

to another saber-toothed clade such as machaeroidine "creodonts" (see Zack, 2019b). Barbourofelid carnivoramorphans first appear in the early Miocene (20–19 Ma; Morales et al., 2001; Morlo et al., 2004) and are last recorded in the late Miocene (6 Ma; Tedford et al., 2004), a range of 13–14 million years. Finally, machairodontine felid carnivorans are recorded as early as the middle Miocene (16 Ma) based on the first appearance of *Pseudaelurus sensu stricto* (Werdelin et al., 2010; Robles et al., 2013) and last appear during the end-Pleistocene extinctions (~ 0.01 Ma), a temporal range of roughly 16 million years. Excluding *Eomakhaira*, the biochron of thylacosmilines spans at least 16 million years, based on a *Patagosmilus*-like upper molar from the early Miocene of Patagonia (Colhuehuapian SALMA, 20.2–20.0 Ma; Goin et al., 2007; Ré et al., 2010). Thus, even excluding *Eomakhaira,* the temporal range of thylacosmilines exceeds that of nimravids and barbourofelids and is comparable to that of machairodontines.

Sabertooth clades are generally characterized by high rates of extinction and turnover relative to other carnivorous mammals (Naples et al., 2011; Piras et al., 2018). This has been suggested to be related to their inferred specialized hunting behavior and comparatively narrow prey base (based on functional morphology and paleoecological data) and their status as hypercarnivorous apex predators, which would make them more vulnerable to ecological distruptions and environmental perturbations (Naples et al., 2011; Antón, 2013; Piras et al., 2018; and references therein). In this respect, the long stratigraphic range of thylacosmilines compared to placental saber-toothed clades is noteworthy considering the many major faunal/climatic changes faced by the former in South America, including the Bisagra Patagónica during the Oligocene (Goin et al., 2010), the faunal

turnover at the Oligocene-Miocene boundary (which, notably, marked the end of all non-thylacosmiline proborhyaenids; Bond and Pascual, 1983), the Middle Miocene Climatic Optimum and subsequent climatic deterioration (Croft et al., 2016), and the expansion of grasslands during the late Miocene (Pascual and Ortiz Jaureguizar, 1990). The shorter stratigraphic ranges of placental sabertooths relative to thylacosmilines do not appear to be attributable to competitive interactions between placental sabertooth clades in North America, Eurasia, and Africa compared to the relative isolation of thylacosmilines in South America, as placental sabertooth clades mostly do not overlap in space and time (e.g., North America's "cat gap" of Hunt and Joeckel, 1988). The large disparity between the temporal ranges of thylacosmiline metatherians and placental sabertooth clades suggests dissimilar ecological requirements, with thylacosmilines perhaps having broader dietary and/or habitat preferences. Thylacosmiline sparassodonts, a distinctive, diverse, and temporally long-lived lineage of machairodont mammals, hardly represent "inferior" or "ineffective" imitations of their placental analogs as frequently claimed (Riggs, 1934; Simpson, 1940; Patterson and Pascual, 1972; Werdelin, 1987; McNab, 2005; Prothero, 2006; Webb, 2006; Leigh et al., 2014; Faurby and Svenning, 2016; Faurby et al., In press). The discovery of *Eomakhaira* clarifies the evolution of machairodonty both within Sparassodonta and in mammals generally and speaks to the enduring utility of the South American fossil record in elucidating the splendid variety of morphological diversity among mammals and nature's fantastic capacity for convergence.

ACKNOWLEDGMENTS

We thank Reynaldo Charrier, an integral member of the field team that collected SGOPV 3490, who has unflaggingly supported paleontological studies in central Andes for decades. A. Charrier and G. Carrasco also were members of that exploration field party and contributed substantially to its success. M. Brown expertly prepared the specimen. We thank Z.-X. Luo and A. Isch of the University of Chicago for their help in CT scanning SGOPV 3490, and N. Gard, C. Holliday, and A. Isch for helpful discussions regarding segmentation and processing of CT data. We thank M.J. Babot, A. Forasiepi, C. Suarez, and T.E. Williamson for useful discussions and additional information regarding the anatomy of sparassodonts and other metatherians, M. Borths for discussions regarding carnassial rotation in "creodonts," and R. Beck for advice on the phylogenetic analysis. We are grateful to J. Galkin, A. Marcato, R. Voss, and E. Westwig (AMNH), R. Muelheim and T. Matson (CMNH), and D. Brinkman, M. Fox, and C. Norris (YPM-VPPU) for access to specimens in their care, and R. McCord (Arizona Museum of Natural History) for loans from the Larry Marshall Marsupial Dentition Collection. We thank R. Beck, M.J. Babot, and R. Voss for their reviews and insightful comments on earlier drafts of this manuscript. Finally, we remain indebted to the Museo Nacional de Historia Natural and Consejo de Monumentos Nacionales, Santiago, Chile, for continuing collaboration in investigations of the fossil history of Chile. This research was completed as part of a master's thesis in biology by R.K.E. at Case Western Reserve University. This research was supported by funding from the National Science Foundation (DEB-9317943, DEB-0317014, and DEB-0513476 to J.J. Flynn; DEB-9020213 and DEB-9318126 to A.R. Wyss) and the Frick Fund, Division of Paleontology, AMNH.

REFERENCES

Abello, M.A., N. Toledo, and E. Ortiz-Jaureguizar. 2020. Evolution of South American Paucituberculata (Metatheria: Marsupialia): adaptive radiation and climate changes at the Eocene-/Oligocene boundary. Historical Biology 32 (4): 476–493.

Akersten, W.A. 1985. Canine function in *Smilodon* (Mammalia, Felidae, Machairodontinae). Contributions in Science, Natural History Museum of Los Angeles County 356: 1–22.

Ameghino, F. 1897. Les mammifères crétacés de l'Argentine. Deuxième contribution à la connaissance de la faune mammalogique des couches à *Pyrotherium*. Boletín del Instituto Geográfico Argentino 18: 406–521.

Anaya Daza, F., B. Shockey, and D.A. Croft. 2010. Sparassodonts of Salla: species richness and new taxa of carnivorous marsupials from the late Oligocene of Bolivia. Journal of Vertebrate Paleontology, SVP Program and Abstracts, 2010: 53A.

Anders, U., W. von Koenigswald, I. Ruf, and B.H. Smith. 2011. Generalized individual dental age stages for fossil and extant placental mammals. Paläontologische Zeitschrift 85 (3): 321–339.

Antón, M. 2013. Sabertooth. Bloomington: Indiana University Press, 264 pp.

Antón, M., and À. Galobart. 1999. Neck function and predatory behavior in the scimitar toothed cat *Homotherium latidens* (Owen). Journal of Vertebrate Paleontology 19 (4): 771–784.

Antón, M., et al. 2004. Implications of the mastoid anatomy of larger extant felids for the evolution and predatory behaviour of sabretoothed cats (Mammalia, Carnivora, Felidae). Zoological Journal of the Linnean Society 140 (2): 207–221.

Antón, M., M.J. Salesa, and G. Siliceo. 2012. Machairodont adaptations and affinities of the Holarctic late Miocene homotherin *Machairodus* (Mammalia, Carnivora, Felidae): the case of *Machairodus catocopis* Cope, 1887. Journal of Vertebrate Paleontology 33 (5): 1202–1213.

Aplin, K.P., K.M. Helgen, and D.P. Lunde. 2010. A review of *Peroryctes broadbenti*, the giant bandicoot of Papua New Guinea. American Museum Novitates 3696: 1–41.

Argot, C. 2003. Functional adaptations of the postcranial skeleton of two Miocene borhyaenoids (Mammalia, Metatheria), *Borhyaena* and *Prothylacinus*, from South America. Palaeontology 46 (6): 1213–1267.

Argot, C. 2004a. Evolution of South American mammalian predators (Borhyaenoidea): anatomical and palaeobiological implications. Zoological Journal of the Linnean Society 140 (4): 487–521.

Argot, C. 2004b. Functional-adaptive features and palaeobiologic implications of the postcranial skeleton of the late Miocene sabretooth borhyaenoid *Thylacosmilus atrox* (Metatheria). Alcheringa: An Australasian Journal of Palaeontology 28 (1): 229–266.

Argot, C., and J. Babot. 2011. Postcranial morphology, functional adaptations and palaeobiology of *Callistoe vincei*, a predaceous metatherian from the Eocene of Salta, north-western Argentina. Palaeontology 54 (2): 447–480.

Averianov, A., E. Obraztsova, I. Danilov, P. Skutschas, and J. Jin. 2016. First nimravid skull from Asia. Scientific Reports 6: 25812.

Averianov, A., E. Obraztsova, I. Danilov, and J. Jin. 2019. Anthracotheriid artiodactyl *Anthracokeryx* and an upper Eocene age for the Youganwo Formation of southern China. Historical Biology 31 (9): 1115–1122.

Babot, M.J. 2005. Los Borhyaenoidea (Mammalia, Metatheria) del Terciario inferior del Noroeste argentino. Aspectos filogenéticos, paleobiológicos y bioestratigráficos. Ph.D. dissertation, Facultad de Ciencias Naturales e Instituto Miguel Lillo, Universidad Nacional de Tucumán, Tucumán, Argentina.

Babot, M.J., J.E. Powell, and C. Muizon, de. 2002. *Callistoe vincei*, a new Proborhyaenidae (Borhyaenoidea, Metatheria, Mammalia) from the early Eocene of Argentina. Geobios 35 (5): 615–629.

Barrett, P.Z. 2016. Taxonomic and systematic revisions to the North American Nimravidae (Mammalia, Carnivora). PeerJ 4: e1658.

Baskin, J.A. 1981. *Barbourofelis* (Nimravidae) and *Nimravides* (Felidae), with a description of two new species from the late Miocene of Florida. Journal of Mammalogy 62 (1): 122–139.

Beck, R.M.D. In press. Current understanding of the phylogeny of Metatheria: a review. *In* F.J. Goin and A.M. Forasiepi (editors), New World marsupials and their extinct relatives: 100 million years of evolution: Springer.

Bi, S., X. Jin, S. Li, and T. Du. 2015. A new Cretaceous metatherian mammal from Henan, China. PeerJ 3: e896.

Billet, G., C. Muizon, de, and B. Mamani Quispe. 2008. Late Oligocene mesotheriids (Mammalia, Notoungulata) from Salla and Lacayani (Bolivia): implications for basal mesotheriid phylogeny and distribution. Zoological Journal of the Linnean Society 152: 153–200.

Blanco, R.E., W.W. Jones, and G.A. Grinspan. 2011. Fossil marsupial predators of South America (Marsupialia, Borhyaenoidea): bite mechanics and palaeobiological implications. Alcheringa: an Australasian Journal of Palaeontology 35 (3): 377–387.

Blanco, R.E., W.W. Jones, and N. Milne. 2013. Is the extant southern short-tailed opossum a pigmy sabretooth predator? Journal of Zoology 291 (2): 100–110.

Bond, M., and R. Pascual. 1983. Nuevos y elocuentes restos craneanos de *Proborhyaena gigantea* Ameghino, 1897 (Marsupialia, Borhyaenidae, Proborhyaeninae) de la Edad Deseadense. Un ejemplo de coevolución. Ameghiniana 20 (1–2): 47–60.

Bryant, H.N. 1988. Delayed eruption of the deciduous upper canine in the sabertoothed carnivore *Barbourofelis lovei* (Carnivora, Nimravidae). Journal of Vertebrate Paleontology 8 (3): 295–306.

Bryant, H.N. 1996. Nimravidae. *In* D.R. Prothero and R.J. Emry (editors), The terrestrial Eocene-Oligocene transition in North America: 453–475. Cambridge: Cambridge University Press.

Bryant, H.N., and A.P. Russell. 1995. Carnassial functioning in nimravid and felid sabertooths: theoretical basis and robustness of inferences. *In* J.J. Thomason (editor), Functional morphology in vertebrate paleontology: 116–135. Cambridge: Cambridge University Press.

Cabrera, Á. 1927. Datos para el conocimiento de los dasiuroideos fósiles argentinos. Revista del Museo de La Plata 30: 271–315.

Carneiro, L.M. 2018. A new protodidelphid (Mammalia, Marsupialia, Didelphimorphia) from the Itaboraí Basin and its implications for the evolution of the Protodidelphidae. Anais da Academia Brasileira de Ciências 90 (suppl. 2): e20180440.

Cassini, G.H., D.A. Flores, and S.F. Vizcaíno. 2012. Postnatal ontogenetic scaling of nesodontine (Notoungulata, Toxodontidae) cranial morphology. Acta Zoologica 93 (3): 249–259.

Cassini, G.H., et al. 2017. Teeth complexity, hypsodonty and body mass in Santacrucian (Early Miocene) notoungulates (Mammalia). Earth and Environmental Science Transactions of the Royal Society of Edinburgh 106 (4): 303–313.

Charrier, R., J.J. Flynn, A.R. Wyss, L. Zapata, and C.C. Swisher, III. 1997. Antecedentes bio y cronoestratigráficos de la Formación Coya-Machalí–Abanico, entre los Ríos Maipo y Teno (33° 55′ y 35° 10′ L.S.), Cordillera Principal, Chile Central. VIII Congreso Geológico Chileno, Actas I: 465–469.

Chemisquy, M.A., and F.J. Prevosti. 2014. It takes more than large canines to be a sabretooth predator. Mastozoología Neotropical 21 (1): 27–36.

Chow, M. 1958. A record of the earliest sabre-toothed cats from the Eocene of Lushih, Honan. Science Record 2: 347–349.

Churcher, C.S. 1985. Dental functional morphology in the marsupial sabre-tooth *Thylacosmilus atrox* (Thylacosmilidae) compared to that of felid sabre-tooths. Australian Mammalogy 8 (3): 201–220.

Congreve, C.R., J.C. Lamsdell, and M. Ruta. 2016. Implied weighting and its utility in palaeontological datasets: a study using modelled phylogenetic matrices. Palaeontology 59 (3): 447–462.

Couto-Ribeiro, G.d. 2010. Avaliação morfológica, taxonômica e cronológica dos mamíferos fósseis da Formação Tremembé (Bacia de Taubate), Estado de São Paulo, Brasil. Master's thesis, Department of Zoology, Universidade de São Paulo, São Paulo, 122 pp.

Croft, D.A., R. Charrier, J.J. Flynn, and A.R. Wyss. 2008a. Recent additions to knowledge of Tertiary mammals from the Chilean Andes. I Simposio Paleontología en Chile, Museo Nacional de Historia Natural, Santiago. Libro de Actas: 91–96.

Croft, D.A., J.J. Flynn, and A.R. Wyss. 2008b. The Tinguiririca Fauna of Chile and the early stages of "modernization" of South American mammal faunas. Arquivos do Museu Nacional, Rio de Janeiro 66 (1): 191–211.

Croft, D.A., et al. 2016. New mammal faunal data from Cerdas, Bolivia, a middle-latitude Neotropical site that chronicles the end of the Middle Miocene Climatic Optimum in South America. Journal of Vertebrate Paleontology 36 (5): e1163574.

Croft, D.A., R.K. Engelman, T. Dolgushina, and G. Wesley. 2018. Diversity and disparity of sparassodonts (Metatheria) reveal non-analogue nature of ancient South American mammalian carnivore guilds. Proceedings of the Royal Society B: Biological Sciences 285: 20172012.

Crompton, A.W., and K. Hiiemae. 1970. Molar occlusion and mandibular movements during occlusion in the American opossum, *Didelphis marsupialis* L. Zoological Journal of the Linnean Society 49: 21–47.

Davis, B.M. 2007. A revision of "pediomyid" marsupials from the Late Cretaceous of North America. Acta Palaeontologica Polonica 52 (2): 217–256.

Dawson, M.R., R.K. Stucky, L. Krishtalka, and C.C. Black. 1986. *Machaeroides simpsoni*, new species, oldest known sabertooth creodont (Mammalia), of the Lost Cabin Eocene. Rocky Mountain Geology 24 (special paper 3): 177–182.

Degrange, F.J., J.I. Noriega, and J.I. Areta. 2012. Diversity and paleobiology of Santacrucian birds. *In* S.F. Vizcaíno, R.F. Kay, and M.S. Bargo (editors), Early Miocene paleobiology in Patagonia: high-latitude paleocommunities of the Santa Cruz Formation: 138–155. Cambridge: Cambridge University Press.

de Queiroz, K., and J. Gauthier. 1990. Phylogeny as a central principle in taxonomy: phylogenetic definitions of taxon names. Systematic Biology 39 (4): 307–322.

DeSantis, L.R.G., et al. 2017. Assessing niche conservatism using a multiproxy approach: dietary ecology of extinct and extant spotted hyenas. Paleobiology 43 (2): 286–303.

DigiMorph Staff. 2003. *Choloepus hoffmanni*. Digital Morphology, online resource (http://www.digimorph.org/specimens/Choloepus_hoffmanni/), accessed March 18, 2019.

DigiMorph Staff. 2004. *Sarcophilus laniarius*. Digital Morphology, online resource (http://digimorph.org/specimens/Sarcophilus_laniarius/), accessed January 28, 2019.

Dunn, R.E., et al. 2013. A new chronology for middle Eocene–early Miocene South American Land Mammal Ages. Geological Society of America Bulletin 125 (3–4): 539–555.

Echarri, S., M.D. Ercoli, M.A. Chemisquy, G. Turazzini, and F.J. Prevosti. 2017. Mandible morphology and diet of the South American extinct metatherian predators (Mammalia, Metatheria, Sparassodonta). Earth and Environmental Science Transactions of the Royal Society of Edinburgh 106 (4): 277–288.

Emerson, S.B., and L. Radinsky. 1980. Functional analysis of sabertooth cranial morphology. Paleobiology 6 (3): 295–312.

Engelman, R.K., and D.A. Croft. 2014. A new species of small-bodied sparassodont (Mammalia, Metatheria) from the middle Miocene locality of Quebrada Honda, Bolivia. Journal of Vertebrate Paleontology 34 (3): 672–688.

Engelman, R.K., F. Anaya, and D.A. Croft. 2015. New specimens of *Acyon myctoderos* (Metatheria, Sparassodonta) from Quebrada Honda, Bolivia. Ameghiniana 52 (2): 204–225.

Engelman, R.K., J.J. Flynn, P. Gans, A.R. Wyss, and D.A. Croft. 2018. *Chlorocyon phantasma*, a late Eocene borhyaenoid (Mammalia: Metatheria: Sparassodonta) from the Los Helados locality, Andean Main Range, Central Chile. American Museum Novitates 3918: 1–22.

Ercoli, M.D., F.J. Prevosti, and A.M. Forasiepi. 2014. The structure of the mammalian predator guild in the Santa Cruz Formation (late early Miocene). Journal of Mammalian Evolution 21: 369–381.

Ewer, R.F. 1954. Some adaptive features in the dentition of hyaenas. Annals and Magazine of Natural History 7 (75): 188–194.

Faurby, S., and J.-C. Svenning. 2016. The asymmetry in the Great American Biotic Interchange in mammals is consistent with differential susceptibility to mammalian predation. Global Ecology and Biogeography 25 (12): 1443–1453.

Faurby, S., L. Werdelin, and A. Antonelli. In press. Dispersal ability predicts evolutionary success among mammalian carnivores. bioRxiv. [doi.org/10.1101/755207]

Fiani, N. 2015. Dental Radiology. *In* L. Vogeinest and G. Allan (editors), Radiology of Australian mammals: 205–222. Collingwood: CSIRO Publishing.

Flynn, J.J., and A.R. Wyss. 2004. A polydolopine marsupial skull from the Cachapoal Valley, Andean Main Range, Chile. *In* G.C. Gould and S.K. Bell (editors), Tributes to Malcolm C. McKenna: his students, his legacy. Bulletin of the American Museum of Natural History 285: 80–92.

Flynn, J.J., A.R. Wyss, D.A. Croft, and R. Charrier. 2003. The Tinguiririca fauna, Chile: biochronology, paleoecology, biogeography, and a new earliest Oligocene South American Land Mammal "Age." Palaeogeography, Palaeoclimatology, Palaeoecology 195: 229–259.

Flynn, J.J., R. Charrier, D.A. Croft, and A.R. Wyss. 2012. Cenozoic Andean faunas: shedding new light on South american mammal evolution, biogeography, environments, and tectonics. *In* B.D. Patterson and L.P. Costa (editors), Bones, clones, and biomes: the history and geography of Recent Neotropical mammals: 51–75. Chicago: University of Chicago Press.

Forasiepi, A.M. 2009. Osteology of *Arctodictis sinclairi* (Mammalia, Metatheria, Sparassodonta) and phylogeny of Cenozoic metatherian carnivores from South America. Monografías del Museo Argentino de Ciencias Naturales 6: 1–174.

Forasiepi, A.M., and A.A. Carlini. 2010. A new thylacosmilid (Mammalia, Metatheria, Sparassodonta) from the Miocene of Patagonia, Argentina. Zootaxa 2552: 55–68.

Forasiepi, A.M., and M.R. Sánchez-Villagra. 2014. Heterochrony, dental ontogenetic diversity, and the circumvention of constraints in marsupial mammals and extinct relatives. Paleobiology 40 (2): 222–237.

Forasiepi, A.M., F.J. Goin, and V. di Martino. 2003. Una nueva especie de *Lycopsis* (Metatheria, Prothylacyninae) de la Formación Arroyo Chasicó (Mioceno Tardío) de la provincia de Buenos Aires. Ameghiniana 40 (2): 249–253.

Forasiepi, A., F.J. Goin, and A.A. Tauber. 2004. Las especies de *Arctodictis* Mercerat, 1891 (Metatheria, Borhyaenidae), grandes carnívoros del Mioceno del América del Sur. Revista Española de Paleontología 19 (1): 1–22.

Forasiepi, A., et al. 2006. A new species of Hathliacynidae (Metatheria, Sparassodonta) from the middle Miocene of Quebrada Honda, Bolivia. Journal of Vertebrate Paleontology 26 (3): 670–684.

Forasiepi, A.M., M.J. Babot, and N. Zimicz. 2015. *Australohyaena antiqua* (Mammalia, Metatheria, Sparassodonta), a large predator from the late Oligocene of Patagonia. Journal of Systematic Palaeontology 13 (6): 505–523.

Forasiepi, A.M., R.D.E. MacPhee, and S.H. del Pino. 2019. Caudal cranium of *Thylacosmilus atrox* (Mammalia, Metatheria, Sparassodonta), a South American predaceous sabertooth. Bulletin of the American Museum of Natural History 433: 1–64.

Futuyma, D.J. 1998. Evolutionary Biology, 3rd ed. Sunderland, MA: Sinauer Associates.

Gazin, C.L. 1946. *Machaeroides eothen* Matthew, the saber-tooth creodont of the Bridger Eocene. Proceedings of the United States National Museum 96: 335–347.

Goin, F.J. 1997. New clues for understanding Neogene marsupial radiations. *In* R.F. Kay, R.H. Madden, R.L. Cifelli, and J.J. Flynn (editors), Vertebrate paleontology in the Neotropics: the Miocene fauna of La Venta, Colombia: 187–206. Washington, DC: Smithsonian Institution Press.

Goin, F.J. 2003. Early marsupial radiations in South America. *In* M. Jones, C. Dickman, and M. Archer (editors), Predators with pouches: the biology of marsupial carnivores: 30–42. Collingwood, Victoria, Australia: CSIRO Publishing.

Goin, F.J., and R. Pascual. 1987. News on the biology and taxonomy of the marsupials Thylacosmilidae (late Tertiary of Argentina). Anales de la Academia Nacional de Ciencias Exactas, Físicas y Naturales de Buenos Aires 39: 219–246.

Goin, F.J., A. Candela, and G. López. 1998. Middle Eocene marsupials from Antofagasta de la Sierra, northwestern Argentina. Geobios 31 (1): 75–85.

Goin, F.J., et al. 2007. Los Metatheria sudamericanos de comienzos del Neógeno (Mioceno Temprano, Edad-mamífero Colhuehuapense). Parte I: Introducción, Didelphimorphia y Sparassodonta. Ameghiniana 44 (1): 29–71.

Goin, F.J., M.A. Abello, and L. Chornogubsky. 2010. Middle Tertiary marsupials from central Patagonia (early Oligocene of Gran Barranca): understanding South America's *Grande Coupure*. *In* R.H. Madden, A.A. Carlini, M.G. Vucetich, and R.F. Kay (editors), The paleontology of Gran Barranca evolution and environmental change through the Middle Cenozoic of Patagonia: 69–105. Cambridge: Cambridge University Press.

Goin, F.J., M.O. Woodburne, A.N. Zimicz, G.M. Martin, and L. Chornogubsky. 2016. A brief history of South American metatherians: evolutionary contexts and intercontinental dispersals. New York: Springer, 225 pp.

Goloboff, P.A. 2009. Rooting by multiple outgroup taxa. Online resource (https://groups.google.com/forum/#!topic/tnt-tree-analysis-using-new-technology/2xKZICp8wtk), accessed 2/14/2019.

Goloboff, P.A., J.A. Farris, and K.C. Nixon. 2008. TNT, a free program for phylogenetic analysis. Cladistics 24 (5): 774–786.

Goloboff, P.A., A. Torres, and J.S. Arias. 2018. Weighted parsimony outperforms other methods of phylogenetic inference under models appropriate for morphology. Cladistics 34 (4): 407–437.

Gordon, C.L. 2003. A first look at estimating body size in dentally conservative marsupials. Journal of Mammalian Evolution 10 (1–2): 1–21.

Goswami, A., N. Milne, and S. Wroe. 2011. Biting through constraints: cranial morphology, disparity and convergence across living and fossil carnivorous mammals. Proceedings of the Royal Society B: Biological Sciences 278 (1713): 1831–1839.

Grossnickle, D.M. 2017. The evolutionary origin of jaw yaw in mammals. Scientific Reports 7: 45094.

Hitz, R.B., J.J. Flynn, and A.R. Wyss. 2006. New basal Interatheriidae (Typotheria, Notoungulata, Mammalia) from the Paleogene of central Chile. American Museum Novitates 3520: 1–32.

Hunt, R.M.J., and R.M. Joeckel. 1988. Mammalian biozones in nonmarine rocks of the North American continental interior: biostratigraphic resolution within the "cat gap." Rocky Mountain Section, Geological Society of America Abstracts with Program 20: 421.

Jäger, K.R.K., P.G. Gill, I. Corfe, and T. Martin. 2019. Occlusion and dental function of *Morganucodon* and *Megazostrodon*. Journal of Vertebrate Paleontology 39 (3): e1635135.

Jones, M.E. 1995. Guild structure of the large marsupial carnivores in Tasmania. Ph.D. dissertation, Department of Zoology, University of Tasmania, Hobart, 143 pp.

Jones, M.E. 2003. Convergence in ecomorphology and guild structure among marsupial and placental carnivores. *In* M. Jones, C. Dickman, and M. Archer (editors), Predators with pouches: the biology of carnivorous marsupials: 285–296. Collingwood, Victoria, Australia: CSIRO Publishing.

Kealy, S., and R. Beck. 2017. Total evidence phylogeny and evolutionary timescale for Australian faunivorous marsupials (Dasyuromorphia). BMC Evolutionary Biology 17 (1): 240.

Kelly, T.S., P.C. Murphey, and S.L. Walsh. 2012. New records of small mammals from the middle Eocene Duchesne River Formation, Utah, and their implications for the Uintan-Duchesnean North American Land Mammal Age transition. Paludicola 8 (4): 208–251.

Koenigswald, W., von. 2011. Diversity of hypsodont teeth in mammalian dentitions – construction and classification. Palaeontographica Abteilung A 294 (1–3): 63–94.

Koenigswald, W., von, and F.J. Goin. 2000. Enamel differentiation in South American marsupials and a comparison of placental and marsupial enamel. Palaeontographica Abteilung A 255 (4–6): 129–168.

Koepfli, K.-P., et al. 2006. Molecular systematics of the Hyaenidae: relationships of a relictual lineage resolved by a molecular supermatrix. Molecular Phylogenetics and Evolution 38 (3): 603–620.

Krause, J.M., et al. 2017. New age constraints for early Paleogene strata of central Patagonia, Argentina: implications for the timing of South American Land Mammal ages. GSA Bulletin 129 (7–8): 886–903.

Kruuk, H. 1976. Feeding and social behavior of the striped hyaena (*Hyaena vulgaris* Desmarest). East African Wildlife Journal 14: 91–111.

Ladevèze, S., C.d. Muizon, R.M.D. Beck, D. Germain, and R. Cespedes-Paz. 2011. Earliest evidence of mammalian social behaviour in the basal Tertiary of Bolivia. Nature 474: 83–86.

Leigh, E.G., A. O'Dea, and G.J. Vermeij. 2014. Historical biogeography of the isthmus of Panama. Biological Reviews 89 (1): 148–172.

López-Aguirre, C., M. Archer, S.J. Hand, and S.W. Laffan. 2017. Extinction of South American sparassodontans (Metatheria): environmental fluctuations or complex ecological processes? Palaeontology 60 (1): 91–115.

Lorente, M., L. Chornogubsky, and F.J. Goin. 2016. Presencia de un posible boriénido (Mammalia, Metatheria) en el Eoceno temprano medio de la localidad de La Barda (Provincia de Chubut, Argentina). Paper presented at the XXX Jornadas Argentinas de Paleontología de Vertebrados, Buenos Aires, Argentina.

Macrini, T.E. 2001. *Monodelphis domestica*. Digital Morphology, online resource (http://digimorph.org/specimens/Dasyurus_hallucatus), accessed January 28, 2019.

Macrini, T.E. 2005a. *Dasyurus hallucatus*. Digital Morphology, online resource (http://digimorph.org/specimens/Dasyurus_hallucatus), accessed January 28, 2019.

Macrini, T.E. 2005b. *Isoodon macrourus*. Digital Morphology, online resource (http://digimorph.org/specimens/Isoodon_macrourus/), accessed November 12, 2019.

Macrini, T.E. 2005c. *Didelphis virginiana*. Digital Morphology, online resource (http://digimorph.org/specimens/Didelphis_virginiana), accessed January 28, 2019.

Macrini, T.E. 2007a. *Macrotis lagotis*. Digital Morphology, online resource (http://digimorph.org/specimens/Macrotis_lagotis/), accessed April 19, 2019.

Macrini, T.E. 2007b. *Pucadelphys andinus*. Digital Morphology, online resource http://digimorph.org/specimens/Pucadelphys_andinus/), accessed November 12, 2019.

Madden, R.H. 2015. Hypsodonty in mammals: Evolution, geomorphology and the role of earth surface processes, Cambridge: Cambridge University Press, 443 pp.

Madden, R.H., R.F. Kay, M.G. Vucetich, and A.A. Carlini. 2010. Gran Barranca: a 23-million-year record of middle Cenozoic faunal evolution in Patagonia. *In* R.H. Madden, A.A. Carlini, M.G. Vucetich, and R.F. Kay (editors), The paleontology of Gran Barranca evolution and environmental change through the Middle Cenozoic of Patagonia: 423–439. Cambridge: Cambridge University Press.

Maddison, W.P., and D.R. Maddison. 2008. Mesquite: a modular system for evolutionary analysis. 2.75.

Madzia, D., and A. Cau. 2017. Inferring 'weak spots' in phylogenetic trees: application to mosasauroid nomenclature. PeerJ 5: e3782.

Maga, A.M., and R.M.D. Beck. 2017. Skeleton of an unusual, cat-sized marsupial relative (Metatheria: Marsupialiformes) from the middle Eocene (Lutetian: 44–43 million years ago) of Turkey. PLoS ONE 12 (8): e0181712.

Marshall, L.G. 1976a. Evolution of the Thylacosmilidae, extinct saber-tooth marsupials of South America. Paleobios 23: 1–30.

Marshall, L.G. 1976b. New didelphine marsupials from the La Venta fauna (Miocene) of Colombia, South America. Journal of Paleontology 50 (3): 402–418.

Marshall, L.G. 1976c. Notes on the deciduous dentition of the Borhyaenidae (Marsupialia: Borhyaenoidea). Journal of Mammalogy 57 (4): 751–754.

Marshall, L.G. 1978. Evolution of the Borhyaenidae, extinct South American predaceous marsupials. University of California Publications in Geological Sciences 117: 1–89.

Marshall, L.G. 1979. Review of the Prothylacyninae, an extinct subfamily of South American "dog-like" marsupials. Fieldiana Geology (new series) 3: 1–49.

Marshall, L.G., J.A. Case, and M.O. Woodburne. 1990. Phylogenetic relationships of the families of marsupials. *In* H.H. Genoways (editor), Current Mammalogy 2: 433–505. New York: Plenum Press.

McKenna, M.C., A.R. Wyss, and J.J. Flynn. 2006. Paleogene pseudoglyptodont xenarthrans from central Chile and Argentine Patagonia. American Museum Novitates 3536: 1–18.

McNab, B.K. 2005. Uniformity in the basal metabolic rate of marsupials: its causes and consequences. Revista Chilena de Historia Natural 78: 183–198.

Meachen-Samuels, J.A. 2012. Morphological convergence of the prey-killing arsenal of sabertooth predators. Paleobiology 38 (1): 1–14.

Mellett, J.S. 1969. Carnassial rotation in a fossil carnivore. American Midland Naturalist 82 (1): 287–289.

Mills, M.G.L. 2015. Living near the edge: a review of the ecological relationships between large carnivores in the arid Kalahari. African Journal of Wildlife Research 45 (2): 127–137.

Molnar, R.E., and F.M. Vasconcellos, de. 2016. Cenozoic dinosaurs in South America – revisited. Memoirs of Museum Victoria 74: 363–377.

Mones, A., and M. Ubilla. 1978. La edad Deseadense (Oligoceno inferior) de la Formación Fray Bentos y su contenido paleontologico, con especial referencia a la presencia de *Proborhyaena* cf. *gigantea* Ameghino (Marsupialia: Borhyaenidae) en el Uruguay. Nota preliminar. Comunicaciones Paleontologicas del Museo de Historia Natural de Montevideo 7 (1): 151–158.

Morales, J., M.J. Salesa, M. Pickford, and D. Soria. 2001. A new tribe, new genus and two new species of Barbourofelinae (Felidae, Carnivora, Mammalia) from the Early Miocene of East Africa and Spain. Earth and Environmental Science Transactions of the Royal Society of Edinburgh 92 (01): 97–102.

Morlo, M., S. Peigné, and D. Nagel. 2004. A new species of *Prosansanosmilus*: implications for the systematic relationships of the family Barbourofelidae new rank (Carnivora, Mammalia). Zoological Journal of the Linnean Society 140 (1): 43–61.

Muizon, C., de. 1998. *Mayulestes ferox*, a borhyaenoid (Metatheria, Mammalia) from the early Palaeocene of Bolivia. phylogenetic and paleobiologic implications. Geodiversitas 20 (1): 19–142.

Muizon, C., de. 1999. Marsupials skulls from the Deseadan (late Oligocene) of Bolivia and phylogenetic analysis of the Borhyaenoidea (Marsupialia, Mammalia). Geobios 32 (3): 483–509.

Muizon, C. de, and B. Lange-Badré. 1997. Carnivorous dental adaptations in tribosphenic mammals and phylogenetic reconstruction. Lethaia 30 (4): 353–366.

Muizon, C., de, S. Ladevèze, C. Selva, R. Vignaud, and F. Goussad. 2018. *Allqokirus australis* (Sparassodonta, Metatheria) from the early Paleocene of Tiupampa (Bolivia) and the rise of the metatherian carnivorous radiation in South America. Geodiversitas 40 (16): 363–459.

Murray, P.F., and D. Megirian. 2006. Cranial morphology of the Miocene thylacinid *Mutpuracinus archibaldi* (Thylacinidae, Marsupialia) and relationships within the Dasyuromorphia. Alcheringa: an Australasian Journal of Palaeontology 30 (suppl. 1): 229–276.

Myers, T.J. 2001. Prediction of marsupial body mass. Australian Journal of Zoology 49 (2): 99–118.

Naples, V.L., L.D. Martin, and J.P. Babiarz. 2011. The other saber-tooths: scimitar-tooth cats of the Western Hemisphere. Baltimore: John Hopkins University Press, 236 pp.

O'Connor, P.M., et al. 2019. A new mammal from the Turonian–Campanian (Upper Cretaceous) Galula Formation, southwestern Tanzania. Acta Palaeontologica Polonica 64 (1): 65–84.

Owens, M.J., and D.D. Owens. 1978. Feeding ecology and its influence on social organization in Brown hyenas (*Hyaena brunnea*, Thunberg) of the Central Kalahari Desert. African Journal of Ecology 16 (113–135).

Palmqvist, P., et al. 2011. The giant hyena *Pachycrocuta brevirostris*: modelling the bone-cracking behavior of an extinct carnivore. Quaternary International 243 (1): 61–79.

Pascual, R., and E. Ortiz Jaureguizar. 1990. Evolving climates and mammal faunas in Cenozoic South America. Journal of Human Evolution 19: 23–60.

Patterson, B., and L.G. Marshall. 1978. The Deseadan, early Oligocene, marsupialia of South America. Fieldiana Geology 41 (2): 37–100.

Patterson, B.D., and R. Pascual. 1972. The fossil mammal fauna of South America. *In* A. Keast, F.C. Erk, and B. Glass (editors), Evolution, mammals, and southern continents: 274–309. New York: State University of New York Press.

Peigné, S. 2003. Systematic review of European Nimravinae (Mammalia, Carnivora, Nimravidae) and the phylogenetic relationships of Palaeogene Nimravidae. Zoologica Scripta 32 (3): 199–229.

Petter, G., and R. Hoffstetter. 1983. Les marsupiaux du Déséadien (Oligocène inférieur) de Salla (Bolivie). Annales de Paléontologie 69 (3): 175–234.

Piras, P., et al. 2018. Evolution of the sabertooth mandible: A deadly ecomorphological specialization. Palaeogeography, Palaeoclimatology, Palaeoecology 496: 166–174.

Pol, D., J.M. Leardi, A. Lecuona, and M. Krause. 2012. Postcranial anatomy of *Sebecus icaeorhinus* (Crocodyliformes, Sebecidae) from the Eocene of Patagonia. Journal of Vertebrate Paleontology 32 (2): 328–354.

Powell, J.E., M.J. Babot, D.A. García-López, M.V. Deraco, and C. Herrera. 2011. Eocene vertebrates of northwestern Argentina: annotated list. *In* J.A. Salfity and R.A. Marquillas (editors), Cenozoic geology of the central Andes of Argentina: 349–370. Salta, Argentina: SCS Publisher.

Prevosti, F.J., and A.M. Forasiepi. 2018. Evolution of South American mammalian predators during the Cenozoic: Palaeobiogeographic and Palaeoenvironmental Contengencies, Cham, Switzerland: Springer, 196 pp.

Prevosti, F.J., A.M. Forasiepi, M.D. Ercoli, and G.F. Turazzini. 2012. Paleoecology of the mammalian carnivores (Metatheria, Sparassodonta) of the Santa Cruz Formation (late early Miocene). *In* S.F. Vizcaíno, R.F. Kay, and M.S. Bargo (editors), Early Miocene paleobiology in Patagonia: high-latitude paleocommunities of the Santa Cruz Formation: 173–193. Cambridge: Cambridge University Press.

Prevosti, F.J., A. Forasiepi, and N. Zimicz. 2013. The evolution of the Cenozoic terrestrial mammal guild in South America: competition or replacement? Journal of Mammalian Evolution 20 (1): 3–21.

Prothero, D.R. 2006. After the dinosaurs. Bloomington: Indiana University Press, 362 pp.

Rangel, C.C., et al. 2019. Diversity, affinities, and adaptations of the South American basal sparassodont *Patene* Simpson, 1935 (Mammalia, Metatheria). Ameghiniana 56 (4): 263–289.

Ré, G.H., et al. 2010. A geochronology for the Sarmiento Formation at Gran Barranca. *In* R.H. Madden, A.A. Carlini, M.G. Vucetich, and R.F. Kay (editors), The paleontology of Gran Barranca evolution and environmental change through the Middle Cenozoic of Patagonia: 46–58. Cambridge: Cambridge University Press.

Riggs, E.S. 1933. Preliminary description of a new marsupial saber-tooth from the Pliocene of Argentina. Geological Series, Field Museum of Natural History 6: 61–66.

Riggs, E.S. 1934. A new marsupial saber-tooth from the Pliocene of Argentina and its relationships to other South American predacious marsupials. Transactions of the American Philosophical Society 24 (1): 1–32.

Robinson, P., et al. 2004. Wasatchian through Duchesnean Biochronology. *In* M.O. Woodburne (editor), Late Cretaceous and Cenozoic mammals of North America: 106–155. New York: Columbia University Press.

Robles, J.M., et al. 2013. New *Pseudaelurus* and *Styriofelis* remains (Carnivora: Felidae) from the middle Miocene of Abocador de Can Mata (Vallès-Penedès Basin). Comptes Rendus Palevol 12 (2): 101–113.

Rose, R.K., D.A. Pemberton, N.J. Mooney, and M.E. Jones. 2016. *Sarcophilus harrisii*. Mammalian Species 49 (942): 1–17.

Rovinsky, D.S., A.R. Evans, and J.W. Adams. 2019. The pre-Pleistocene fossil thylacinids (Dasyuromorphia: Thylacinidae) and the evolutionary context of the modern thylacine. PeerJ 7: e7457.

Salesa, M.J., M. Anton, A. Turner, and J. Morales. 2005. Aspects of the functional morphology in the cranial and cervical skeleton of the sabre-toothed cat *Paramachairodus ogygia* (Kaup, 1832) (Felidae, Machairodontinae) from the Late Miocene of Spain: implications for the origins of the machairodont killing bite. Zoological Journal of the Linnean Society 144 (3): 363–377.

Scott, W.B. 1937. A history of land mammals in the Western Hemisphere. New York: Macmillan Company, 786 pp..

Scott, W.B., and G.L. Jepsen. 1936. The mammalian fauna of the White River Oligocene: Part I. Insectivora and Carnivora. Transactions of the American Philosophical Society 28 (1): 1–153.

Shockey, B.J., and F. Anaya. 2008. Postcranial osteology of mammals from Salla, Bolivia (late Oligocene): form, function, and phylogenetic implications. *In* E.J. Sargis and M. Dagosto (editors), Mammalian evolutionary morphology: a tribute to Frederick S. Szalay: 135–157. New York: Springer.

Simpson, G.G. 1930. Post-Mesozoic Marsupialia. *In* J.F. Pompeckj (editor), Fossilium catalogus I: Animalia: 1–87. Berlin: W. Junk.

Simpson, G.G. 1940. Mammals and land bridges. Journal of the Washington Academy of Sciences 30: 137–163.

Simpson, G.G. 1945. The principles of classification and a classification of mammals. Bulletin of the American Museum of Natural History 85: 1–350.

Simpson, G.G. 1948. The beginning of the age of mammals in South America. Part I, Introduction. Systematics: Marsupialia, Edentata, Condylarthra, Litopterna and Notioprogonia. Bulletin of the American Museum of Natural History 91 (1): 1–232.

Simpson, G.G. 1970. Mammals from the early Cenozoic of Chubut, Argentina. Breviora 360: 1–13.

Sinclair, W.J. 1906. Mammalia of the Santa Cruz Beds. Marsupialia. *In* W.B. Scott (editor), Reports of the Princeton University Expeditions to Patagonia, 1896–1899: 333–460. Stuttgart: Princeton University, E. Schweizerbart'sche Verlagshandlung (E. Nägele).

Sinclair, W.J. 1930. New carnivorous Marsupialia from the Deseado Formation of Patagonia. Field Museum of Natural History, Geological Memoirs 1: 35–39.

Slater, G.J., and B. Van Valkenburgh. 2008. Long in the tooth: evolution of sabertooth cat cranial shape. Paleobiology 34 (3): 403–419.

Solé, F., and S. Ladevèze. 2017. Evolution of the hypercarnivorous dentition in mammals (Metatheria, Eutheria) and its bearing on the development of tribosphenic molars. Evolution and Development 19 (2): 56–68.

Suarez, C., A.M. Forasiepi, F.J. Goin, and C. Jaramillo. 2016. Insights into the Neotropics prior to the Great American Biotic Interchange: new evidence of mammalian predators from the Miocene of northern Colombia. Journal of Vertebrate Paleontology 36 (1): e1029581.

Suyin, D., Z. Jiajian, Z. Yuping, and T. Yongsheng. 1977. The age and characteristic of the Liuniu and the Dongjun faunas, Bose Basin of Guangxi. Vertebrata PalAsiatica 15 (1): 35–45.

Tambussi, C.P., and F.J. Degrange. 2013. The dominance of zoophagous birds: just a cliché? *In* C.P. Tambussi, and F. Degrange (editors), South American and Antarctic continental Cenozoic birds: paleobiogeographic affinities and disparities: 87–102. Dordrecht: Springer Netherlands.

Tedford, R.H., et al. 2004. Mammalian biochronology of the Arikareean through Hemphillian interval (late Oligocene through early Pliocene epochs). *In* M.O. Woodburne (editor), Late Cretaceous and Cenozoic mammals of North America: biostratigraphy and geochronology: 169–231. New York: Columbia University Press.

Tejada-Lara, J.V., et al. 2015. Life in proto-Amazonia: Middle Miocene mammals from the Fitzcarrald Arch (Peruvian Amazonia). Palaeontology 58 (2): 341–378.

Tomiya, S. 2013. New carnivoraforms (Mammalia) from the middle Eocene of California, USA, and comments on the taxonomic status of '*Miacis*' *gracilis*. Palaeontologia Electronica 16 (2): 1–29.

Tseng, Z.J., G.T. Takeuchi, and X. Wang. 2010. Discovery of the upper dentition of *Barbourofelis whitfordi* (Nimravidae, Carnivora) and an evaluation of the genus in California. Journal of Vertebrate Paleontology 30 (1): 244–254.

Turnbull, W.D. 1978. Another look at dental specialization in the extinct sabre-toothed marsupial, *Thylacosmilus*, compared with its placental counterparts. *In* P.M. Butler and K.A. Joysey (editors), Development, function and evolution of teeth: 399–413. New York: Academic Press.

Turnbull, W.D., and W. Segall. 1984. The ear region of the marsupial sabertooth, *Thylacosmilus*: influence of the sabertooth lifestyle upon it, and convergence with placental sabertooths. Journal of Morphology 181 (3): 239–270.

Van Valkenburgh, B. 1989. Carnivore dental adaptations and diet: a study of trophic diversity within guilds. *In* J.L. Gittleman (editor), Carnivore behavior, ecology, and evolution: 410–436. Boston: Springer US.

Van Valkenburgh, B. 1999. Major patterns in the history of carnivorous mammals. Annual Review of Earth and Planetary Sciences 27 (1): 463–493.

Van Valkenburgh, B., and C.B. Ruff. 1987. Canine tooth strength and killing behavior in large carnivores. Journal of the Zoological Society of London 212: 379–397.

Van Valkenburgh, B., X. Wang, and J. Damuth. 2004. Cope's rule, hypercarnivory, and extinction in North American canids. Science 306: 101.

Vieira, E.V., and D. Astúa de Moraes. 2003. Carnivory and insectivory in Neotropical marsupials. *In* M. Jones, C. Dickman, and M. Archer (editors), Predators with pouches: the biology of carnivorous marsupials: 271–284. Collingwood, Victoria, Australia: CSIRO Publishing.

Voss, R.S., and S.A. Jansa. 2009. Phylogenetic relationships and classification of didelphid marsupials, an extant radiation of New World metatherian mammals. Bulletin of the American Museum of Natural History 322: 1–177.

Wang, X., S.C. White, and J. Guan. 2020. A new genus and species of sabretooth, Oriensmilus liupanensis (Barbourofelinae, Nimravidae, Carnivora), from the middle Miocene of China suggests barbourofelines are nimravids, not felids. Journal of Systematic Palaeontology: 1–21.

Warburton, N.M., K.J. Travouillon, and A.B. Camens. 2019. Skeletal atlas of the Thylacine (*Thylacinus cynocephalus*). Palaeontologia Electronica 22.2.29A: 1–56.

Webb, S.D. 2006. The Great American Biotic Interchange: patterns and processes. Annals of rhe Missouri Botanical Garden 93 (2): 245–257.

Werdelin, L. 1987. Jaw geometry and molar morphology in marsupial carnivores; analysis of a constraint and its macroevolutionary consequences. Paleobiology 13 (3): 342–350.

Werdelin, L. 1989. Constraint and adaptation in the bone-cracking canid *Osteoborus* (Mammalia: Canidae). Paleobiology 15 (4): 387–401.

Werdelin, L., N. Yamaguchi, W.E. Johnson, and S.J. O'Brien. 2010. Phylogeny and evolution of cats (Felidae). *In* D. Macdonald and A. Loveridge (editors), Biology and conservation of wild felids: 59–82. Oxford: Oxford University Press.

West, A.R. 2017. Multidisciplinary investigations on the origins and evolution of the extinct ungulate order Notoungulata (Mammalia: Placentalia) and the extinct muskox genus *Bootherium* (Mammalia: Artiodactyla: Bovidae). Ph.D. dissertation, Department of Earth and Environmental Sciences, Columbia University, New York, 353 pp.

West, A.R., et al. 2014. New high-precision $^{40}Ar/^{39}Ar$ geochronology of fossil-bearing strata of the Cachapoal Valley, Andean Main Range, Chile. Journal of Vertebrate Paleontology, SVP Program and Abstracts 2014: 254.

Wheeler, H.T. 2011. Experimental paleontology of the scimitar-tooth and dirk-tooth killing bites. *In* V.L. Naples, L.D. Martin, and J.P. Babiarz (editors), The other saber-tooths: scimitar-tooth cats of the Western Hemisphere: 19–34. Baltimore: John Hopkins University Press.

Wible, J.R. 2003. On the cranial osteology of the short-tailed opossum *Monodelphis brevicaudata* (Didelphidae, Marsupialia). Annals of Carnegie Museum 72 (3): 137–202.

Williamson, T.E., S.L. Brusatte, T.D. Carr, A. Weil, and B.R. Standhardt. 2012. The phylogeny and evolution of Cretaceous-Palaeogene metatherians: cladistic analysis and description of new early Palaeocene specimens from the Nacimiento Formation, New Mexico. Journal of Systematic Palaeontology 10 (4): 625–651.

Woolley, P.A. 2011. *Pseudantechinus mimulus*: a little known dasyurid marsupial. Australian Mammalogy 33 (1): 57–67.

Wroe, S. 1999. The geologically oldest dasyurid, from the Miocene of Riversleigh, north-west Queensland. Palaeontology 42 (3): 501–527.

Wroe, S., et al. 2013. Comparative biomechanical modeling of metatherian and placental saber-tooths: A different kind of bite for an extreme pouched predator. PLoS ONE 8 (6): e66888.

Wysocki, M.A. 2019. Fossil evidence of evolutionary convergence in juvenile dental morphology and upper canine replacement in sabertooth carnivores. Ecology and Evolution n/a (n/a).

Wysocki, M.A., R.S. Feranec, Z.J. Tseng, and C.S. Bjornsson. 2015. Using a novel absolute ontogenetic age determination technique to calculate the timing of tooth eruption in the saber-toothed cat, *Smilodon fatalis*. PLoS ONE 10 (7): e0129847.

Yates, A.M. 2014. New craniodental remains of *Thylacinus potens* (Dasyuromorphia: Thylacinidae), a carnivorous marsupial from the late Miocene Alcoota local fauna of central Australia. PeerJ 2: e547.

Zack, S.P. 2019a. The first North American *Propterodon* (Hyaenodonta: Hyaenodontidae), a new species from the late Uintan of Utah. PeerJ 7: e8136.

Zack, S.P. 2019a. A skeleton of a Uintan machaeroidine 'creodont' and the phylogeny of carnivorous eutherian mammals. Journal of Systematic Palaeontology 17 (8): 653–689.

Zack, S.P. 2019b. The first North American *Propterodon* (Hyaenodonta: Hyaenodontidae), a new species from the late Uintan of Utah. PeerJ 7: e8136.

Zimicz, A.N. 2012. Ecomorfología de los marsupiales paleógenos de América del Sur. Ph.D. dissertation, Facultad de Ciencias Naturales y Museo de La Plata, Universidad Nacional de La Plata, La Plata.

Zimicz, N. 2014. Avoiding competition: the ecological history of late Cenozoic metatherian carnivores in South America. Journal of Mammalian Evolution 21 (4): 383–393.

Zimmer, C. 2009. The tangled bank: an introduction to evolution, 1st ed. Greenwood Village, CO: Roberts and Company Publishers, 385 pp.

APPENDIX 1

List of Comparative Material Examined

"Specimens" refers to specimens or casts that could be observed firsthand; "References" refer to data and observation based in part or solely on the primary literature.

Taxon	Specimens	References
Acrocyon riggsi	FMNH P13433	Goin et al. (2007)
Acrocyon sectorius	MACN-A 9364	Marshall (1978)
Acyon myctoderos	UATF-V-000926, UF 26921-26941	Forasiepi et al. (2006)
Allqokirus australis	—	Muizon et al. (2018)
Anachlysictis gracilis	—	Goin (1997)
Arctodictis sinclairi	MLP 77-VI-13-1, MLP 85-VII-3-1	Forasiepi (2009); Goin et al. (2007)
Arctodictis munizi	—	Forasiepi et al. (2004)
Arminiheringia auceta	MACN-A 10970/10972	Babot et al. (2002); Zimicz (2012)
Arminiheringia contigua	MACN-A 10317 (cast)	—
Arminiheringia cultrata	MACN-A 10329 (cast)	—
Arminiheringia sp.	—	Zimicz (2012); Forasiepi and Sánchez-Villagra (2014); Forasiepi, personal commun.

APPENDIX 1 *continued*

Taxon	Specimens	References
Australohyaena antiquua	MACN-A 52-322, FMNH P13633 (cast), FMNH P193800 (cast)	Forasiepi et al. (2015)
Borhyaena macrodonta	MACN-A 52-366, MACN-A 52-390 (cast)	—
Borhyaena tuberata	MACN-A 5780, MACN-A 6203-6265	Sinclair (1906); Cabrera (1927); Forasiepi (2009)
Callistoe vincei	—	Babot et al., 2002; Argot and Babot (2011); Babot, personal commun.
Cladosictis patagonica	MACN-A 674; MACN-A 5927, MACN-A 5950, MACN-A 6280 (cast)	Sinclair (1906)
aff. *Eomakhaira*? (MLP 88-V-10-4)	—	Goin et al. (1998)
Fredszalaya hunteri	—	Anaya Daza et al. (2010); Shockey and Anaya (2008)
Hondadelphys fieldsi	UCMP 37960	Goin (1997)
Lycopsis longirostrus	UCMP 38061	—
Lycopsis padillai	—	Suarez et al. (2016)
Lycopsis torresi	MLP 11-113	—
Lycopsis viverensis	—	Forasiepi et al. (2003)
Mayulestes ferox	—	Muizon (1998)
cf. *Nemolestes*	AMNH 29433	Forasiepi et al. (2015)
Notogale mitis	YPM-VPPU 21871	Patterson and Marshall (1978)
Paraborhyaena boliviana	UATF-V-000129	Petter and Hoffstetter (1983)
Patagosmilus goini	—	Forasiepi and Carlini (2010); Forasiepi, personal commun.
Patene coluapiensis	AMNH 28448	—
Patene simpsoni	MNRJ 1331-V	—
Pharsophorus lacerans	MACN-A 52-391	Patterson and Marshall (1978); Petter and Hoffstetter (1983)
Pharsophorus tenax	AC 3004 (cast), AC 3192 (cast)	Marshall (1978)
Pharsophorus cf. *P. lacerans*	MPEF-PV 4190	Goin et al. (2010); Zimicz (2012)
Plesiofelis schlosseri	MLP 11-114	—
Proborhyaena gigantea	AMNH 29576, MACN-A 52-382	Babot et al. (2002), Mones and Ubilla (1978)
cf. *Proborhyaena*	MLP 79-XII-18-1	Bond and Pascual (1983)
Proborhyaenidae sp. nov? (Tremembé Formation)	—	Couto-Ribeiro (2010)
Prothylacynus patagonicus	MACN-A 707, MACN-A 5931; MACN-PV 14453	Forasiepi (2009)
Pseudothylacynus rectus	MACN-A 52-369	
Sarcophilus harrissii	CMNH 18915	—

APPENDIX 1 *continued*

Taxon	Specimens	References
Sipalocyon gracilis	AMNH 9254, MACN-A 692; YPM-VPPU 15373	Sinclair (1906)
Sparassodonta gen. et sp. nov.	UF 27881	—
Stylocynus paranensis	MLP 11-94	—
Thylacinus cynocephalus	CMNH 18916	Murray and Megirian (2006)
Thylacosmilinae? gen. et sp. nov. (IGM 251108)	—	Goin (1997)
Thylacosmilinae indet.	—	Goin et al. (2007)
Thylacosmilus atrox	FMNH 14344; FMNH P14531 (cast); MLP 35-X-4-1	Riggs (1933); Riggs (1934); Turnbull (1978); Goin and Pascual (1987); Argot (2004b)

All issues of *Novitates* and *Bulletin* are available on the web (http://digitallibrary.amnh.org/dspace). Order printed copies on the web from:
http://shop.amnh.org/a701/shop-by-category/books/scientific-publications.html

or via standard mail from:

American Museum of Natural History—Scientific Publications
Central Park West at 79th Street
New York, NY 10024

♾ This paper meets the requirements of ANSI/NISO Z39.48-1992 (permanence of paper).